Answers Research Journal 19 (2026): 19–94.
https://assets.answersresearchjournal.org/doc/v19/radioisotope_dating_meteorites_6.pdf

ARJ

Radioisotope Dating of Meteorites: VI. The SNC and Other Martian Meteorites

Andrew A. Snelling, Answers in Genesis, PO Box 510, Hebron, Kentucky, 41048.

Abstract

More than 260 meteorites have been identified as coming from Mars, all igneous rocks classified into shergottites, nakhlites, chassignites, orthopyroxenite and polymict regolith breccias. More than 60 have been radioisotope dated using the K-Ar, Ar-Ar, Rb-Sr, Sm-Nd, U-Th-Pb, Lu-Hf and Re-Os methods. Some 3.0–4.57 Ga radioisotope "ages" coincide with the postulated formation of Mars and the subsequent giant impact cratering, massive volcanism and water outflows that deposited sedimentary layers and carved canyons during the Martian Noachian and Hesperian eras. Other younger <3.0 Ga Amazonian era radioisotope "ages" are sporadically distributed, coinciding with minor, scattered, lingering igneous activity. The radioisotope "ages" are generally concordant, so they provide no definitive evidence of accelerated radioisotope decay having occurred during and since the formation of these Martian igneous rocks. Contrary to the naturalistic paradigm, God specifically tells us in His eyewitness account that He created the earth on Day One of the Creation Week, and Mars, the other planets, and earth's Moon were created on Day Four from the same "primordial material" He had created on Day One. Today's measured radioisotope compositions of these Martian meteorites may thus partially reflect the isotopic signature of that created "primordial material" consisting of atoms of all elemental isotopes including isotopes and their now daughter isotopes that were not derived by radioactive decay. However, it is assumed that radioisotope decay with its emitted damaging radiation did not occur during the Creation Week because God declared at the end of Day Six that everything He had made as "very good" (Genesis 1:31). Thus it is assumed that radioisotope decay only commenced when God cursed the ground. Similarly, the impact cratering of earth, its Moon, Mars and the other planets would likewise not have occurred during the Creation Week to damage God's "very good" creation. Instead, the giant impact cratering, massive volcanism and water outflows that deposited sedimentary layers and carved canyons during the Martian Noachian and Hesperian eras (3.0–4.1 Ga) might correlate with the global Flood cataclysm on the earth. In the subsequent Martian Amazonian era (<3.0 Ga) geologic activity was minor, localized, and sporadic, as recorded in many of the Martian meteorites. There is thus a major "disconnect" between the radioisotope "ages" for these Martian 3.0–4.1 Ga major geologic events and rocks, and the radioisotope "ages" of < 600 Ma for rocks formed during the earth's global Flood cataclysm. This "disconnect" may be due to the earth having suffered from the Day Three Great Upheaval in which the primordial isotopic endowment was mixed and redistributed producing younger radioisotope "ages" in the resultant rocks, whereas Mars being subsequently created on Day Four was not so affected and thus maintained its primordial mantle isotopic endowment. Then when earth's global Flood cataclysm occurred with its accompanying accelerated radioisotope decay and stirring of mantle reservoirs due to plate subduction and mantle plumes during catastrophic plate tectonics, Mars was also affected with giant impact cratering and massive volcanism, in which its mantle reservoirs were stirred and their isotopic endowment mixed. However, whereas the radioisotope "clocks" in the earth's rocks were accelerated from their pre-Flood settings through some 600 million years, the Martian rocks' radioisotope "clocks" may have been mixed, reset and accelerated through some 4 billion years from their pre-Flood settings. This has implications for earth's Moon, since it also did not suffer from the Day Three Great Upheaval and early in it supposed geologic history it also suffered from giant impact cratering and massive volcanism, which thus could also correlate with the earth's global Flood cataclysm. In any case, even though these Martian meteorites yield consistent radioisotope "ages", these cannot be their true real-time ages, which according to the biblical paradigm are only about 6,000 and less real-time years.

Keywords: Martian meteorites, radioisotope ages, created primordial isotopic endowment, mantle reservoirs, Day Three Great Upheaval, "very good" creation, impact cratering, massive volcanism, global Flood cataclysm, accelerated radioisotope decay

Introduction

In 1956 Claire Patterson at the California Institute of Technology in Pasadena reported a Pb-Pb isochron age of 4.55±0.07 Ga for three stony and two iron meteorites, which since then has been declared the age of the earth (Patterson 1956). Adding weight to that claim is the fact that many meteorites appear to consistently date to around the same "age" (Dalrymple 1991, 2004), thus bolstering the evolutionary community's confidence that they have successfully dated the age of the earth and the solar system at around 4.56 Ga. Of course, the evolutionary community still argues that the collapse of the solar (proto-stellar) nebula occurred "only"

100,000 years–10 million years before the earth had coalesced from it (Montmerle et al. 2006). Yet these apparent successes have also strengthened their case for the supposed reliability of the increasingly sophisticated radioisotope dating methods.

Creationists have commented little on the radioisotope dating of meteorites, apart from acknowledging the use of Patterson's geochron to establish the age of the earth, and that many meteorites give a similar old age. Morris (2007) did focus on the Allende carbonaceous chondrite as an example of a well-studied meteorite analysed by many radioisotope dating methods, but he only discussed the radioisotope dating results from one, older paper (Tatsumoto, Unruh, and Desborough 1976).

In order to rectify this lack of engagement by the creationist community with the meteorite radioisotope dating data, Snelling (2014a) obtained as much radioisotope dating data as possible for the Allende CV3 carbonaceous chondrite meteorite (due to its claimed status as the most studied meteorite), displayed the data, and attempted to analyse them. He found that both isochron and model ages for the total rock, separated components, or combinations of these strongly clustered around a Pb-Pb age of 4.56–4.57 Ga, the earliest (Tatsumoto, Unruh, and Desborough 1976) and the latest (Amelin et al. 2010) determined Pb-Pb isochron ages at 4.553 ± 0.004 Ga and 4.56718 ± 0.0002 Ga respectively being essentially the same. Apart from scatter of the U-Pb, Th-Pb, Rb-Sr, and Ar-Ar ages, no systematic pattern was found in the Allende isochron and model ages similar to the systematic pattern of isochron ages found in Precambrian rock units during the RATE project that was interpreted as produced by an episode of past accelerated radioisotope decay (Snelling 2005c, Vardiman, Snelling, and Chaffin 2005).

Snelling (2014b) then grouped together all the radioisotope ages obtained for ten ordinary (H, L, and LL) and five enstatite (E) chondrites and similarly displayed the data. They generally clustered, strongly in the Richardton (H5), St. Marguerite (H4), Bardwell (L5), Bjurbole (L4), and St. Séverin (LL6) ordinary chondrite meteorites, at 4.55–4.57 Ga, dominated by Pb-Pb and U-Pb isochron and model ages, but confirmed by Ar-Ar, Rb-Sr, Re-Os, and Sm-Nd isochron ages. There was also scatter of the U-Pb, Th-Pb, Rb-Sr, and Ar-Ar model ages, in some cases possibly due to thermal disturbance. However, the systematic deviations among the different radioisotope systems observed in the RATE studies were not found in these meteorites' isochron ages.

Snelling (2014e) subsequently compiled all the radioisotope ages for 12 eucrite (basaltic) achondrites. The data for many of these meteorites again strongly clustered at 4.55–4.57 Ga, dominated by Pb-Pb and U-Pb isochron and model ages but confirmed by Rb-Sr, Lu-Hf, and Sm-Nd isochron ages. There was also scatter of the U-Pb, Pb-Pb, Th-Pb, Rb-Sr, K-Ar, and Ar-Ar model ages, in most cases likely due to thermal disturbances resulting from metamorphism or impact cratering of the parent asteroid, identified as 4-Vesta. Again, no pattern was found in these meteorites' isochron ages similar to the systematic patterns of isochron ages found in Precambrian rock units during the RATE project.

Snelling (2015b) also tabulated all the radioisotope ages of ten further achondrites that have been repeatedly dated—primitive achondrites, angrites, aubrites, mesosiderites, and irons. The data again strongly clustered at 4.55–4.57 Ga, dominated by Pb-Pb and U-Pb isochron and model ages, and sometimes confirmed by Ar-Ar, Rb-Sr, Lu-Hf, Re-Os, and Sm-Nd isochron and/or model ages. There was also again scattering of many K-Ar, Ar-Ar, Rb-Sr, Re-Os, Sm-Nd, and a few U-Pb, Pb-Pb, Th-Pb ages, in most cases likely due to thermal disturbances resulting from impact cratering of the parent asteroids. And again, no pattern was found in these meteorites' isochron ages matching that of the RATE studies.

Snelling (2015d) then tabulated all the radioisotope ages of groups of meteorites. The data strongly clustered at 4.55–4.57 Ga in the groups of chondrites, stony achondrites, and irons, dominated by Pb-Pb, U-Pb, and Pb-Pb calibrated isochron ages. These ages were often confirmed by Rb-Sr, Lu-Hf, Re-Os, and Sm-Nd isochron ages. But there was also scattering of many Rb-Sr, Lu-Hf, Re-Os, Sm-Nd isochron ages, and a few Pb-Pb isochron ages, in most cases likely due to thermal disturbances resulting from impact cratering of the parent asteroids. Again, no pattern was found in the isochron ages for these groups of meteorites similar to that identified in the RATE investigations.

Snelling (2014a, b, e, 2015b, d) thus sought to discuss the possible significance of this clustering in terms of various potential creationist models for the history of radioisotopes and their decay. He favoured the idea that asteroids and the meteorites derived from them represent residual "primordial material" from the formation of the solar system, which is compatible with the Hebrew text of Genesis that could suggest God made "primordial material" on Day One of the Creation Week, from which He subsequently made the non-earth portion of the solar system on Day Four. Thus he argued that today's measured radioisotope compositions of all these meteorites may reflect a geochemical signature of that "primordial material," which included atoms of all elemental isotopes, "inherited" at their creation. So if some (or most) of the daughter isotopes were already in

all these meteorites when they were formed, then the 4.55–4.57 Ga "ages" for them obtained by Pb-Pb and U-Pb isochron and model age dating are likely not their true real-time ages, which according to the biblical paradigm is only about 6,000 real-time years.

However, Snelling (2014a, b, e, 2015b, d) suggested that drawing final conclusions from the radioisotope dating data for just these 16 chondrite, 12 eucrite meteorites, ten primitive and other achondrites, and the groups of meteorites was somewhat premature, and recommended further studies of the radioisotope dating data for Martian and lunar meteorites, for lunar rocks, and for rocks from every level in the earth's geologic record so as to hopefully confirm or modify these initial conclusions. This present contribution is therefore designed to document the radioisotope dating data for the Martian meteorites, so as to continue the discussion of the potential significance of the meteorites' radioisotope ages.

The Classification of Meteorites

Meteorites have been classified into distinct groups and subgroups that show similar chemical, isotopic, mineral, and physical relationships. Within the evolutionary community the ultimate goal of such a classification scheme is to group all known specimens that apparently share a common origin on a single, identifiable parent body, or even a body yet to be identified. This could be another planet, moon, asteroid, or other current solar system object, or one that is believed to have existed in the past (for example, a shattered asteroid). However, several meteorite groups classified this way appear to have come from a single, heterogeneous parent body, or even a single group may contain members that may have come from a variety of similar but distinct parent bodies. So any meteorite classification system is not absolute, and is only as valid as the criteria used to develop it.

More than 24,000 meteorites had been catalogued by 2002 (Norton 2002), and that number rapidly grew to more than 40,000 meteorites by 2014 (Krot et al. 2014) due to the ongoing discovery of large concentrations of meteorites in the world's cold and hot deserts (for example, in Antarctica, and Australia and Africa, respectively). Officially recognized meteorites and their classifications are listed in the Meteoritical Bulletin Database Meteoritical Bulletin: Search the Database, which now lists more than 78,940 meteorites with valid names.

Traditionally meteorites have been divided into three overall categories based on whether they are dominantly composed of rocky materials (stones or stony meteorites), metallic material (irons or iron meteorites), or mixtures (stony-irons or stony-iron meteorites). These categories have been in use since at least the early nineteenth century, but they are merely descriptive and do not have any genetic connotations. In reality, the term "stony-iron" is a misnomer, as the meteorites in one group (the CB chondrites) have over 50% metal by volume and were called stony-irons until their affinities with chondrites were recognized. Similarly, some iron meteorites also contain many silicate inclusions but are rarely described as stony-irons.

Nevertheless, these three categories are still part of the most widely used meteorite classification systems. Stony meteorites are traditionally divided into two other categories—chondrites (meteorites that are characterized by containing chondrules and which apparently have undergone little change since their parent bodies originally formed), and achondrites (meteorites that appear to have had a complex origin involving asteroidal or planetary differentiation). Iron meteorites were traditionally divided into objects with similar internal structures (octahedrites, hexahedrites, and ataxites), but these terms are now only used for descriptive purposes and have given way to chemical group names. Stony-iron meteorites have always been divided into pallasites (which now comprise several distinct groups) and mesosiderites (a textural term which is also synonymous with the name of a modern group).

The most recent classification scheme for the meteorites is that of Weisberg, McCoy, and Krot (2006), which is reproduced in fig. 1. Based on their bulk compositions and textures, Krot et al. (2005, 2014) divided meteorites into two major categories,

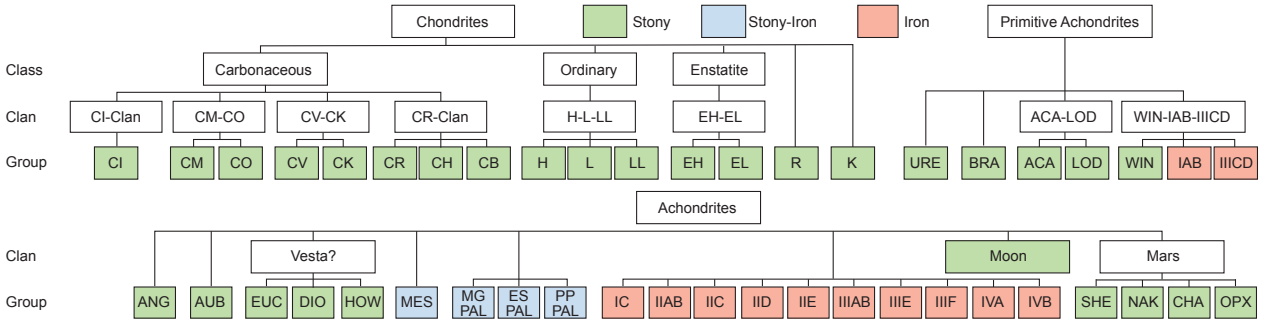

Fig. 1. The classification system for meteorites (after Weisberg, McCoy and Krot 2006).

chondrites (meteorites containing chondrules) and achondrites (or non-chondritic meteorites, that is, meteorites not containing chondrules). They further subdivided the achondrites into primitive achondrites and igneously differentiated achondrites. However, Weisberg, McCoy, and Krot (2006) simply subdivided all meteorites into three categories—chondrites, primitive achondrites, and achondrites (fig. 1). As in Krot et al.'s (2005, 2014) classification scheme, Weisberg, McCoy and Krot (2006) have included the IAB and IIICD irons in the primitive achondrites because of their silicate inclusions, while the rest of the groups of irons, the stony-irons, the Martian and lunar meteorites are included with the other achondrite groups in the achondrites.

The meteorites are further classified into groups using a classification scheme based on their chemistry, oxygen isotopes, mineralogy, and petrography (fig. 1). The goals of this classification scheme are to provide descriptive labels for classes of meteorites with similar supposed origins or formation histories that could be derived from the same asteroidal or planetary body, and to reveal possible genetic links between various classes. Recent advances in high-precision isotope measurements have revealed the importance of stable-isotope anomalies of bulk meteorites for understanding genetic relationships between meteorite groups (Warren 2011).

About 82% of all meteorite falls are chondrites (Norton 2002). The chondrites derive their name from their interior texture, which is unlike any found in terrestrial rocks. Dispersed more or less uniformly throughout these meteorites are spherical, sub-spherical and sometimes ellipsoidal structures called chondrules. These range in size from about 0.1 to 4 mm (0.0039 to 0.15 in) diameter, with a few reaching centimeter size. Their abundance within a given chondrite can vary enormously from only a few per cent of the total volume of the meteorite to as much as 70%, with fine-grained matrix material dispersed between the chondrules. Most chondrules are rich in the silicate minerals olivine and pyroxene. The other major components of chondrites are refractory inclusions—Ca-Al-rich inclusions (CAIs) and amoeboid olivine aggregates (AOAs)—and Fe-Ni metal alloys and sulfides (Brearley and Jones 1998; Scott and Krot 2005), set in fine-grained matrix material. It is generally believed conventionally that the refractory inclusions, chondrules, and FeNi-metal were formed in the postulated solar nebula by high-temperature processes that included condensation and evaporation. Many CAIs and most chondrules and FeNi-metal were subsequently melted during multiple brief heating episodes. Although most chondrites experienced thermal processing on their parent asteroids, such as aqueous or hydrothermal alteration, thermal, and shock metamorphism, they did not experience melting and igneous differentiation, and thus largely preserve records of physical and chemical processes in the solar nebula.

The chondrites have been subdivided into three classes—carbonaceous (C), ordinary (O), and enstatite (E) chondrites—and 15 groups, including the rare R and K chondrites (fig. 1). The carbonaceous (C) chondrites, representing almost 4% of all chondrites, are so named because their matrix is carbon-rich, containing various amounts of carbon in the form of carbonates and complex organic compounds including amino acids (Cronin, Pizzarello, and Cruikshank 1988). The ordinary (O) chondrites are by far the most common type of meteorite to fall to earth. About 77% of all meteorites and nearly 94% of chondrites are ordinary chondrites. They have been divided into three groups—H, L, and LL chondrites—the letters designating their different bulk iron contents (H for high and L for low) and their different amounts of metal (L for low) (Krot et al. 2005; Norton 2002). The E chondrites comprise only 1.4% of the chondrites, and are named after their primary silicate mineral, enstatite. Enstatite is the Mg-rich end member of the orthopyroxene solid-solution series, and makes up 60–80 vol. % of these meteorites (Krot et al. 2005; Norton 2002). Further details of the classification of the chondrites are provided by Snelling (2014a, b).

Nonchondritic meteorites or achondrites lack chondritic textures contain virtually none of the components found in chondrites. It is conventionally claimed that they were derived from chondritic materials by partial or complete melting and planetary differentiation of chondritic precursor asteroids or larger planetary bodies such as Mars and the moon, and that fractionation caused their bulk compositions to deviate to various degrees from chondritic materials (Krot et al. 2005). Several groups of nonchondritic meteorites experienced low degrees of melting, and have largely retained their chondritic bulk compositions. To emphasize the relatively unprocessed nature of these achondrites and their intermediate status relative to chondrites and highly differentiated meteorites, they are often referred to as primitive achondrites in contrast to the other major category the differentiated achondrites (fig. 1). However, the distinctions between these categories are not clear-cut as many different chemical, textural, and isotopic properties are used to distinguish them.

The differentiated achondrites (fig. 1) are conventionally regarded as having been derived from parent bodies that experienced large-scale partial melting, isotopic homogenization (ureilites are the only exception), and subsequent differentiation. Based on abundance of Fe-Ni metal, these meteorites are commonly divided into three types—achondrites,

stony-irons, and irons. Each of these types contains several meteorite groups and ungrouped members (fig. 1). According to uniformitarians, several groups of achondrites and iron meteorites are likely to be genetically related and were possibly derived from single asteroids or planetary bodies.

The achondrites account for about 8% of meteorites overall, and the majority of them (about two-thirds) are HED meteorites (howardites, eucrites, and diogenites), believed to have originated from the crust of asteroid 4-Vesta (Norton 2002) (fig. 1). Other types include the primitive achondrites, angrites, aubrites, Martian, lunar, and several types thought to originate from as-yet unidentified asteroids, as well as the pallasites, mesosiderites, and various groups of irons. These groups have been determined on the basis of, for example, their bulk Fe/Mn and $^{17}O/^{18}O$ ratios, which are thought to be characteristic "fingerprints" for each parent body (Mittlefehldt et al. 1998). The achondrites represent the products of classical igneous processes acting on the silicate-oxide system of asteroidal bodies—partial to complete melting, differentiation, and magmatic crystallization (Mittlefehldt 2005). Thus the achondrites consist of materials similar to terrestrial basalts and plutonic rocks, so they exhibit igneous textures, or igneous textures modified by impact and/or thermal metamorphism, and distinctive mineralogies indicative of igneous processes. Iron meteorites represent the complimentary metal-sulfide system products of this process. The structural parameters in irons have been combined with several chemical parameters such as nickel and trace element contents to produce a more definite classification with meaningful distinct genetic groups that could represent different parent bodies. Also, certain trace elements such as gallium (Ga), germanium (Ge), and iridium (Ir) that like Ni are siderophile (or iron-loving) have been used to sub-divide the iron meteorites into distinct chemical groups. Further details about the achondrites and their classification are provided by Snelling (2014e, 2015b)

The Martian Meteorites

There are currently more than 260 individual samples of Martian meteorites available for study, suggested to represent 150 pairing groups (Meteoritical Bulletin Database Meteoritical Bulletin: Search the Database), with more being discovered each year. Paired meteorites are believed to have originated from the same parent meteoroid that broke up into several pieces upon ejection from Mars or upon entry into the earth's atmosphere. The total mass of Martian meteorites is ~211kg, with the most massive meteorites, including recovered strewn field stones, being Zagami (~18kg), Tissint (~12kg), and Nakhla (~9.9kg).

The suite of meteorites known to be derived from Mars are predominantly igneous, and consist of the shergottite (>80% of all known Martian meteorites), nakhlite (~10%) and chassignite (~3%) groups, the acronym SNC for the suite being formally derived from the "original three" meteorites (Shergotty, Nakhla, and Chassigny) (fig. 2). However, this designation is no longer comprehensive, and the simple term "Martian meteorites" is recommended instead (Treiman, Gleason and Bogard 2000). Two other types of Martian meteorites have more recently added to their classification scheme (fig. 2). These additional types are the orthopyroxenite Allan Hills (ALH) 84001 (Mittlefehldt 1994), and the unique polymict regolith breccia (originally classified as a "basaltic breccia") Northwest Africa (NWA) 7034 (Agee et al. 2013) and its pairs (Humayun et al. 2013; Wittmann et al. 2015).

The rate of recovery of Martian meteorites has varied significantly over the last two centuries. Five witnessed meteorite falls have been reported, including: the first discovered Martian meteorite Chassigny in 1815 (Champagne-Ardenne, France), Shergotty in 1865 (Bihar, India), Nakhla in 1911 (Al Buhayrath in Egypt) (fig. 3), Zagami in 1962 (Katsina, Nigeria) (fig. 4), and Tissint in 2011 (Guelmim-Es-Semara, Morocco). A total of thirty samples have been recovered in Antarctica by the US Antarctic Search for Meteorites and Japanese National Institute of Polar Research missions. Since 2014 (representing the year where the Eighth International Conference on Mars took place), 73 Martian meteorites have been recovered, constituting 48% of the current collection, with all of them being found in Morocco, Algeria, Mali, Mauritania, Libya, Oman, and Chile. They included 68 shergottites, four nakhlites, and one chassignite.

With the exception of the polymict breccia lithologies, all other Martian meteorites are volcanic or subvolcanic and plutonic rocks. In general terms, these igneous rocks range in composition from mafic to ultramafic and contain variable proportions of augite, pigeonite, maskelynite (plagioclase that has been shock metamorphosed to a diaplectic glass in most specimens), olivine, and orthopyroxene, and minor minerals including Cr-spinel, phosphates (merrillite, apatite), sulfides, titanomagnetite, ilmenite, ± baddeleyite, and ± silica. The textures of the different groups of Martian meteorites are aphanitic, porphyritic, diabasic (= micro gabbroic), and oikocrystic.

Their diverse, highly fractionated compositions, and comparatively young crystallization "ages" (1.3Ga and possibly ~180Ma) suggested that they are derived from a large, planet-sized body (Ashwal, Warner, and Wood 1982; Jones 1986; Wood

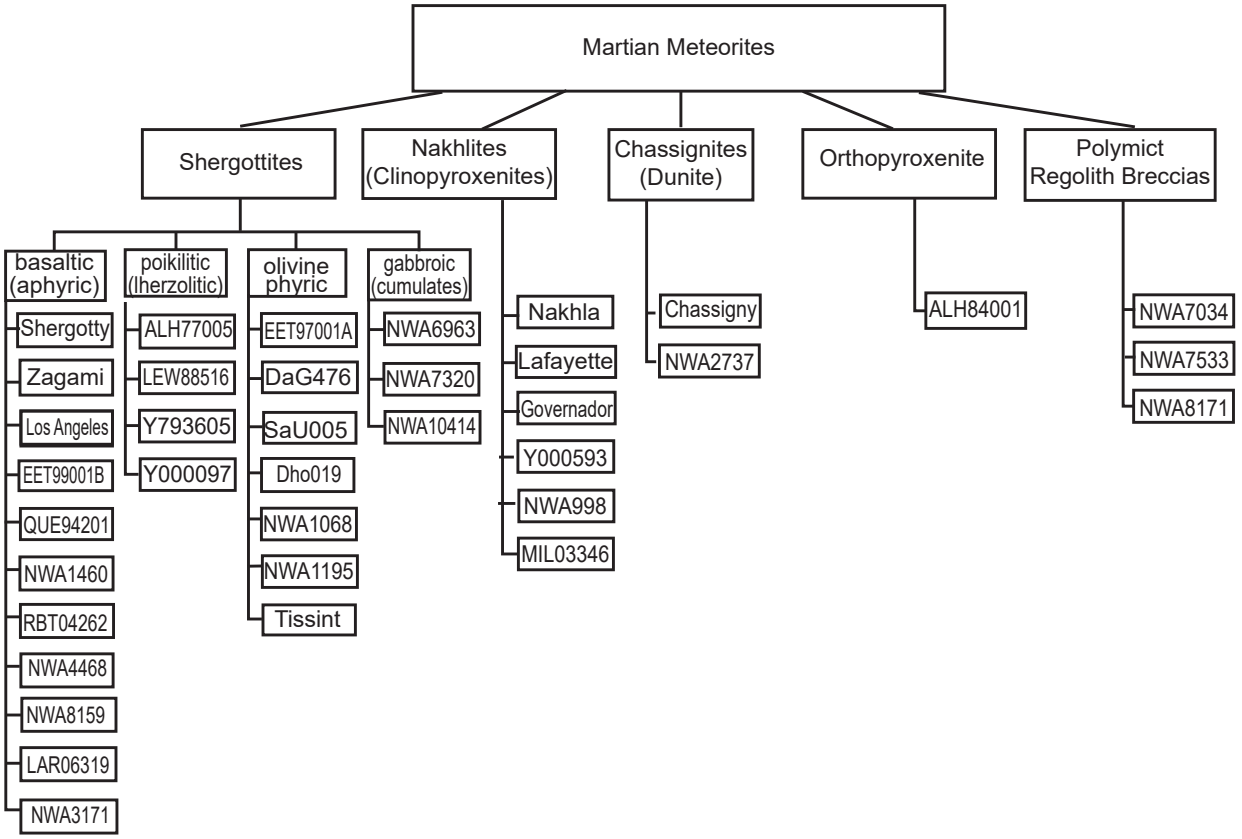

Fig. 2. The classification system for Martian meteorites (after Krot et al. 2014; Udry et al. 2020). There are now five distinctive groups, with the shergottites subdivided into four types. Representative meteorites are listed, many of which have been radioisotope dated.

and Ashwal 1981). Their unique oxygen isotopic compositions and FeO/MnO ratios of their pyroxenes (fig. 5) indicate that this body is not the earth or the moon. Similarities between the isotopic compositions of nitrogen and noble gases of the Martian atmosphere (as determined by the Viking Landers) and those trapped in impact-produced glasses in some shergottites suggest that these meteorites are from Mars (Bogard, Garrison, and McCoy 2000; McSween 2002, 2008; McSween and Treiman 1998; Nyquist et al. 2001b).

Shergottites

The shergottites are the most abundant type of

Fig. 3. The Nakhla meteorite is the prototype of the nakhlite Martian meteorites. Some 40 fragments of the Nakhla meteorite totaling 40 kg were seen to fall as a shower in the hamlets surrounding the village of El-Nakhla, El-Baharîya in Egypt (near Alexandria) on June 28th, 1911, at 9:00 a.m. (a) Inside surfaces after breaking in 1998. (Public domain photo courtesy of NASA.) (b) This is a 4.02 g sample from one of the forty fragments. This specimen is 19 mm across and is housed in the Institute of Meteoritics, University of New Mexico (after Norton 2002).

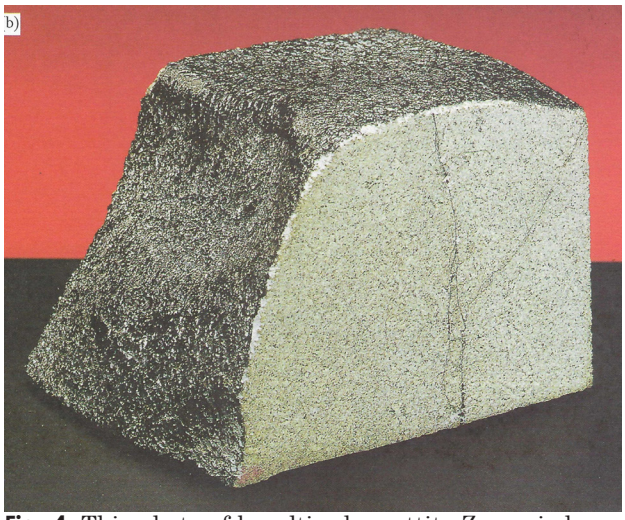

Fig. 4. This photo of basaltic shergottite Zagami shows a shiny black fusion crust typical of all shergottites (after Norton 2002). Zagami is from Katsina Province in Nigeria, found on October 3, 1962. It weighed ~18 kg and is fine-grained with the very small augite and plagioclase grains being best viewed by a magnifying glass. The specimen measures 76 mm across.

Martian meteorites (fig. 2), accounting for 89% of the total collection by number and 82% by mass, and are the most diverse of the Martian meteorite subgroups.. The shergottites may be subdivided on the basis of texture (grain sizes and shapes) and mineralogy (modal abundances) (Papike et al. 2009) (fig. 6). The different textures represent mineral formation and emplacement in the shallow subsurface or perhaps eruption at the surface.

First in abundance are the basaltic (aphyric) shergottites, which mostly contain the clinopyroxenes pigeonite and augite (average lengths of 0.3 mm, up to 1 mm) and plagioclase (now shock produced glass or maskelynite) in subequal proportions (fig. 7). They have basaltic or diabasic textures and are characterized by the absence of olivine phenocrysts or megacrysts (He et al. 2015; Howarth, Udry, and Day 2018; McSween et al. 1996; Rubin et al. 2000). Pyroxene in the basaltic shergottites varies in composition, although most commonly low- and high-Ca pyroxene are present in subequal proportions. The absence of olivine in these rocks and their low mg# (23–52) indicate that they crystallized from fractionated magmas (Stolper and McSween 1979). Many of them (including the type shergottite, Shergotty) contain cumulus pyroxene, and have strongly foliated textures suggesting crystal accumulation in near-surface dikes or lava flows (McCoy, Taylor, and Keil 1992; Stolper and McSween 1979). However, some (QUE94201 and Los Angeles) have higher plagioclase contents and may represent magma compositions (McKay et al. 2002; McSween et al. 1996; Rubin et al. 2000).

Second, but third in abundance, are the poikilitic shergottites that contain large oikocrysts of low-Ca pyroxene (from 3 to 10 mm in length) enclosing olivine chadacrysts (up to 1.8 mm), or variations thereof, with later-crystallizing olivine, pyroxene, and maskelynite (Combs et al. 2019; Howarth et al. 2014; Kizovski et al. 2019; Rahib et al. 2019; Walton et al. 2012). Poikilitic shergottites were previously termed

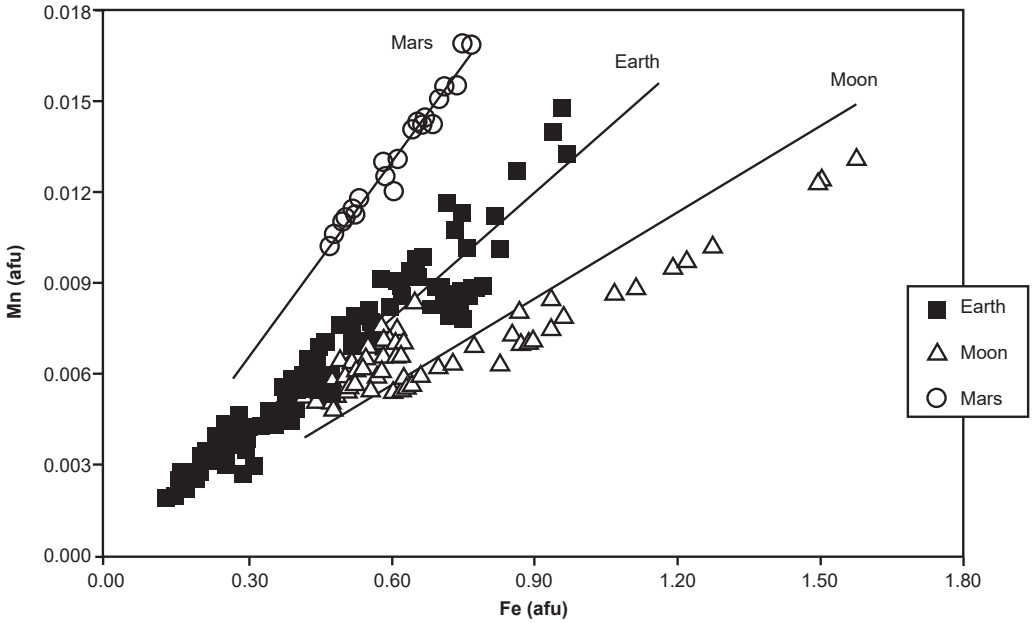

Fig. 5. Mn versus Fe in atoms per formula unit (afu) per 6-oxygen for representative olivine analyses from the earth, moon, and Mars (after Karner, Papike and Shearer 2003). The trend of data points shown for each planet represents 25–200 actual electron microprobe analyses. Linear regression lines for each planetary suite are constrained to pass through the origin.

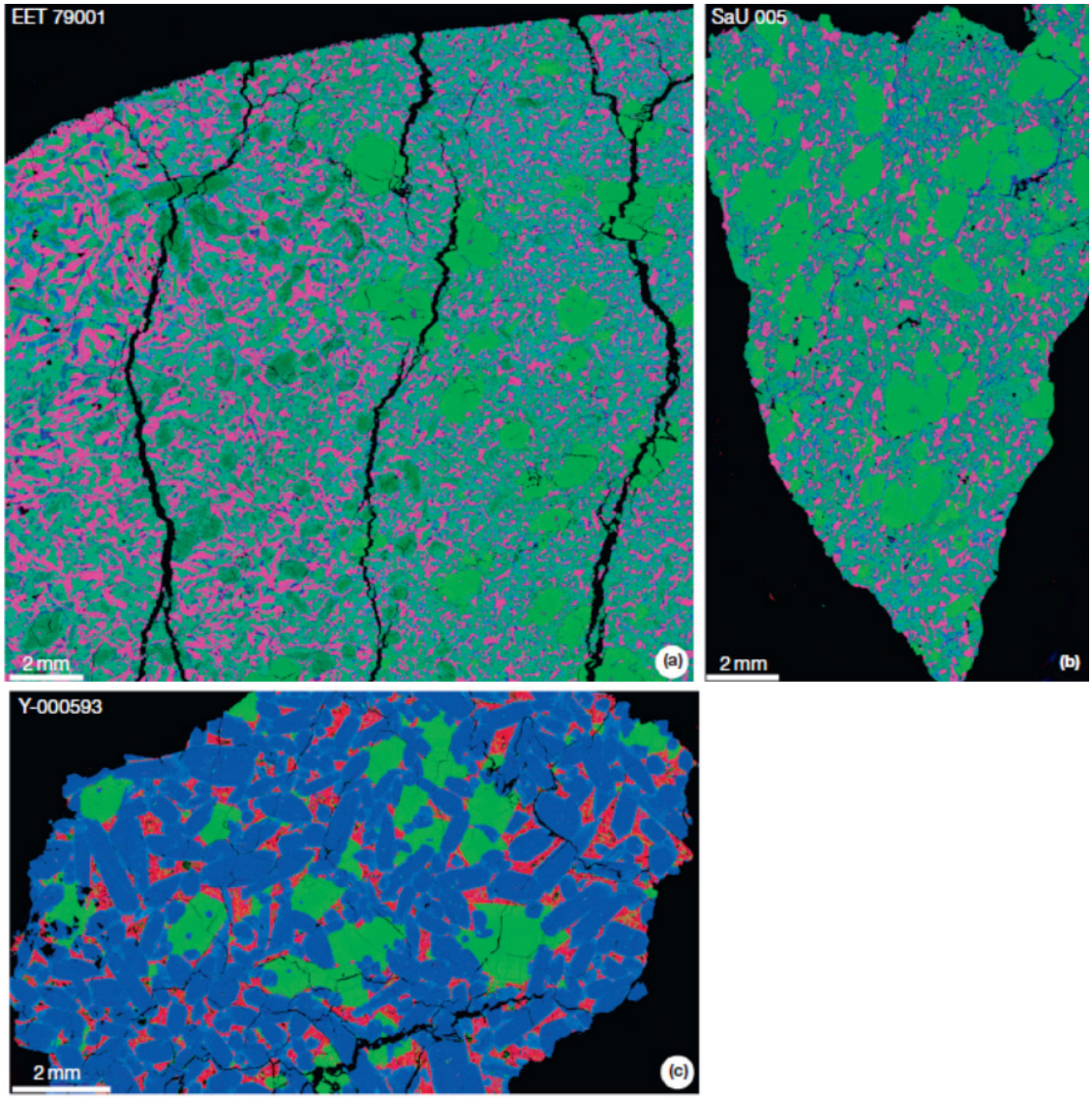

Fig. 6. Combined elemental maps (a–c) in Al (red), Fe (green) and Ca Kα (blue) X-rays of Martian meteorites (after Krott et al. 2014). (a) Elephant Moraine (EET) 79001 shergottite shows a contact between lithology A (right) and lithology B (left). Lithology A is an olivine–phyric basalt containing megacrysts of olivine in a finer-grained groundmass consisting principally of pigeonite (green–blues) and maskelynite (magenta). Lithology B is a pyroxene–plagioclase (maskelynite) basalt. It lacks olivine, is coarser grained than the groundmass of lithology A, and has a higher augite content (some of the blues). (b) Sayh al Uhaymir (SaU) 005 is an olivine–phyric basalt mineralogically similar to lithology A of EET 79001. Olivine megacrysts is a finer grained groundmass consisting principally of pigeonite (green–blues) and maskelynite (magenta). (c) Yamato (Y) 000593 is a nakhlite containing augite (blue), olivine (green), and interstitial areas (red) consisting principally of radiating sprays of plagioclase and alkali feldspars.

lherzolitic shergottites (Mikouchi and Kurihara, 2008). They are magnesian (mg# ~70) olivine–clinopyroxene–chromite cumulates, dominated by coarse grained poikilitic pigeonite enclosing rounded olivine (and chromite) crystals, with interstitial areas of finer-grained, FeO-rich olivine, pigeonite, augite, maskelynite, and other late phases (Ikeda 1997; McSween et al. 1979; McSween, Taylor, and Stolper 1979; Treiman et al. 1994). McSween et al. (1979) and McSween, Taylor, and Stolper (1979) noted that the dominant mineralogy of these rocks is consistent with early crystallization from magmas having the crystallization sequence inferred for basaltic shergottites such as Shergotty. This led to their classification as shergottites, although some authors feel that they should be referred to simply as Martian lherzolites (Treiman et al. 1994).

EET79001 is a unique shergottite (fig. 8) consisting of two lithologies (designated A and B) separated by an obvious contact (fig. 6a). Lithology B is a clinopyroxene–plagioclase rock resembling the basaltic shergottites. Lithology A, however, is distinct from either the basaltic or the lherzolitic shergottites. It has a porphyritic texture consisting of

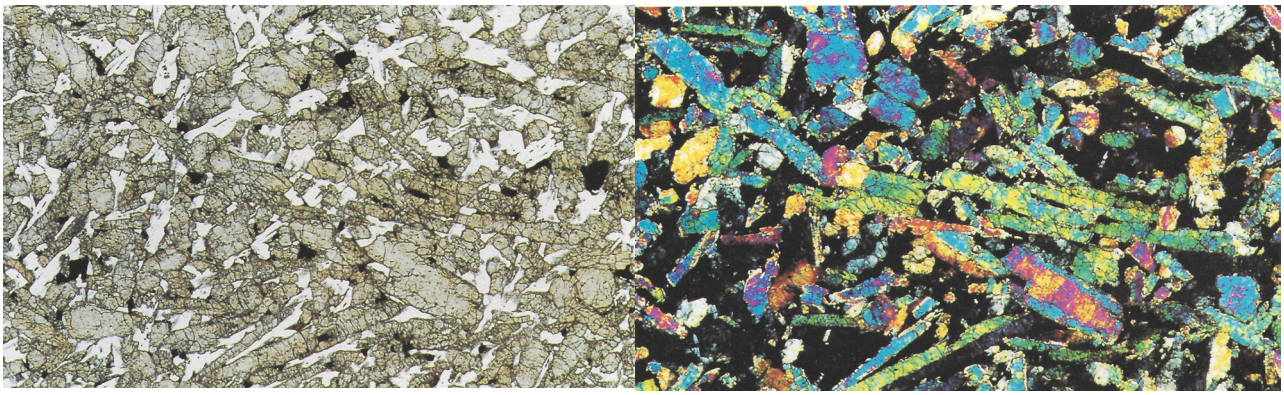

Fig. 7. Thin section of the Martian basaltic shergottite meteorite Zagami (after Norton 2002). (a) Viewed in transmitted light, large augite prisms are oriented along a preferred plane suggesting a cumulate. The white spaces between the grains is glassy maskelynite (shock melted plagioclase). The field of view is 9.15 mm across. (b) The same field of view at the same scale viewed under crossed polars. Note that the glass being isotropic has gone to extinction.

Fig. 8. End cut after first saw cut of EETA79001 Martian meteorite. It was found on January 13, 1980, in the Elephant Moraine area of Antarctica and weighed 7.9 kg. Sawing was done with a steel band saw without any lubricant. Vertical stripes are saw marks. The cube in the lower left corner is 1 cm^3. (Public domain photo courtesy of NASA.)

megacrysts of olivine, orthopyroxene, and chromite, in a finer-grained pigeonite–plagioclase groundmass. Four new shergottites (including Dar al Gani 476 and Sayh al Uhaymir 005 [fig. 6b]) consist entirely of olivine–porphyritic lithologies resembling EET79001 lithology A. These meteorites have been referred to by various terms, including basaltic shergottite (on the basis of plagioclase content), transitional shergottite, or mixed shergottite, but are currently called olivine–phyric shergottites to emphasize their differences from basaltic shergottites such as Shergotty or QUE94201 and avoid genetic implications (Goodrich 2002).

These olivine-phyric shergottites, which are now second in abundance, are thus porphyritic and contain olivine phenocrysts (sometimes megacrystic with sizes up to 2.5 mm), with later-crystallizing olivine, pyroxene, and maskelynite grains in the groundmass of ~0.25 mm (Balta et al. 2015; Basu Sarbadhikari et al. 2009, Basu Sarbadhikari, Babu, and Kumar 2017; Chen et al. 2015; Dunham et al. 2019; Goodrich 2002; Liu et al. 2016). However, in the last decade, numerous new finds and descriptions of this group of shergottites have shown that many of them have >10% plagioclase, and thus are not lherzolites sensu stricto (Walton et al. 2012). A recent discovery among the olivine-phyric shergottites is the presence of olivine phenocrysts that display concentric core-to-rim color differences in transmitted light, from amber to red brown to clear, for example, NWA 7042 (Izawa et al. 2015; Kizovski et al. 2020) and NWA10416 (Piercy et al. 2020; Vaci et al. 2020). While the alteration of olivine to iddingsite is not uncommon in the Martian meteorites (attributable to either low-temperature aqueous alteration on Mars or a similar process on the earth), this particular texture is distinct and has been suggested to be due to deuteric alteration (that is, reaction with magmatic fluids during crystallization) (Kizovski et al. 2020; Kuebler 2013; Vaci et al. 2020) or, alternatively, preferential terrestrial alteration (Piercy et al. 2020).

A newly recognized fourth type are the gabbroic shergottites, which contain cumulate pyroxene or plagioclase (Filiberto, Gross, and McCubbin 2016, 2018; Udry et al. 2017). Most shergottites studied before 2014 were fine-grained or diabasic, but new gabbroic specimens (apparently having crystallized at depth under the Martian surface) have now been recovered, including NWA6963 (pyroxene cumulate) and NWA7320 (plagioclase cumulate) (Filiberto et al. 2014, 2018; Hewins et al. 2019; Udry et al. 2017). Gabbroic shergottites are similar to basaltic shergottites but have a cumulate texture (with average grain size of cumulus grains of pyroxene or plagioclase >1 mm up to 5 mm in length) and geochemically show indications of crystal accumulation. They may be related to basaltic shergottites through magmatic processes. Hewins et al. (2019) describe NWA 10414,

which is a pigeonite-rich (73 mod.%) cumulate shergottite, with pigeonite grain lengths up to 4 mm. It is a distinctive shergottite, as it does not contain augite in any significant quantity.

Two more recently described shergottites, NWA7635 and NWA8159, are distinct in texture and crystallization age from the other shergottites, but which overlap in ejection age. Northwest Africa 7635, dated at 2.40±0.14 Ga, consists of phenocrysts of maskelynite (up to 20 µm in length), augite, and olivine in a maskelynite and pyroxene groundmass, but lacks pigeonite (Lapen et al. 2017). Northwest Africa 8159, originally described as an augite basalt (Herd et al. 2017a), is dated at 2.37±0.25 Ga, has an intergranular texture of plagioclase (partially converted to maskelynite), augite, and olivine (with grain sizes varying from 100 to 200 µm), and also lacks pigeonite. Orthopyroxene in this rock is the result of a subsolidus reaction (Herd et al. 2017a). Both rocks are depleted in LREE (light rare earth elements) with $(La/Yb)_{CI}$ ~0.1, but with a slightly different Dy/Lu ~0.84 (compared to Dy/Lu >1 in other shergottites). Nevertheless, the depleted nature, geochemistry, and radiogenic isotopic characteristics of NWA7635 suggest that it is derived from the same mantle sources as the depleted shergottites (Lapen et al. 2017).

Shergottites are geochemically classified based on their relative enrichment or depletion in incompatible trace elements (ITE). Those ITE compositions are believed to be largely inherited from their Martian mantle sources, which supposedly formed during silicate planetary differentiation and crystallization after a magma ocean phase very early in Mars' history (Borg and Draper 2003; Borg, Brennecka, and Symes 2016; Debaille et al. 2007, 2008). Postulated subsequent partial melting of these mantle sources would seem to have imparted distinct isotopic compositions to the shergottites derived from them (Borg et al. 2003; Lapen et al. 2017).

Coupled variations in ITE, including bulk rock rare earth elements (REEs), and radiogenic isotopic compositions ($^{147}Sm/^{144}Nd$ and $^{176}Lu/^{177}Hf$) are used to distinguish three groupings of shergottites. However, these groups include specimens that are either relatively enriched in ITE, depleted in ITE, or have compositions intermediate between the enriched and depleted groupings. Depleted shergottites have bulk REE compositions with $(La/Yb)_{CI}$ <0.3 and have relatively low initial $^{87}Sr/^{86}Sr$, $^{207, 206, 208}Pb/^{204}Pb$, and $^{187}Os/^{188}Os$ ratios, and relatively high initial $^{142, 143}Nd/^{144}Nd$ and $^{176}Hf/^{177}Hf$ ratios. Enriched shergottites have REE compositions relatively enriched in the more incompatible REE resulting in $(La/Yb)_{CI}$ >0.8. The relative enrichment in ITE is associated with relatively high initial $^{87}Sr/^{86}Sr$, $^{207, 206, 208}Pb/^{204}Pb$, and $^{187}Os/^{188}Os$ ratios, and relatively low initial $^{142,143}Nd/^{144}Nd$ and $^{176}Hf/^{177}Hf$ ratios. Intermediate shergottites, with $(La/Yb)_{CI}$ of 0.3–0.8, represent compositions intermediate between the enriched and depleted end-member compositions (Armytage et al. 2018; Borg et al. 2002, 2003, 2016; Brandon et al. 2000, 2012; Brennecka, Borg, and Wadhwa 2014; Combs et al. 2019; Debaille et al. 2008; Ferdous et al. 2017; Filiberto et al. 2012; Lapen et al. 2017; McSween 2015; Nyquist et al. 2001b; Paquet et al. 2021; Shafer et al. 2010b; Symes et al. 2008; Tait and Day 2018; Usui et al. 2010).

Nakhlites (Clinopyroxenites/Wehrlites)

Nakhlites and chassignites make up ~10% of the total Martian meteorite collection by number and 17% by mass and are highly distinctive Martian meteorites (Udry et al. 2020). At least 12 of the Martian meteorites are nakhlites and are clinopyroxenites or wehrlites, dominated by cumulus augite (clinopyroxene) and lesser olivine (average lengths between 0.3 and 0.4 mm). Their coarse-grained textures and the presence of exsolution lamellae in augite (which require slow cooling) suggest that they are cumulates. They also contain intercumulus interstitial material consisting of a microcrystalline groundmass (mesostasis) of radiating crystalline plagioclase, the orthopyroxene pigeonite, ferroaugite, titanomagnetite, fayalite, pyrite, troilite, chlorapatite, and rare silica-rich glass, as well as alteration phases such as iddingsite (Berkley, Keil, and Prinz 1980; Treiman 1986, 1990, 1993, 2005).

Initial studies have suggested that the nakhlites were emplaced as one magmatic body, often called a "cumulate pile" (Berkley, Keil, and Prinz 1980; Day et al. 2006; Mikouchi, Makishima, and Kurihara 2012). According to their mineral chemistry, nakhlites seem to represent different degrees of thermal processing, attributed to their relative position in the "cumulate pile" (Day et al. 2006; Jambon et al. 2002; Mikouchi et al. 2003; Sautter et al. 2002; Treiman 2005; Treiman and Irving 2008).

Nakhlites and chassignites have similar crystallization (~1.3 Ga) and ejection (~11 Ma) "ages" (Cohen et al. 2017; Nyquist et al. 2001b; Udry and Day 2018). The similar ejection "ages" suggest that they all likely originate from the same location on Mars. Nakhlites and chassignites have the same depleted radiogenic isotopic compositions, with high $^{142}Nd/^{144}Nd$ and $^{182}W/^{184}W$, and low $^{87}Sr/^{86}Sr$, but these compositions are distinct from shergottites (Carlson and Boyet 2009; Caro et al. 2008; Debaille et al. 2009; Foley et al. 2005; Nyquist et al. 2001b). Although the nakhlites and chassignites were previously suggested to be unrelated (Wadhwa and Crozaz, 1995), their compositions,

textures, and volatile-bearing minerals suggest that they may originate from the same volcanic system (McCubbin et al. 2013; Udry and Day 2018).

However, the recovery and study of new nakhlites and chassignites since 2014 (Balta et al. 2017; Corrigan, Velbel, and Vicenzi 2015; Krämer Ruggiu et al. 2020; Tomkinson et al. 2015; Udry and Day 2018) show greater variation in mineralogy and composition compared to the previously observed samples, suggesting that these rocks were emplaced as several shallow sills and/or lava flows, and may not represent a singular magmatic body. Textural evidence also suggests that the nakhlites have undergone different emplacement and/or shock histories (Corrigan, Velbel, and Vicenzi 2015; Griffin et al. 2019; Krämer Ruggiu et al. 2020; Udry and Day 2018).

Chassignites (Dunites)

The two chassignites, Chassigny (fig. 9) and NWA2737, are Martian dunites with similar textures and mineralogy, and their oxygen isotope compositions lie on the mass fractionation line defined by the other Martian meteorites (Beck et al. 2006; Franchi et al. 1999). They are olivine–chromite cumulates composed of millimeter-sized (average 0.6 mm in length) anhedral to subhedral olivine (90%) with a few vol% chromite inclusions and interstitial plagioclase, orthopyroxene, and phosphate minerals (Beck et al. 2006; Floran et al., 1978). Olivine is fairly uniform in composition but in NWA2737 it is more forsteritic (Fo79, cf. Fo69 in Chassigny). Melt inclusions in olivine contain hydrous amphibole, suggesting that the rocks formed under highly oxidizing conditions (Floran et al. 1978; Treiman et al. 2007). In hand specimens, Chassigny is green, whereas NWA2737 is black. In thin section, the olivine in NWA2737 appears brown due to shock-produced nanophase metallic iron particles (Pieters et al. 2008). Both chassignites are highly shocked rocks containing mosaicized olivine and diaplectic glass (maskelynite) (Langenhorst and Greshake 1999; Treiman et al. 2007).

As already noted above, chassignites have similar crystallization (~1.3 Ga) and ejection (~11 Ma) "ages" to nakhlites (Cohen et al. 2017; Nyquist et al. 2001b; Udry and Day 2018), although NWA2737 has a younger shock reset age of 160–190 Ma (Bogard 2011). The similar ejection "ages" suggest that they all likely originate from the same location on Mars. Chassignites have the same depleted radiogenic isotopic compositions as nakhlites, with high $^{142}Nd/^{144}Nd$ and $^{182}W/^{184}W$, and low $^{87}Sr/^{86}Sr$, but these compositions are distinct from shergottites (Carlson and Boyet 2009; Caro et al. 2008; Debaille et al. 2009; Foley et al. 2005; Nyquist et al. 2001b). Although the chassignites and nakhlites were previously suggested to be unrelated (Wadhwa and Crozaz 1995), their compositions, textures, and volatile-bearing minerals suggest that they may originate from the same volcanic system (McCubbin et al. 2013; Udry and Day 2018). The recently studied ferroan chassignite NWA8694 may represent the link between the nakhlites and chassignites based on bulk, mineral, and melt inclusion compositions (Hewins et al. 2020).

Allan Hills 84001 (Orthopyroxenite)

The notorious ALH84001 meteorite (fig. 10) is the only known Martian orthopyroxenite. Originally

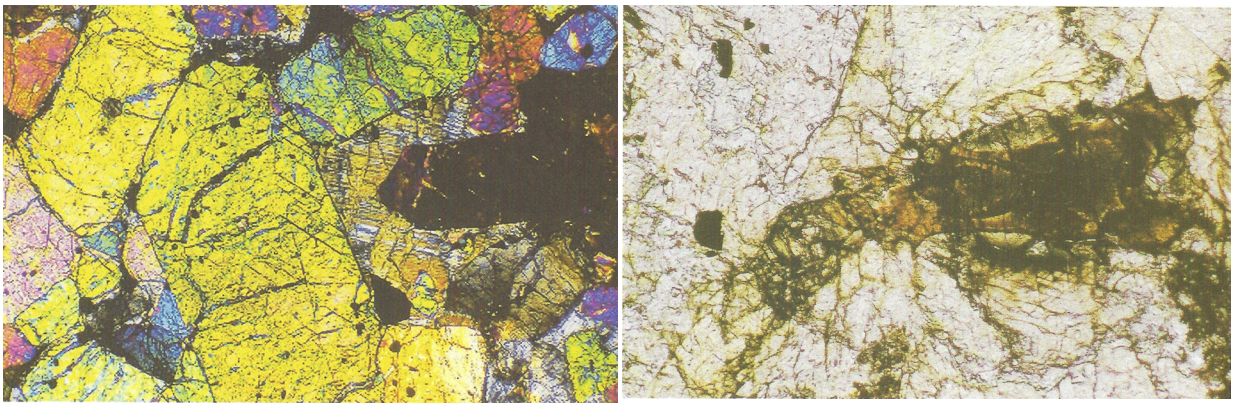

Fig. 9. The Chassigny meteorite was found at Chassigny in France on October 3, 1815, and its total mass was ~4 kg. (a) A thin section view under crossed polars (after Norton 2002). The colorful grains are all olivine, by far the most abundant mineral in Chassigny. The black grain on the right extending toward the center is a subhedral olivine crystal near extinction. Surrounding this extinguished olivine crystal are grains of orthopyroxene with typical multiple twinning and low interference colors. The small black grains scattered in the olivine are chromite. The field of view is 2.8 mm across. (b) Evidence of shock in Chassigny is seen in this thin section viewed under plane-polarized light (after Norton 2002). Visible is a large brown area of diaplectic glass of olivine composition, quenched from shock-melted olivine. Some fine, elongated olivine crystals grew from the shock-melt before the shock-melt quenched to glass. The clear white areas surrounding the glass is crystalline olivine and the black grains are chromite. The field of view is 0.7 mm across.

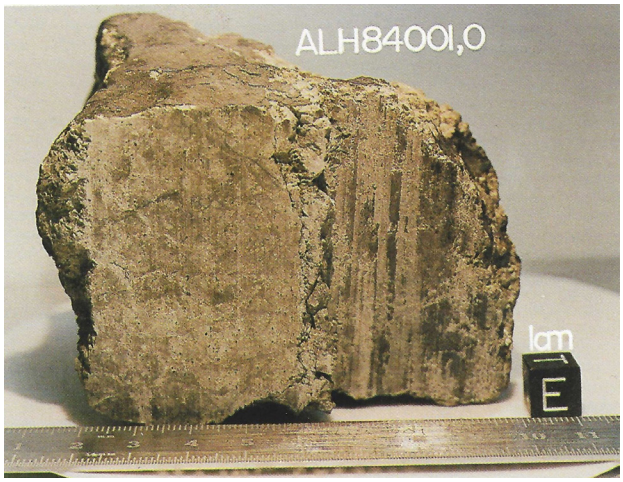

Fig. 10. Martian orthopyroxenite meteorite ALH84001 which was found on December 27, 1984, in the Alan Hills of Antarctica. This is a sliced portion from the 1.94 kg total mass measuring ~22 cm. The scale cube is 1 cm^3. (Public domain photo courtesy of the Johnson Space Center and NASA).

classified as a diogenite (that is, a pyroxenite of the HED clan [fig. 1]), it was shown by Mittlefehldt (1994) to be a unique Martian cumulate orthopyroxenite. While all other SNCs apparently have crystallization ages of a few hundred million years, the "age" of ALH 84001 is 4.09 ± 0.03 Ga (Lapen et al. 2010) and thus is presumed to be a fragment of the ancient Martian crust.

Allan Hills 84001 is a coarse-grained igneous cumulate orthopyroxenite. It consists mainly of large (up to 6 mm long) orthopyroxene crystals (96%) with 2% chromite, 1% plagioclase (maskelynite), and 0.15% phosphate (apatite), and with accessory minerals including olivine, augite, pyrite, and Fe-Mn-Mg carbonates, which contain magnetite, periclase, and hematite inclusions and organic matter (Barber and Scott 2003; Bradley, Harvey, and McSween 1996; McKay et al. 1996; Mittlefehldt 1994, Steele et al. 2007; Thomas-Keprta et al. 2009) (fig. 11). Its chemical composition is consistent with an origin as a cumulate orthopyroxenite (Barrat and Bollinger 2010; Mittlefehldt 1994). The carbonates are evidently younger and thus secondary, being "dated" at 3.95 Ga (Beard et al. 2013; Borg et al. 1999). This meteorite was apparently ejected from Mars 14.2 Ma ago (Eugster et al. 2002).

This meteorite became famous after McKay et al. (1996) declared that ALH84001 showed evidence of past life on Mars. This was due to the presence of possible indigenous organic molecules (polycyclic aromatic hydrocarbons) and putative bacteria nanofossils (fig. 12). Furthermore, the magnetite inclusions in carbonate globules (fig. 13) showed chemical and physical characteristics similar to magnetite formed by magnetobacteria on the earth

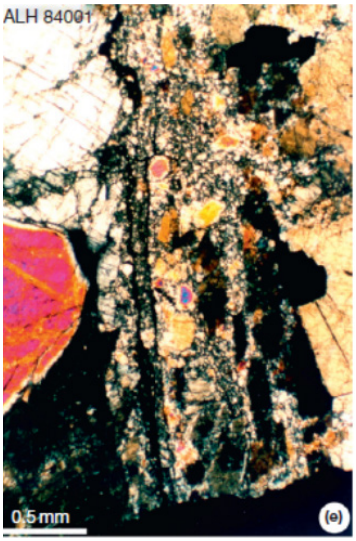

Fig. 11. Thin section photomicrograph in transmitted light with crossed polars of Martian meteorite ALH 84001, a coarse-grained orthopyroxenite containing abundant carbonates (after Krott et al. 2014). The large colorful crystals are all orthopyroxene (96% of the meteorite's mineral content), the center crystal showing signs of alteration. Other minerals include 2% chromite, 1% plagioclase (maskelynite), and 0.15% phosphate (apatite), and with accessory minerals including olivine, augite, pyrite, and Fe-Mn-Mg carbonates, which contain magnetite, periclase, and hematite inclusions and organic matter.

(Thomas-Keprta et al. 2000). However, several studies demonstrated that these features are likely to be abiotic (Anders et al. 1996; Treiman 2019). A subsequent study by Koike et al. (2020) presented evidence for ancient N-bearing organic compounds preserved in secondary carbonate in ALH 84001, likely formed through neutral water at ~25°C (Halevy, Fischer, and Eiler 2011; Valley et al. 1997).

Fig. 12. High resolution SEM (scanning electron microscope) image within a carbonate globule in Martian meteorite ALH84001 reveals a tiny bacteria-like structure 100 mm in length that was reported as maybe the remnants of early Martian bacteria. These structures are equivalent in size to the smallest bacteria found in 3.5 Ga rocks on earth. (Public domain photo courtesy of the Johnson Space Center and NASA).

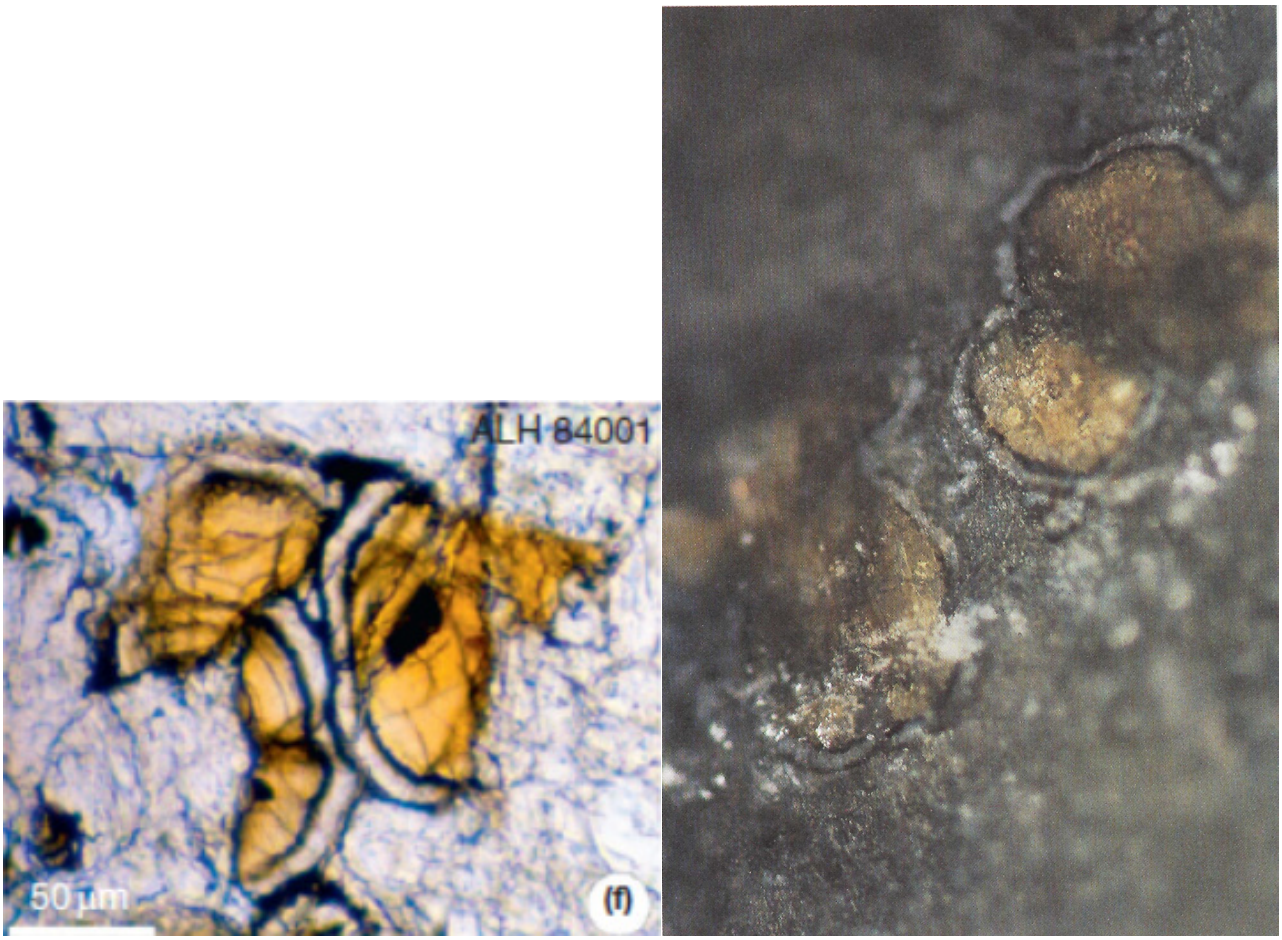

Fig.13. Thin section photomicrographs in transmitted light with crossed polars of Martian meteorite ALH 84001, a coarse-grained orthopyroxenite containing abundant carbonate globules. (a) After Krott et al. 2014. (b) Public domain photo courtesy of the Johnson Space Center and NASA. Compounds rich in magnesium and iron (black) encircle the carbonate globules (yellow).

The magnetite may have formed through shock metamorphism from the Fe-carbonates during rapid temperature increase along carbonate grain faces and edges (Treiman 2003). In spite of the lack of convincing evidence for ancient life in this rock, the conditions seemingly recorded by the carbonates are suggestive to uniformitarians of a habitable environment during their supposed Noachian period on Mars (McSween 2019; Treiman 2019).

Polymict Regolith Breccia NWA 7034 and Its Pairs

The polymict regolith breccia Northwest Africa 7034 (fig. 14) and its 16 paired meteorites totaling a mass of ~941 g, including NWA 7533, are perhaps the most significant discovery among the Martian meteorites in recent years. These rocks show similar reflectance spectra and bulk composition to the average crust (Agee et al. 2013; Cannon, Mustard, and Agee 2015; Humayun et al. 2013).

The NWA7034 meteorite group contains a variety of igneous clasts that include basalt, mugearite, trachyandesite, norite, gabbro, and monzonite (area sizes between 0.04 and 3 mm^2), some of which originate from distinct parent melts (Hewins et al. 2017; Santos et al. 2015; Wittmann et al. 2015). They also contain impact melt clasts (Wittmann et al. 2015), at least one of which has the same composition as the surface Gusev basalt Humphrey (Udry, Balta, and McSween 2014). The clasts in NWA7034 apparently represent the conventionally-named early Noachian lithified portion of the Martian regolith, which has undergone hydrothermal activity (McCubbin et al. 2016; Nyquist et al. 2016). The variability in rock type and compositions of the different clasts observed in this breccia, including some sedimentary clasts (Wittmann et al., 2015), show that there are many lithologies in this meteorite not previously represented in the other Martian meteorites.

NWA7034 igneous clasts contain the oldest dated Martian minerals, which are zircons >4300 Ma up to 4476 ± 1 Ma, with a minimum source model age of 4547 Ma, suggesting the formation of an andesitic primordial crust, as the postulated last stage of magma ocean crystallization (Bellucci et al. 2018; Bouvier et al. 2018; Hu et al. 2019; McCubbin et al. 2016; Nyquist et al. 2016). The fact that some

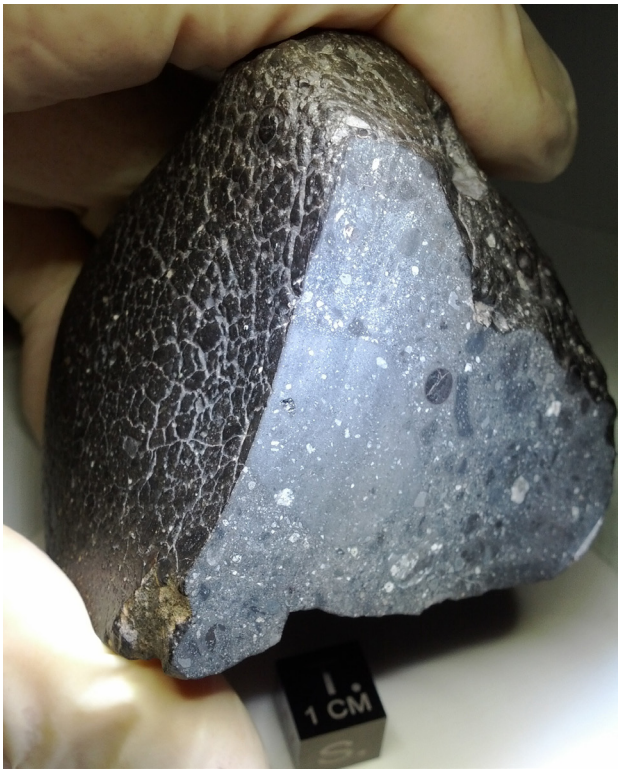

Fig. 14. Designated Northwest Africa (NWA) 7034, and nicknamed "Black Beauty," this Martian meteorite is classified as a polymict regolith breccia. It was found in the Sahara Desert during 2011 and weighs approximately 11 ounces (320 grams). The cube beneath it is 1 cm^3. (Public domain photo courtesy of NASA).

alkaline clasts have crystallization ages of ~4.4 Ga appears to show that alkaline magmatism occurred early in Martian history.

This polymict regolith breccia likely assembled by pyroclastic eruption(s) and/or impact event(s), then evidently underwent lithification represented by a thermal event at ~1,500–1,100 Ma (Bridges et al. 2017; Goderis et al. 2016; MacArthur et al. 2019; McCubbin et al. 2016). Alternatively, Cassata et al. (2018) proposed that contact metamorphism occurred between ~1,500 and 1,200 Ma based on $^{40}Ar/^{39}Ar$ ages, with brecciation and lithification happening at ≤225 Ma. The regolith breccia was apparently launched from Mars between ~5 and 9 Ma ago and underwent relatively little shock metamorphism (Cartwright et al. 2014; Wittmann et al. 2015).

The Radioisotope Dating of the Martian Meteorites

To thoroughly investigate the radioisotope dating of the Martian meteorites all the copious relevant literature was searched for reported radioisotope dates using all the major methods. While it cannot be claimed that all the papers, articles and abstracts which have ever been published containing radioisotope dating results for sixty-three (63) of these Martian meteorites have thus been obtained, the cross-checking undertaken between these publications does indicate the data set obtained is very comprehensive.

The reported radioisotope dates obtained for each of the five types of Martian meteorites (45 shergottites, 12 nakhlites, two chassignites, one orthopyroxenite, and three polymict regolith breccias) were tabulated in lists for each meteorite according to the different radioisotope dating methods used—shergottites (table 1), nakhlites (table 2), chassignites (table 3), orthopyroxenite (table 4,) and polymict regolith breccias (table 5). Whether the whole rock, a mineral, or minerals were radioisotope dated, the category of age whether model, plateau, isochron or discordia, and the published sources are also indicated, along with any relevant explanatory notes.

The tabulated data were then plotted on histogram diagrams for each of the five types of Martian meteorites displaying the frequency (numbers of ages) for the various small age ranges—shergottites (fig.15), nakhlites (fig. 16), chassignites (fig. 17), orthopyroxenite (fig. 18), and polymict regolith breccias (fig. 19).

Discussion

All the major radioisotope dating methods have been used to obtain ages for these Martian meteorites—K-Ar and Ar-Ar, Rb-Sr, Sm-Nd, U-Th-Pb, Lu-Hf and Re-Os (tables 1–5). The K-Ar method provided both model and isochron ages, whereas the more popular, dominantly-used Ar-Ar method, due to supposedly being more accurate, yielded plateau and isochron ages via step-heating of whole rocks and minerals, primarily plagioclase but sometimes pyroxene. The next frequently used Rb-Sr method only provided isochron ages based on whole rocks and minerals separates, primarily plagioclase and pyroxene, but sometimes glass, olivine (when present), opaques, leachates, and/or residues. The Ar-Ar and Rb-Sr methods were also used on the carbonates in the orthopyroxenite ALH 84001 (table 4) and on iddingsite in the nakhlite Lafayette (table 2). Similarly, the Sm-Nd method produced isochron ages using whole rocks, plagioclase, pyroxene, olivine (when present), opaques, leachates and/or residues, often being obtained on the same fractions of a meteorite from which the Rb-Sr isochron ages were obtained.

In contrast, while the popular U-Th-Pb methods were also used for some meteorites on whole rock samples and mineral separates (primarily pyroxene and plagioclase, and sometimes olivine, oxides, leachates and/or residues), it has been often used to target zircon ($ZrSiO_4$), baddeleyite (ZrO_2) and phosphate grains, and carbonates in the

Table 1. Radioisotope ages of Shergottites.

Sample	Method	Reading	Err +/-	Note	Source	Type
BASALTIC						
SHERGOTTY						
Whole rock	K-Ar	580	50		Geiss and Hess 1958	model age
Plagioclase	K-Ar	170			Eugster, Polnau, and Terribilini 1997	K-Ar isochron age
Three points—whole rock, pyroxene, plagioclase + glass	K-Ar	196	40		Terribilini et al. 1998	K-Ar isochron age
Plagioclase	Ar-Ar	254	10		Bogard, Husain, and Nyquist 1979	plateau age
Whole rock	Ar-Ar	167			Bogard and Garrison 1999	plateau age
Whole rock	Ar-Ar	360	50		Shankar et al. 2008	plateau age
Whole rock	Ar-Ar	391	11	22–75% ^{39}Ar release	Korochantseva et al. 2009	plateau age
Plagioclase	Ar-Ar	161	9		Cohen et al. 2023	isochron age
Eight points—whole rock, plagioclase, pyroxene	Rb-Sr	164	12		Wooden et al. 1979	isochron age
Ten points—whole rock, glass, pyroxene	Rb-Sr	165	11		Nyquist et al. 1979	isochron age
Nine points—whole rock, pyroxene, glass	Rb-Sr	186	11		Shih et al. 1982	isochron age
Six points—whole rock, leachates and residues	Rb-Sr	360	12		Jagoutz and Wänke 1986	isochron age
Four points—plagiclase, whole rock and leachates	Rb-Sr	167	4		Jagoutz and Wänke 1986	isochron age
Four points—plagiclase, whole rock and leachates	Rb-Sr	167			Jagoutz 1991	isochron age
Phosphates and whole rocks, leachates	Rb-Sr	360			Jagoutz 1991	isochron age
Ten points—whole rock and pyroxene leachates and residues	Sm-Nd	147	20		Jagoutz and Wänke 1986	isochron age
Twelve points—whole rock and pyroxene, plus leachates and residues	Sm-Nd	360	16		Jagoutz and Wänke 1986	isochron age
Whole rock and minerals	Sm-Nd	170	41		Blichert-Toft et al. 2007	isochron age
Five points - whole rock, plagioclase, pyroxenes	Sm-Nd	620	171		Shih et al. 1982	isochron age
Four points—whole rock, plagioclase, pyroxenes	Sm-Nd	172	40		Bouvier et al. 2008	isochron age

Whole rock and minerals	Lu-Hf	187	89		Blichert-Toft et al. 2007	isochron age
Four points—whole rock, plagioclase, pyroxenes	Lu-Hf	188	91		Bouvier et al. 2008	isochron age
Four points—hree leachates, residue	U-Pb	200	4		Chen and Wasserburg 1986	U-Pb isochron age
Seven points—plagioclae, pyroxene, whole rock, leachates, residues	U-Pb	437	36		Chen and Wasserburg 1986	Th-Pb isochron age
Five points—plagioclase, pyroxene, whole rock, leachates	U-Pb	600	20		Chen and Wasserburg 1986	U-Pb isochron age
Phosphates	U-Pb	217	110		Sano et al. 2000	U-Pb isochron age
Phosphates	U-Pb	189	83		Sano et al. 2000	Th-Pb isochron age
Five points—whole rock, plagioclase, pyroxenes	U-Pb	4100			Bouvier et al. 2008	Pb-Pb isochron age
ZAGAMI						
Feldspars	Ar-Ar	242			Bogard and Garrison 1999	plateau age
Plagioclases	Ar-Ar	209	2	uncorrected for ^{36}Ar	Bogard and Park 2007	isochron age
Plagioclases	Ar-Ar	223	6	3–100% ^{39}Ar release	Bogard and Park 2007	isochron age
Plagioclase (coarse-grained)	Ar-Ar	217	2	3–97% ^{39}Ar release	Bogard and Park 2008	isochron age
Whole rock, pyroxene, plagioclase separates	Ar-Ar	225	25		Korochantseva et al. 2009	plateau ages
Plagioclase grain	Ar-Ar	240	28	weighted mean high T	Park et al. 2013a	plateau age
Plagioclase grain	Ar-Ar	240	24	weighted mean high T	Park et al. 2013a	plateau age
Plagioclase grain	Ar-Ar	216	46	weighted mean high T	Park et al. 2013a	plateau age
Plagioclase grain	Ar-Ar	205	27		Park et al. 2013a	isochron age
Plagioclase grains	Ar-Ar	261	16	pooled data	Park et al. 2013a	isochron age
K-rich melt—four samples	Ar-Ar	187	12	most radiogenic samples	Park et al. 2013a	isochron age
Plagioclase	Ar-Ar	189	56		Cohen et al. 2023	isochron age
Seven points—whole rock, pyroxene, plagioclase	Rb-Sr	180	4		Shih et al. 1982	isochron age
Fine-grained whole rock portions	Rb-Sr	186	5		Nyquist et al. 1995	isochron age
Coarse-grained whole rock portions	Rb-Sr	183	6		Nyquist et al. 1995	isochron age
Ten points—whole rock, plagioclase, pyroxenes, opaques	Rb-Sr	166	6		Borg, Edmunson, and Asmeron 2005	isochron age

Fine-grained whole rock portions	Rb-Sr	166	12		Nyquist, Shih, and Reese 2006	isochron age
Coarse-grained whole rock portions	Rb-Sr	177	9		Nyquist, Shih, and Reese 2006	isochron age
Four points—fine-grained whole rock, pyroxene, plagioclase	Rb-Sr	174	14		Nyquist 2006	isochron age
Four points—coarse-grained whole rock, pyroxene, plagioclase	Rb-Sr	163	19		Nyquist 2006	isochron age
Eleven points—dark mottled lithology	Rb-Sr	167	18		Nyquist, Shih and Reese 2010	isochron age
Twelve points—fine-grained lithology	Rb-Sr	179	18		Nyquist, Shih, and Reese 2010	isochron age
Eleven points—coarse-grained lithology	Rb-Sr	167	12		Nyquist, Shih, and Reese 2010	isochron age
Seven points—whole rock, pyroxene, phosphate	Sm-Nd	116	47		Shih et al. 1982	isochron age
Fine and coarse grained portions combined	Sm-Nd	180	7		Nyquist et al. 1995	isochron age
Twelve points—whole rock, plagioclase, pyroxenes, olivine, opaques	Sm-Nd	166	12		Borg et al. 2005	isochron age
Whole rock and minerals	Sm-Nd	155	6		Bouvier et al. 2005a	isochron age
Three points—whole rock, plagioclase, pyroxene	Sm-Nd	155	9		Bouvier et al. 2005b	isochron age
Three points—fine-grained pyroxene, plagioclase	Sm-Nd	198	21		Nyquist 2006; Nyquist, Shih, and Reese 2010	isochron age
Four points—coarse-grained whole rock, pyroxene, plagioclase	Sm-Nd	163	7		Nyquist 2006, Nyquist, Shih and Reese 2010	isochron age
Nine points—dark mottled lithology	Sm-Nd	166	29		Nyquist, Shih and Reese 2010	isochron age
Eight points—fine-grained lithology	Sm-Nd	151	34		Nyquist, Shih, and Reese 2010	isochron age
Nine points—coarse-grained lithology	Sm-Nd	177	18		Nyquist, Shih, and Reese 2010	isochron age
Whole rock and minerals	Lu-Hf	190	11		Bouvier et al. 2005a	isochron age
Three points—whole rock, plagioclase, pyroxene	Lu-Hf	185	36		Bouvier et al. 2005b	isochron age

Three points—leachates and residue	U-Pb	230	5		Chen and Wasserburg 1986	U-Pb isochron age
Three points—leachate, residue, whole rock	U-Pb	229	8		Chen and Wasserburg 1986	Th-Pb isochron age
Two points—plagioclase, pyroxene, residues	U-Pb	186	13	^{238}U-^{206}Pb isochron	Borg, Asmeron, and Edmunson 2003	U-Pb isochron age
Two points—plagioclase, pyroxene, residues	U-Pb	225	180	^{235}U-^{207}Pb isochron	Borg, Asmeron and Edmunson 2003	U-Pb isochron age
Five points—whole rocks, plagioclase, pyroxenes	U-Pb	163	4	U-Pb concordia lower inercept	Borg, Asmeron, and Edmunson 2003	U-Pb isochron age
Five points—whole rocks, plagioclase, pyroxenes	U-Pb	4550	2	U-Pb concordia upper inercept	Borg, Asmeron, and Edmunson 2003	U-Pb isochron age
Five points—plagioclase, pyroxenes	U-Pb	156	6		Borg, Asmeron, and Edmunson 2005	U-Pb isochron age
Whole rock, pyroxene, plagioclase, residues	U-Pb	4044	1		Bouvier et al. 2005a	Pb-Pb isochron age
Four points—whole rock, plagioclase, pyroxene	U-Pb	4808	17		Bouvier et al. 2005b	Pb-Pb isochron age
Baddeleyite	U-Pb	70	35		Herd, Simonetti, and Peterson 2007	U-Pb isochron age
Baddeleyites	U-Pb	183	7	Tera-Wasserburg concordia	Zhou et al. 2013	U-Pb isochron age
Phosphates	U-Pb	153	81	Tera-Wasserburg concordia	Zhou et al. 2013	U-Pb isochron age
Baddeleyites - five	U-Pb	183	9	Tera-Wasserburg discordia	Staddon et al. 2021; Zhou et al. 2013	U-Pb isochron age
LOS ANGELES						
Whole rock	Ar-Ar	329	12	14 extractions at high T	Garrison and Bogard 2001	isochron age
Plagioclase	Ar-Ar	170	14	0.04-100% ^{39}Ar release	Bogard, Park, and Garrison 2009	isochron age
Plagioclase	Ar-Ar	170	47		Cohen et al. 2023	isochron age
Nine points—whole rock, plagioclase, pyroxene, residues	Rb-Sr	165	11		Nyquist et al. 2000	isochron age
Eight point—whole rocks, pyroxenes, residues, leachates	Rb-Sr	165	7		Nyquist et al. 2018	isochron age
Six points—whole rocks, pyroxenes, residues, leachates	Rb-Sr	158	15		Nyquist et al. 2018	isochron age
Nine points—whole rock, plagioclase, pyroxene, residues	Sm-Nd	172	8		Nyquist et al. 2001b	isochron age

Whole rock and minerals	Sm-Nd	179	5		Blichert-Toft et al. 2007	isochron age
Four points—whole rock, plagioclase, pyroxenes	Sm-Nd	181	13		Bouvier at al. 2008	isochron age
Fourteen points—whole rocks, pyroxenes, residues, leachates	Sm-Nd	172	8		Nyquist et al. 2018	isochron age
Ten points—whole rocks, pyroxenes, residues, leachates	Sm-Nd	173	24		Nyquist et al. 2018	isochron age
Whole rock and minerals	Lu-Hf	158	14		Blichert-Toft et al. 2007	isochron age
Three points—whole rock, plagioclase, pyroxene	Lu-Hf	159	42		Bouvier at al. 2008	isochron age
Six points—whole rock, plagioclase, pyroxene	U-Pb	4100			Bouvier at al. 2008	Pb-Pb isochron age
Phosphates—ninety-three analyses	U-Pb	174	5	Tera-Wasserburg discordia	McFarlane and Spray 2022	U-Pb isochron age
EETA79001B						
Five points—whole rock, pyroxene, plagiocalse	Rb-Sr	185	25		Wooden et al. 1982	isochron age
Seven points–whole rock, plagioclase, pyroxene	Rb-Sr	177	12		Nyquist et al. 1986	isochron age
Five points–whole rock, pyroxene	Rb-Sr	174	3		Nyquist et al. 2001a	isochron age
Seven points –whole rock, plagioclase, pyroxene	Sm-Nd	169	23		Nyquist et al. 2001a	isochron age
QUE94201						
Feldspars	Ar-Ar	730	100		Bogard and Garrison 1999	plateau age
Ten points–whole rock, plagioclase, pyroxene, opaques, glass	Rb-Sr	327	12		Borg et al. 1997	isochron age
Nine points–whole rock, plagioclase, pyroxene, opaques, glass	Sm-Nd	327	19		Borg et al. 1997	isochron age
Twelve points–whole rock, plagioclase, pyroxenes, oxides, phosphates	U-Pb	4326	32		Gaffney, Borg, and Connelly 2007	Pb-Pb isochron age
NWA5990						
Four points–plagioclase, pyroxene, opaques, residues	Rb-Sr	389	12		Shih et al. 2011b	isochron age
Ten points–whole rock, plagioclase, pyroxene, olivine, resdiues, leachates	Sm-Nd	402	22		Shih et al. 2011b	isochron age

NWA480						
Eleven points–whole rocks, plagioclase, pyroxene, leachates	U-Pb	4092	74		Bouvier, Blichert-Toft, and Alberède 2009	Pb-Pb isochron age
NWA856						
Four points–whole rock, plagioclase, pyroxene, residues	Rb-Sr	150	32		Brandon et al. 2004	isochron age
Seven points–whole rocks, pyroxenes, leachates, residues	Rb-Sr	162	15		Ferdous et al. 2017	isochron age
Four points–whole rock, pyroxene, residues	Sm-Nd	186	24		Brandon et al. 2004	isochron age
Nine points–whole rocks, pyroxenes, plagioclases, residues, leachates	Sm-Nd	163	6		Ferdous et al. 2017	isochron age
Baddeleyite	U-Pb	186	12		Misawa and Yamaguchi 2007	U-Pb isochron
NWA1460						
Plagioclase	Ar-Ar	360	6		Bogard and Park 2007	plateau age
Plagioclase	Ar-Ar	346	6		Bogard and Park 2007	isochron age
Plagioclase	Ar-Ar	360	6	7 extractions	Nyquist et al. 2009	plateau age
Plagioclase	Ar-Ar	353	16	12 extractions	Nyquist et al. 2009	isochron age
Plagioclase	K-Ar	358	3		Nyquist et al. 2009	model age
Nine points–whole rock, plagioclase, pyroxene, and magnetic "opaques"	Rb-Sr	336	14		Nyquist et al. 2006a	isochron age
Sixteen points–whole rock, plagioclase, pyroxene, opaques, fines, leachates	Rb-Sr	336	15		Nyquist et al. 2009	isochron age
Nine points–whole rock, plagioclase, pyroxene, and magnetic "opaques"	Sm-Nd	345	14		Nyquist et al. 2006a	isochron age
Sixteen points–whole rock, plagioclase, pyroxene, opaques, fines, leachates	Sm-Nd	350	16		Nyquist et al. 2009	isochron age
NWA2626						
Pyroxene (10 grains), plagioclase (3 grains)	Ar-Ar	514	24	laser step-heated	Lindsay et al. 2012	isochron age
Pyroxene (10 grains), plagioclase (3 grains)	Ar-Ar	500	14	laser step-heated	Lindsay et al. 2012	plateau age

NWA2975						
Plagioclase	Ar-Ar	366	3	18-100% ^{39}Ar release	Bogard, Park, and Garrison 2009	isochron age
Plagioclase–seven grains	Ar-Ar	314	7	weighted average	Lindsay et al. 2013	plateau age
Plagioclase–seven grains	Ar-Ar	296	14	corrected for ^{36}Ar	Lindsay et al. 2013	isochron age
Whole rock	Ar-Ar	184	17	corrected for ^{36}Ar step-wise	Cassata and Borg 2016	isochron age
Whole rock and minerals	Sm-Nd	177	11		Bogard, Park and Garrison 2009	isochron age
NWA3171						
Plagioclase	Ar-Ar	225	4		Park and Bogard 2007	isochron age
Plagioclase	Ar-Ar	232	7	20-100% ^{39}Ar release	Bogard, Park and Garrison 2009	isochron age
Whole rock and minerals	Sm-Nd	193	21		Bogard, Park and Garrison 2009	isochron age
Baddeleyite	U-Pb	171	129		Herd, Simonetti, and Peterson 2007	U-Pb isochron age
RBT04262						
Plagioclase	Ar-Ar	171	8		Park et al. 2013c	isochron age
Plagioclase	Ar-Ar	228	7		Park et al. 2013c	plateau age
Plagioclases–five grains	Ar-Ar	236	3	weighted average	Park et al. 2014	plateau age
Plagioclases–six grains	Ar-Ar	227	4		Park et al. 2013c, 2014	isochron age
Six points–whole rock, plagioclase, pyroxene, olivine, opaques	Rb-Sr	167	6		Shih, Nyquist, and Reese 2009	isochron age
Eleven points–whole rock, plagioclase, pyroxene, olivine, residues, leachates	Sm-Nd	174	14		Shih, Nyquist, and Reese 2009	isochron age
Four points–pyroxene, olivine, plagioclase, chromite	Lu-Hf	225	21		Lapen et al. 2008	isochron age
Ten points–whole rock, pyroxene, olivine, plagioclase, leachates	U-Pb	4092	74		Bouvier, Blichert-Toft, and Alberède 2009	Pb-Pb isochron age
NWA10299						
Baddeleyite	U-Pb	196	11	Tera-Wasserburg plot	Sheen et al. 2024	Pb-Pb isochron age
NWA12919						
Baddeleyite	U-Pb	188	11	Tera-Wasserburg plot	Sheen et al. 2024	Pb-Pb isochron age
JaH479						
Baddeleyite	U-Pb	210	9	Tera-Wasserburg plot	Sheen et al. 2024	Pb-Pb isochron age
NWA4468						
Whole rock	Ar-Ar	188	17	corrected for ^{36}Ar step-wise	Cassata and Borg 2016	isochron age

Two points–whole rock, plagioclase, residues	Rb-Sr	187	5		Marks et al. 2010	isochron age
Three points–whole rock, leachate, residue	Sm-Nd	150	29		Borg, Gaffney, and De Paulo 2008	isochron age
Three points–whole rock, oxides, residue	Lu-Hf	179	27		Lapen et al. 2009	isochron age
NWA4880						
Plagioclase–three samples	Ar-Ar	700	140	unweighted average	Turrin et al. 2018	isochron age
Three points–whole rock, plagioclases	Lu-Hf	716	81		Righter, Lapen, and Irving 2018	isochron age
NWA5298						
Baddeleyites–three grains	U-Pb	187	33	least disturbed U-Pb ages	Moser et al. 2013	Pb-Pb isochron age
Baddeleyites–three grains (five spot analyses)	U-Pb	175	30	weighted mean	Darling et al. 2016	U-Pb isochron age
NWA7635						
Six points–whole rock, fines, olivine, pyroxene, phosphate, leachates	Sm-Nd	2326	130		Righter et al. 2014	isochron age
Seven points–whole rocks, pyroxene, olivine, phosphates, leachates, residues	Sm-Nd	2403	140		Lapen et al. 2017	isochron age
Five points–whole rock and mineral strong-acid leachates	U-Pb	4390	16		Andreasen et al. 2014	Pb-Pb isochron age
NWA8159						
Shock melt (plagioclase-pyroxene) glass–step-heated	Ar-Ar	2150	100		Herd et al. 2017a	isochron age
Six points–Whole rocks, fine-grained bulk rock, residues	Sm-Nd	2370	250		Herd et al. 2017a	isochron age
Forty-nine analyses–plagioclase, pyroxene, phosphate, shock melt glass	U-Pb	3370	2100		Bellucci et al. 2020	Pb-Pb isochron age
Forty-nine analyses–plagioclase, pyroxene, phosphate, shock melt glass	U-Pb	2400	860		Bellucci et al. 2020	Pb-Pb model age
NWA8653						
Feldspathic intergrowth and plagioclase	U-Pb	4135	960		Wu et al. 2021	Pb-Pb iscohron age
Baddeleyite–eleven analyses	U-Pb	186	10	weighted mean	Wu et al. 2021	U-Pb age
Baddeleyite–eleven analyses	U-Pb	166	260		Wu et al. 2021	Pb-Pb iscohron age

NWA8679						
Baddeleyites–ten	U-Pb	220	23	Tera-Wasserburg discordia	Staddon et al. 2021	U-Pb isochron age
NWA7257						
Baddeleyites–seventeen	U-Pb	195	15	Tera-Wasserburg discordia	Staddon et al. 2021	U-Pb isochron age
LAR06319						
Whole rock	Ar-Ar	163	13		Park et al. 2013c	isochron age
Nine points–whole rock, pyroxene, olivine, plagiocalse, leachates, residues	Rb-Sr	207	14		Shih, Nyquist, and Reese 2009	isochron age
Nine points–whole rock, pyroxene, olivine, plagiocalse, leachates, residues	Sm-Nd	190	26		Shih, Nyquist, and Reese 2009	isochron age
Seven points–whole rock, pyroxene, olivine, plagioclase, leachates	Sm-Nd	183	12		Shafer et al. 2010a, b	isochron age
Five points–bulk rock, plagioclase, pyroxene	Lu-Hf	197	29		Shafer et al. 2009	isochron age
Five points–bulk rock, plagioclase, pyroxene	Lu-Hf	197	29		Shafer et al. 2010b	isochron age
LAR12011						
Six points–whole rocks, plagioclase, pyroxene, olivine	Sm-Nd	183	12		Righter, Andreason and Lapen 2015	isochron age
Four points–whole rocks, plagioclase, pyroxene	Lu-Hf	197	29		Righter, Andreason and Lapen 2015	isochron age
Dho378						
K-enriched pahses	Ar-Ar	143	4	8 extractions	Park and Bogard 2006	isochron age
Four points–whole rock, plagioclase, residues, glasses	Rb-Sr	159			Nyquist et al. 2018	isochron age
Whole rock and minerals	Sm-Nd	157	24		Nyquist et al. 2006b	isochron age
Four points–whole rocks, pyroxenes, residues	Sm-Nd	157	23		Nyquist et al. 2018	isochron age
KG002						
Phosphates–nine grains	U-Pb	395	240	T-W concordia, lower intercept	Roszjar et al. 2019	U-Pb isochron age
OLIVINE-PHYRIC						
EETA79001A						
Whole rock	Ar-Ar	2035			Bogard and Garrison 1999	plateau age
Four points–whole rock, plagioclase, pyroxene	Rb-Sr	173	10		Nyquist et al. 1986; Wooden et al. 1982	isochron age
Whole rock	Rb-Sr	160			Jagoutz 1991	isochron age

Whole rock	Sm-Nd	240	150		Wooden et al. 1982	isochron age
Four points–whole rocks	Re-Os	164	12		Brandon et al. 2000, 2012	isochron age
Five points–leachates, residue, whole rock	U-Pb	150	15		Chen and Wasserburg 1986	U-Pb isochron age
Four points–leachates, residue, whole rock	U-Pb	170	36		Chen and Wasserburg 1986	Th-Pb isochron age
DaG476						
Plagioclase–step heated	Ar-Ar	619	31	36–71% ^{39}Ar release	Park, Bogard, and Garrison 2008	isochron age
Pyroxene–step heated	Ar-Ar	408	172	25–83% ^{39}Ar release	Park, Bogard, and Garrison 2008	isochron age
Plagioclase–step heated	Ar-Ar	1000			Bogard, Park, and Garrison 2009	plateau age
Plagioclase	Ar-Ar	481	24		Cohen et al. 2023	isochron age
Eight points–whole rock, olivine, plagiocalse, pyroxenes, leachates	Sm-Nd	474	11		Borg et al. 2000; Borg et al. 2003	isochron age
Four points–whole rock leachates and residues, olivine	Sm-Nd	775	25		Jagoutz et al. 1999; Jagoutz and Jotter 2000	isochron age
SaU094 / 005						
Whole rock	Ar-Ar	2000			Bogard, Park, and Garrison 2009	plateau age
Olivine–three extractions	Ar-Ar	885	66	83% ^{39}Ar release	Korochantseva et al. 2009	plateau age
Plagioclase	Ar-Ar	437	24		Cohen et al. 2023	isochron age
Nine points–whole rocks, pyroxenes, residues, leachates	Sm-Nd	445	18		Shih, Nyquist, and Reese 2007	isochron age
Dho019						
Plagioclase	Ar-Ar	707	16		Bogard, Park and Garrison 2009	isochron age
Plagioclase	Ar-Ar	642	72	9–100% ^{39}Ar release	Korochantseva et al. 2009	plateau age
Four points–whole rock, plagioclase, pyroxene	Rb-Sr	525	56		Borg et al. 2001a	isochron age
Eleven points–whole rock, pyroxenes, plagiocalse, olivine, leachates, residues	Sm-Nd	575	7		Borg et al. 2001a	isochron age
Whole rocks and minerals	Sm-Nd	575	7		Borg and Drake 2005	isochron age
NWA1068						
Five points–whole rock, pyroxene, olivine, plagioclase, residues, leachates	Rb-Sr	166	37		Shih et al. 2009	isochron age
Nine points–whole rock, pyroxene, olivine, residues, leachates	Sm-Nd	185	11		Shih et al. 2003	isochron age

Four points–whole rock and leachates	U-Pb	4092	74		Bouvier, Blichert-Toft, and Albarède 2009	Pb-Pb isochron age
NWA1195						
Five points–whole rocks, pyroxenes, olivine	Sm-Nd	348	19		Symes et al. 2005	isochron age
Five points–whole rocks, pyroxenes, olivine, residues	Sm-Nd	347	13		Symes et al. 2008	isochron age
Four points–whole rock and leachates	U-Pb	4319	47		Bouvier, Blichert-Toft and Albarède 2009	Pb-Pb isochron age
TISSINT						
Whole rock–pyroxene-plagioclase groundmass	Ar-Ar	707	29		Park et al. 2013b	plateau age
Whole rock–pyroxene-plagioclase groundmass	Ar-Ar	610	33		Park et al. 2013b	isochron age
Plagioclase	Ar-Ar	540	63		Cohen et al. 2023	isochron age
Six points–whole rock, plagioclases, pyroxene, olivine	Rb-Sr	621	17		Park et al. 2013b	isochron age
Five points–pyroxenes, olivines, plagiaoclase	Rb-Sr	560	30		Brennecka, Borg, and Wadhwa 2014	isochron age
Eight points–whole rock, plagioclases, pyroxenes, olivine, residues	Rb-Sr	495	35		Shih et al. 2014	isochron age
Three points–whole rock, residue, leachate	Sm-Nd	596	23		Brennecka et al. 2013	isochron age
Three points–whole rock, plagioclase, pyroxene	Sm-Nd	616	67		Grosshans et al. 2013	isochron age
Six points–whole rocks, fines, leachates, residues	Sm-Nd	587	28		Brennecka, Borg, and Wadhwa 2014	isochron age
Fifteen points–whole rocks, plagioclase, olivine, pyroxene, residues, leachates	Sm-Nd	472	36		Shih et al. 2014	isochron age
Three points–whole rock, plagioclase, pyroxene	Lu-Hf	583	86		Grosshans et al. 2013	isochron age
Twelve points–four whole rocks, residues and leachates	U-Pb	574	20	weighted average	Moriwaki et al. 2017	Pb-Pb isochron age

POIKILITIC (LHERZOLITIC)						
ALHA77005						
Whole rock	K-Ar	1330	130		Miura et al. 1995	model age
Whole rock	Ar-Ar	3500			Bogard and Garrison 1999	plateau age
Three points–plagioclase, pyroxene, olivine	Ar-Ar	194	77		Walton, Kelley, and Herd 2008	isochron age
Plagioclase–seven grains	Ar-Ar	205	10	tight cluster	Turrin et al. 2013	plateau age
Plagioclase–seven grains	Ar-Ar	177	6	corrected for trapped ^{40}Ar	Turrin et al. 2013	isochron age
Three points–whole rock, plagioclase, pyroxene	Rb-Sr	184	6		Wooden et al. 1979	isochron age
Ten points–whole rock, pyroxenes, olivine	Rb-Sr	156	6		Jagoutz 1989	isochron age
Six points–whole rock, olivine, pyroxene, plagioclase	Rb-Sr	188	11		Shih et al. 1982	isochron age
Eight points–whole rock, plagioclase, pyroxene, olivine	Rb-Sr	185	11		Borg et al. 2001b, 2002	isochron age
Four points–whole rock, pyroxene	Sm-Nd	325			Shih et al. 1982	isochron age
Four points–whole rock, pyroxene, olivine	Sm-Nd	135	40		Jagoutz 1989	isochron age
Eight points–whole rock, plagioclase, pyroxene, olivine	Sm-Nd	173	6		Borg et al. 2001b, 2002	isochron age
ALHA77009						
Pyroxenes	Rb-Sr	154	6		Jagoutz 1991	isochron age
NWA1950						
Plagioclase–two step heated	Ar-Ar	362			Walton, Kelley, and Herd 2008	plateau age
Eleven points–pyroxe, olivine, plagioclase	Ar-Ar	382	36		Walton, Kelley, and Herd 2007, 2008	isochron age
LEW88516						
Whole rock	K-Ar	2600			Bogard and Garrison 1999	model age
Seven points–whole rock, plagioclase, olivine, pyroxene, opaques	Rb-Sr	183	10		Borg, Nyquist, and Weismann 1998; Borg et al. 2001b, 2002	isochron age
Eleven points–whole rock, plagiocalse, pyroxene, opaques, glass, leachates	Sm-Nd	166	16		Borg et al. 1998a, 2001b, 2002	isochron age
Four points–whole rocks, leachates, residue	U-Pb	170			Chen and Wasserburg 1993	U-Pb isochron age
Y000097						
Plagioclase	Ar-Ar	260			Misawa et al. 2008	plateau age

Four points–whole rock, plagioclase, pyroxene, olivine	Rb-Sr	147	28		Misawa et al. 2008	isochron age
Six points–whole rocks, pyroxene, plagioclase, residues, leachates	Sm-Nd	152	13		Misawa et al. 2008	isochron age
Y793605						
Whole rock	Ar-Ar	1595			Bogard and Garrison 1999	plateau age
Five points–whole rock, pyroxene, plagioclase, olivine	Rb-Sr	173	14		Morikawa et al. 2001	isochron age
Six points–whole rock, pyroxene, olivine	Sm-Nd	156	14		Misawa et al. 2006a	isochron age
Five points–whole rocks, pyroxene, olivine, leachates, residues	Sm-Nd	185	16		Misawa et al. 2006c	isochron age
Four points - pyroxene leachates and residue	U-Pb	212	62	T-W concordia, lower intercept	Misawa et al. 1997	U-Pb isochron age
Four points–pyroxene leachates and residue	U-Pb	4439	9	T-W concordia, upper intercept	Misawa et al. 1997	U-Pb isochron age
Five points–whole rock, pyroxene, plagioclase, olivine, residues	U-Pb	3812	870		Misawa et al. 1997	Pb-Pb isochron age
Five points–whole rocks, plagioclase	U-Pb	4174	29		Misawa et al. 2006c	Pb-Pb isochron age
Y980459						
Whole rock	Ar-Ar	866	35		Bogard, Park, and Garrison 2009	plateau age
Seven points–whole rock, plagioclase, pyroxene, glass, residues	Rb-Sr	296	90		Shih et al. 2004	isochron age
Nine points - whole rocks, pyroxene, olivine, glass	Rb-Sr	298	80		Shih et al. 2005	isochron age
Four points–whole rocks, pyroxene, glass, residues	Sm-Nd	290	45		Shih et al. 2004	isochron age
Six points–whole rock, pyroxene, glass, residues, leachates	Sm-Nd	472	27		Shih et al. 2005, 2007	isochron age
Y984028						
Seven points–whole rock, plagioclase, pyroxene, olivine, opaques, residues, leachates	Rb-Sr	170	9		Shih et al. 2009, 2011a	isochron age
Nine Points–whole rock, plagioclase, pyroxene, opaques, residues, leachates	Sm-Nd	170	10		Shih et al. 2011a	isochron age

GRV99027						
Five points–pyroxenes, olivines, plagioclase, residues	Rb-Sr	177	5		Liu, Li, and Lin 2011	isochron age

Table 2. Radioisotope ages of Nakhlites.

Sample	Method	Reading	Err +/-	Note	Source	Type
NAKHLA						
Whole rock	K-Ar	1300	30		Stauffer 1962	model age
Whole rock	Ar-Ar	1300			Podosek 1973	plateau age
Whole rock, pyroxene, olivine,acid-washed residue	Ar-Ar	1397	16	averaged	Burgess et al. 2000	plateau age
Whole rock	Ar-Ar	1332	10		Swindle and Olsen 2004	plateau age
Whole rock	Ar-Ar	1323	11		Swindle and Olsen 2004	plateau age
Whole rock	Ar-Ar	1357	11		Park, Garrison and Bogard 2009	plateau age
Plagioclase	Ar-Ar	1332	24		Cassata et al. 2010	isochron age
Whole rock–step heating	Ar-Ar	1418	18	6–90% ^{39}Ar release	Korochantseva et al. 2011	plateau age
Mesostasis (Plagioclase and glass)–step heating	Ar-Ar	1415	67	0–88% ^{39}Ar release	Korochantseva et al. 2011	plateau age
Mesostasis (Plagioclase and glass)–step heating	Ar-Ar	1364	54	0–88% ^{39}Ar release	Korochantseva et al. 2011	plateau age
Pyroxene–step heating	Ar-Ar	1399	28	1–84% ^{39}Ar release	Korochantseva et al. 2011	plateau age
Whole rock	Ar-Ar	1382.5	6.6		Cohen et al. 2017	plateau age
Thirteen points–whole rock, olivine, pyroxene, plagioclase, opaques	Rb-Sr	1230	10		Gale, Arden, and Hutchinson 1975	isochron age
Nine points–whole rock, plagioclase, pyroxene, glass	Rb-Sr	1310	20		Papanastassiou and Wasserburg 1974	isochron age
Five points–plagiocalse, glass	Rb-Sr	1370	20		Papanastassiou and Wasserburg 1974	isochron age
Two points–whole rocks	Re-Os	1417	15		Brandon et al. 2000	isochron age
Seven points–whole rock, olivine, pyroxene	Sm-Nd	1260	70		Nakamura et al. 1982	isochron age
Four points–whole rock residue and leachates, olivine, pyroxene	Sm-Nd	1297			Jagoutz and Jotter 2000	isochron age
Ten points–whole rocks, plagioclase, glass, pyroxenes, olivine, residues, leachates	Sm-Nd	1380	70		Shih et al. 2010	isochron age
Seven points–whole rock, olivine, pyroxene	U-Pb	1280	50		Nakamura et al. 1982	U-Pb isochron age

Seven points–whole rock, olivine, pyroxene	U-Pb	1240	110		Nakamura et al. 1982	U-Th-Pb isochron age
GOVERNADOR						
Whole rock	Ar-Ar	1320	40		Bogard and Husain 1977	plateau age
Three points–whole rock, pyroxenes	Rb-Sr	1330	10		Wooden et al. 1979	isochron age
Five points–whole rocks, pyroxenes, glass	Rb-Sr	1200	5		Shih, Nyquist, and Weismann 1999	isochron age
Five points–whole rocks, pyroxenes, olivine	Sm-Nd	1360	30		Shih, Nyquist, and Weismann 1996	isochron age
Eight points–whole rocks, pyroxene, olivine, leachates	Sm-Nd	1370	20		Shih, Nyquist, and Weismann 1999	isochron age
LAFAYETTE						
Iddingsite	K-Ar	670	91		Swindle et al. 2000	model age
Whole rock	Ar-Ar	1330	30		Podosek 1973	plateau age
Whole rock	Ar-Ar	1322	10		Swindle and Olsen 2004	plateau age
Pyroxene–step heating	Ar-Ar	1350	32	2–95% ^{39}Ar release	Korochantsova et al. 2011	plateau age
Whole rock–step heating	Ar-Ar	1306	7	6–95% ^{39}Ar release	Korochantsova et al. 2011	plateau age
Whole rock	Ar-Ar	1321.7	9.6		Cohen et al. 2017	plateau age
Whole rock	Ar-Ar	1322	16		Cohen et al. 2017	isochron age
Iddingsite	Rb-Sr	679	66		Shih et al. 1998	isochron age
Ten points–whole rocks, olivine, pyroxene, iddingsite	Rb-Sr	1250	80		Shih et al. 1998	isochron age
Ten points–whole rocks, olivine, pyroxene, iddingsite	Sm-Nd	1320	50		Shih et al. 1998	isochron age
Apatite–nine SHRIMP spot analyses	U-Pb	1120	270		Terada and Sano 2004	U-Pb isochron age
Y000593						
Whole rock	Ar-Ar	1359	5		Bogard and Garrison 2006	isochron age
Whole rock	Ar-Ar	1359	20	8 extractions	Misawa et al. 2005c	isochron age
Whole rock	Ar-Ar	1359	5	cosmic ^{36}Ar corrected	Park, Garrison, and Bogard 2007	isochron age
Plagioclase	Ar-Ar	1434	12	cosmic ^{36}Ar corrected	Park, Garrison, and Bogard 2007	isochron age
Whole rock	Ar-Ar	1367	7		Park, Garrison, and Bogard 2009	plateau age
Whole rock	Ar-Ar	1346	7.8		Cohen et al. 2017	plateau age
Whole rock	Ar-Ar	1340	8		Cohen et al. 2017	isochron age
Five points–whole rock, pyroxene, non-magnetic opaques, residues	Rb-Sr	1300	20		Misawa et al. 2003, 2005c	isochron age
Six points–whole rock, pyroxene, non-magnetic opaques, residues, leachates	Sm-Nd	1310	30		Misawa et al. 2003, 2005c	isochron age

Apatite–twelve SHRIMP spot analyses	U-Pb	1530	460		Terada and Sano 2004	U-Pb isochron age
Fourteen points–whole rocks, pyroxenes, oxides, leachates	U-Pb	1330	140		Bouvier, Blichert-Toft, and Albarède 2009	Pb-Pb isochron age
Y000749						
Whole rock	Ar-Ar	1380	100	98% release	Shankar et al. 2008	isochron age
Whole rock	Ar-Ar	1415.6	7		Cohen et al. 2017	plateau age
Apatite–twelve SHRIMP spot analyses	U-Pb	1530	460		Terada and Sano 2004	U-Pb isochron age
NWA998						
Whole rock	Ar-Ar	1334	11		Park, Garrison, and Bogard 2009	plateau age
Four points–pyroxenes, magnetic opaques	Rb-Sr	1470	21		Carlson and Irving 2004	isochron age
Five points–pyroxene, plagioclase, magnetic opaques, leachate	Sm-Nd	1290	50		Carlson and Irving 2004	isochron age
Four points–pyroxene, olivine, plagioclase, magnetic opaques	Lu-Hf	1540	300		Carlson and Irving 2004	isochron age
Five points–pyroxene, plagioclase, olivine, magnetic opaques	U-Pb	4290	40		Carlson and Irving 2004	Pb-Pb isochron age
Large apatite grain–spot analyses	U-Pb	3954	158	mean	Udry and Day 2018	Pb-Pb model age
NWA5790						
Four points–whole rock, glass, pyroxenes	Sm-Nd	1380	100		Shih et al. 2010	isochron age
NWA10153						
Five points–whole rocks, pyroxene, plagioclase, leachates	Sm-Nd	1419	56		Righter et al. 2016	isochron age
Four points–whole rocks, pyroxene, oxides	Lu-Hf	1360	33		Righter et al. 2016	isochron age
MIL03346						
Whole rock	Ar-Ar	1440	20		Bogard and Garrison 2006	isochron age
Whole rock	Ar-Ar	1360	2		Anand et al. 2006	total (plateau) age
Whole rock	Ar-Ar	1419	8	cosmic ^{36}Ar corrected	Park, Garrison, and Bogard 2007	isochron age
Plagioclase	Ar-Ar	1382	6	cosmic ^{36}Ar corrected	Park, Garrison, and Bogard 2007	isochron age
Mesostasis (plagioclase)	Ar-Ar	1368	83		Park, Garrison, and Bogard 2009	isochron age
Pyroxene	Ar-Ar	1334	54		Park, Garrison, and Bogard 2009	plateau age
Plagioclase	Ar-Ar	1339	8		Cassata et al. 2010	isochron age

Whole rock	Ar-Ar	1390.9	8.9		Cohen et al. 2017	plateau age
Eight points–whole rock, pyroxene, olivine, glass, residues	Rb-Sr	1294	122		Shih, Nyquist, and Reese 2006	isochron age
Eight points–whole rock, pyroxene, olivine, glass, residues	Sm-Nd	1356	30		Shih, Nyquist, and Reese 2006	isochron age
Ten points–whole rock, pyroxenes, olivines, oxides, leachates	U-Pb	1330	140		Bouvier, Blichert-Toft, and Albarède 2009	Pb-Pb isochron age
MIL090030 / 090032 / 090136						
Mesostatis (090030)	Ar-Ar	1373	4	average	Park et al. 2016	isochron age
Mesostatis (090032)	Ar-Ar	1404	9	average	Park et al. 2016	isochron age
Whole rock (090136)	Ar-Ar	1492	4	average	Park et al. 2016	isochron age

Table 3. Radioisotope ages of Chassignites.

Sample	Method	Reading	Err +/-	Note	Source	Type
CHASSIGNY						
Whole rock	K-Ar	1390	170		Lancet and Lancet 1971	model age
Whole rock	Ar-Ar	1320	70		Bogard and Garrison 1999	plateau age
Whole rock–12 extractions	Ar-Ar	1354	13		Misawa et al. 2006b	isochron age
Whole rock	Ar-Ar	1354	12		Bogard and Garrison 2006	isochron age
Nine points–whole rock, plagioclase, pyroxene, olivine, magnetic opaques	Rb-Sr	1226	12		Nakamura, Komi, and Kagami 1982	isochron age
Ten points–whole rocks, plagioclase, pyroxene, olivines, opaques	Rb-Sr	1406	14		Misawa et al. 2006b	isochron age
Two points–whole rocks	Re-Os	1417	15		Brandon et al. 2000	isochron age
Three points–whole rock leachates and residues	Sm-Nd	1362	62		Jagoutz 1996	isochron age
Eight points–whole rock, pyroxene, olivine, plagioclase, opaques	Sm-Nd	1360	30		Misawa et al. 2005b	isochron age
Nine points–whole rocks, pyroxene, olivines, opaques	Sm-Nd	1386	28		Misawa et al 2006b	isochron age
Four points–whole rock, leachates	U-Pb	1330	140		Bouvier, Blichert-Toft, and Albarède 2009	Pb-Pb isochron age
NWA2737						
Whole rock–two points	K-Ar	376	168		Marty et al. 2006	isochron age

Whole rock	Ar-Ar	169	1		Bogard and Garrison 2006	isochron age
Whole rock	Ar-Ar	163	5	0–48% ^{39}Ar, total ^{36}Ar	Bogard and Garrison 2008	isochron age
Whole rock	Ar-Ar	189	18	10–48% ^{39}Ar, total ^{36}Ar	Bogard and Garrison 2008	isochron age
Three points–whole rocks (added to Chassigny)	Sm-Nd	1380	30		Misawa et al. 2005a	isochron age
Three points–whole rocks (added to Chassigny)	Sm-Nd	1416	57		Misawa et al. 2005a	isochron age
Baddeleyites	U-Pb	1640	70		Ozawa et al. 2009	U-Pb isochron age

Table 4. Radioisotope ages of Orthopyroxenites.

Sample	Method	Reading	ERR +/-	NOTE	SOURCE	TYPE
ALH 84001						
Whole rock	K-Ar	3560	280		Miura et al 1995	model age
Whole rock	K-Ar	4050	290		Miura et al 1995	model age
Silicates	K-Ar	3910	150		Turner et al. 1997	isochron age
Whole rock aliquots	Ar-Ar	4010	14		Ash, Knott, and Turner 1996	plateau and isochron age
Pyroxene	Ar-Ar	4175	25		Knott, Ash, and Turner 1996	plateau age
Silicates	Ar-Ar	3920	100		Turner et al. 1997	plateau age (mean)
Plagioclase grains	Ar-Ar	4070	40		Ilg, Jessburger, and El Gorsey 1997	plateau age
Feldspars	Ar-Ar	4095	200		Bogard and Garrison 1999	plateau age
Plagioclase grains	Ar-Ar	4160	200		Cassata et al. 2010	plateau age
Plagioclase grains	Ar-Ar	4163	35		Cassata et al. 2010	isochron age
Six points–plagioclase, pyroxene, whole rock leachates	Rb-Sr	4550	30		Nyquist et al. 1995	isochron age
Whole rock samples, pyroxene and plagioclase separates	Rb-Sr	3890	50		Wadhwa and Lugmair 1996	isochron age
Four points–whole rock, pyroxene, plagioclases	Rb-Sr	4344	230		Beard et al. 2013	isochron age
Five points–fine and coarse whole rock separates, leachates and residues	Sm-Nd	4560			Jagoutz et al. 1994	isochron age
Six points–whole rock leachates and residues	Sm-Nd	4500	120		Nyquist et al. 1995	isochron age
Whole rock, pyroxene	Sm-Nd	4410	30		Lapen et al. 2010	isochron age
Twenty-two points–whole rocks, pyroxenes, residues, leachates	Sm-Nd	4568	88		Nyquist and Shih 2013	isochron age

Four points–whole rock, pyroxene, chromite	Lu-Hf	4086	30		Righter et al. 2009	isochron age
Four points–chromite, pyroxene, whole rocks	Lu-Hf	4091	30		Lapen et al. 2010	isochron age
Six points–whole rock leachates and residues	U-Pb	4135	12		Jagoutz et al. 2009	Pb-Pb isochron age
Thirteen points–whole rock, pyroxene, leachates	U-Pb	4074	99		Bouvier, Blichert-Toft, and Albarède 2009	Pb-Pb isochron age
Pyroxenes and plagioclases	U-Pb	4089	73		Bellucci et al. 2015a	Pb-Pb isochron age
Carbonates	Ar-Ar	3600			Knott et al. 1996	isochron age
Carbonates in whole ropck	Ar-Ar	3270	17		Kring et al. 1998	plateau age
Carbonates in whole ropck	Ar-Ar	3520	24		Kring et al. 1998	plateau age
Carbonates in whole ropck	Ar-Ar	3910	120		Kring et al. 1998	plateau age
Carbonates–eight leachates	Rb-Sr	3900	40		Borg et al. 1999	isochron age
Carbonates	Rb-Sr	1410	100		Wadhwa and Lugmair 1996	isochron age
Carbonates–three leachates	Rb-Sr	3900	40		Borg et al. 1998b	isochron age
Carbonates–five leachates	Rb-Sr	3940	40		Borg et al. 1998b	isochron age
Carbonates–eight leachates	Rb-Sr	3924	19	recalculated data	Borg and Drake 2005	isochron age
Seven points–carbonates, carbonate-rich aliquots	Rb-Sr	3952	22		Beard et al. 2013	isochron age
Carbonates–eight leachates	U-Pb	4038	140		Borg et al. 1999	Pb-Pb isochron age
Carbonates–eight leachates	U-Pb	4045	90	recalculated data	Borg and Drake 2005	Pb-Pb isochron age
Phosphates–twelve grains, SHRIMP spot analyses	U-Pb	4018	81		Terada, Monde and Sano 2003	concordia intercept age
Phosphates–twelve grains, SHRIMP spot analyses	Th-Pb	3971	860		Terada, Monde and Sano 2003	isochron age
Phosphate single grain	U-Pb	3830	470		Koike et al. 2014	concordia intercept age
Phosphate single grain	U-Pb	4220	180		Koike et al. 2014	concordia intercept age
Phosphate single grain	U-Pb	3770	540		Koike et al. 2014	concordia intercept age
Phosphate multi-grain	U-Pb	3990	160		Koike et al. 2014	concordia intercept age

Table 5. Radioisotope ages of Polymict Regolith Breccias.

Sample	Method	Reading	Err +/-	Note	Source	Type
NWA7034						
Whole rock	K-Ar	1600		approx. maximum	Cartwright et al. 2013, 2014	model age
Plagioclase	Ar-Ar	2120	90		Lindsay et al. 2016	plateau age
Plagioclase	Ar-Ar	1620	40		Lindsay et al. 2016	plateau age
Feldspar	Ar-Ar	1374	7		Cassata et al. 2018	plateau age
Whole rock	Ar-Ar	1391	16	oldest of 7 of 13	Cassata et al. 2018	plateau age
Whole rock	Ar-Ar	1327	12	youngest of 7 of 13	Cassata et al. 2018	plateau age
Whole rock	Ar-Ar	1367	44	oldest of 7 of 13	Cassata et al. 2018	isochron age
Whole rock	Ar-Ar	1224	52	youngest of 7 of 13	Cassata et al. 2018	isochron age
Five analyses–whole rock plus four mineral fractions	Rb-Sr	2089	81	basaltic crustal rock	Agee et al. 2013	isochron age
Ten points–whole rocks, plagioclases, pyroxene, residues, leachates	Rb-Sr	2700	600	dispersion; apparent age	Nyquist et al. 2013, 2016	isochron age
Five analyses–whole rock plus four mineral fractions	Sm-Nd	2190	1400	basaltic crustal rock	Agee et al. 2013	isochron age
Four points–whole rocks, pyroxene, leachates	Sm-Nd	4390	80		Nyquist et al. 2013	isochron age
Seven points–whole rocks, plagioclases, pyroxene, phosphates	Sm-Nd	4420	70	coarse-grained minerals	Nyquist et al. 2016	isochron age
Eight points–whole rocks, plagioclases, pyroxenes, residues, leachates	Sm-Nd	4460	100	^{146}Sm-^{142}Nd	Nyquist et al. 2016	isochron age
Zircons	U-Pb	1570	30	U-Pb concordia intercept	Tartèse et al. 2014	U-Pb isochron age
Zircons	U-Pb	4370	70	U-Pb concordia intercept	Tartèse et al. 2014	U-Pb isochron age
Two baddeleyite grains–five analyses (weighted average age)	U-Pb	4350	4	U-Pb discordia intercepts	Tartèse et al. 2014	U-Pb isochron age
Five zircon grains and one baddeleyite grain	U-Pb	4439	17	average	Yin et al. 2014	U-Pb isochron age
One zircon grain	U-Pb	4350	13	concordia upper intercept	Yin et al. 2014	U-Pb isochron age
Five other zircon grains	U-Pb	1410	56	average	Yin et al. 2014	U-Pb isochron age
Zircons (older)	U-Pb	4431	27	upper intercept	McCubbin et al. 2016	U-Pb concordia age
Zircons (younger)	U-Pb	1502	98	upper intercept	McCubbin et al. 2016	U-Pb concordia age
Zircon	U-Pb	4476	1	oldest of 7 concordant	Bouvier et al. 2018	Pb-Pb model age

Zircon	U-Pb	4430	1	youngest of 7 concordant	Bouvier et al. 2018	Pb-Pb model age
Zircon	U-Pb	4483	9	oldest of 7 concordant	Bouvier et al. 2018	U-Pb model age
Zircon	U-Pb	4160	13	youngest of 7 concordant	Bouvier et al. 2018	U-Pb model age
Baddeleyite (two grains)	U-Pb	4340	7	average	McCubbin et al. 2016	U-Pb isochron age
Zircons	U-Pb	4465	73	concordia upper intercept	Hu et al. 2019	U-Pb isochron age
Zircons	U-Pb	1634	93	concordia lower intercept	Hu et al. 2019	U-Pb isochron age
Zircons	U-Pb	4425	23	weighted average/ mean	Hu et al. 2019	Pb-Pb isochron age
Phosphates	U-Pb	1345	47	T-W concordia lower intercept	Yin et al. 2014	U-Pb isochron age
Phosphates–apatite grains (17)	U-Pb	1495	88	T-W concordia upper intercept	McCubbin et al. 2016	U-Pb isochron age
Apatites	U-Pb	1530	65	T-W concordia lower intercept	Hu et al. 2019	U-Pb isochron age
NWA7533						
Feldspars	Ar-Ar	1400		two best, approximate	Lindsay et al. 2014	plateau age
Apatites	Sm-Nd	1490	480		Shang et al. 2022	isochron age
Six igneous clasts and two zircons	Lu-Hf	4440	41		Jensen et al. 2025	isochron age
Chloroapatite in monzonitic clasts	U-Pb	1357	81	regolith breccia, concordia lower intercept	Bellucci et al. 2015b	U-Pb isochron age
Zircons (10)–SHRIMP spot analyses discordia upper intercept	U-Pb	4428	25	regolith breccia	Humayun et al. 2013	U-Pb discordia age
Zircons (10)–SHRIMP spot analyses discordia lower intercept	U-Pb	1712	85	later disturbance	Humayun et al. 2013	U-Pb discordia age
Zircons (39) and baddeleyites (2)	U-Pb	4474	10	mean concordia upper inetercept	Costa et al. 2020	Pb-Pb isochron age
Zircons (39) and baddeleyites (2)	U-Pb	4442	17	mean concordia upper inetercept	Costa et al. 2020	Pb-Pb isochron age
Zircons (39) and baddeleyites (2)	U-Pb	4486	2	oldest concordia upper intercept	Costa et al. 2020	Pb-Pb isochron age
Zircons (39) and baddeleyites (2)	U-Pb	4331	1	youngest concordia upper intercept	Costa et al. 2020	Pb-Pb isochron age
Zircons (8)	U-Pb	1548	9	oldest in range, detrital grain	Costa et al. 2020	U-Pb concordia age
Zircons (8)	U-Pb	300	1	youngest in range, detrital grain	Costa et al. 2020	U-Pb concordia age
Zircon in Basaltic clast	U-Pb	4453	39		Jensen et al. 2025	U-Pb concordia age
Zircon in Basaltic andesite clast	U-Pb	4426	10		Jensen et al. 2025	U-Pb concordia age
Zircon in Monzonitic clast	U-Pb	4375	190	upper intercept	Jensen et al. 2025	U-Pb discordia model age
Zircon in Basaltic clast	U-Pb	4456	68	upper intercept	Jensen et al. 2025	U-Pb discordia model age
Zircon in Basaltic clast	U-Pb	4422	12	upper intercept	Jensen et al. 2025	U-Pb discordia model age

Zircon in Basaltic andesite clast	U-Pb	4447	8	upper intercept	Jensen et al. 2025	U-Pb discordia model age
Zircon in Basaltic andesite clast	U-Pb	4464	12	upper intercept	Jensen et al. 2025	U-Pb discordia model age
NWA8171						
Apatites	Sm-Nd	1490	480		Shang et al. 2022	isochron age

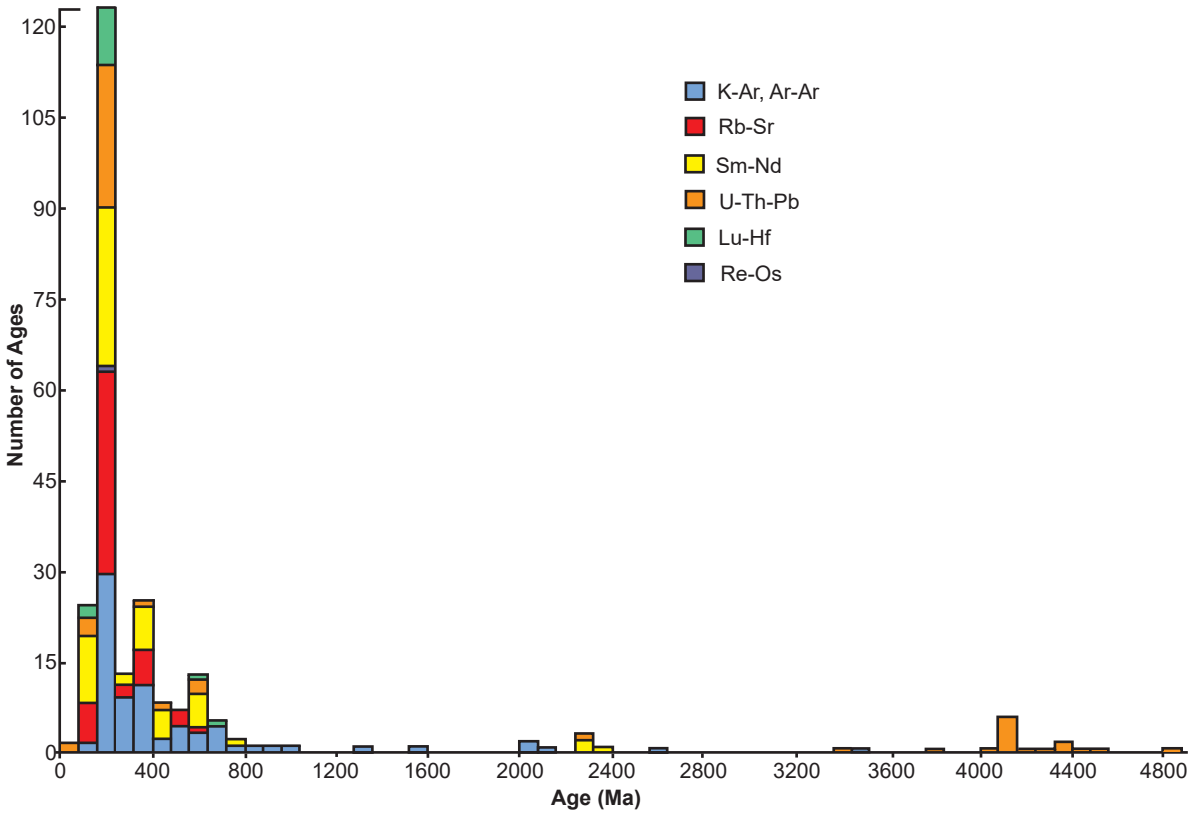

Fig. 15. Frequency versus radioisotope ages histogram diagram for all the shergottites listed in table 1, color-coded according to the radioisotope methods utilized to obtain them.

orthopyroxenite ALH 84001. U-Th-Pb ages were derived from U-Pb, Th-Pb, and Pb-Pb isochrons, including upper and lower intercepts on U-Pb concordia, and Tera-Wasserburg concordia and discordia. In several instances, model Pb-Pb and U-Pb ages from concordant grains were obtained, and in other instances the isochrons were based on means, weighted means, and averages. In other words, the analytical data were manipulated to produce meaningful ages that were statistically valid.

The Re-Os method has only been used three times, on whole rock samples of olivine-phyric shergottite EETA79001A (table 1 and fig. 15), Nakhla (table 2 and fig. 16) and Chassigny (table 3 and fig. 17) and yields isochron ages. That method primarily relies on the presence of sulfides which are generally absent from these Martian meteorites. On the other hand, the Lu-Hf method has been used on eight basaltic shergottites and the olivine-phyric shergottite Tissint (table 1 and fig. 15), two nakhlites (table 2 and fig. 16), the orthopyroxenite ALH 84001 (table 4 and fig. 18), and the polymict regolith breccia NWA7533 (table 5 and fig. 19). In all instances, except one, whole rock and minerals (plagioclase and pyroxene, and sometimes oxides and/or chromite, or residues and/or leachates) were used to obtain isochron ages. With the exception, for the polymict regolith breccia NWA7533 six igneous clasts and two zircons were used.

Shergottites

The radioisotope ages of forty-five (45) shergottites are spread between 0 and 4800Ma, but most of the radioisotope ages are between 0 and 1040Ma (fig. 15). The 4800Ma age is clearly an outlier as a Marian meteorite cannot be older that the supposed age of its 4.57Ga Mars source. Nevertheless, 123 of the 251 radioisotope ages (49%) plotted in fig. 15 are in the 160–240Ma range, with agreement between all six methods—twenty-nine (29) K-Ar and Ar-Ar ages, thirty-four (34) Rb-Sr ages, twenty-six (26) Sm-Nd

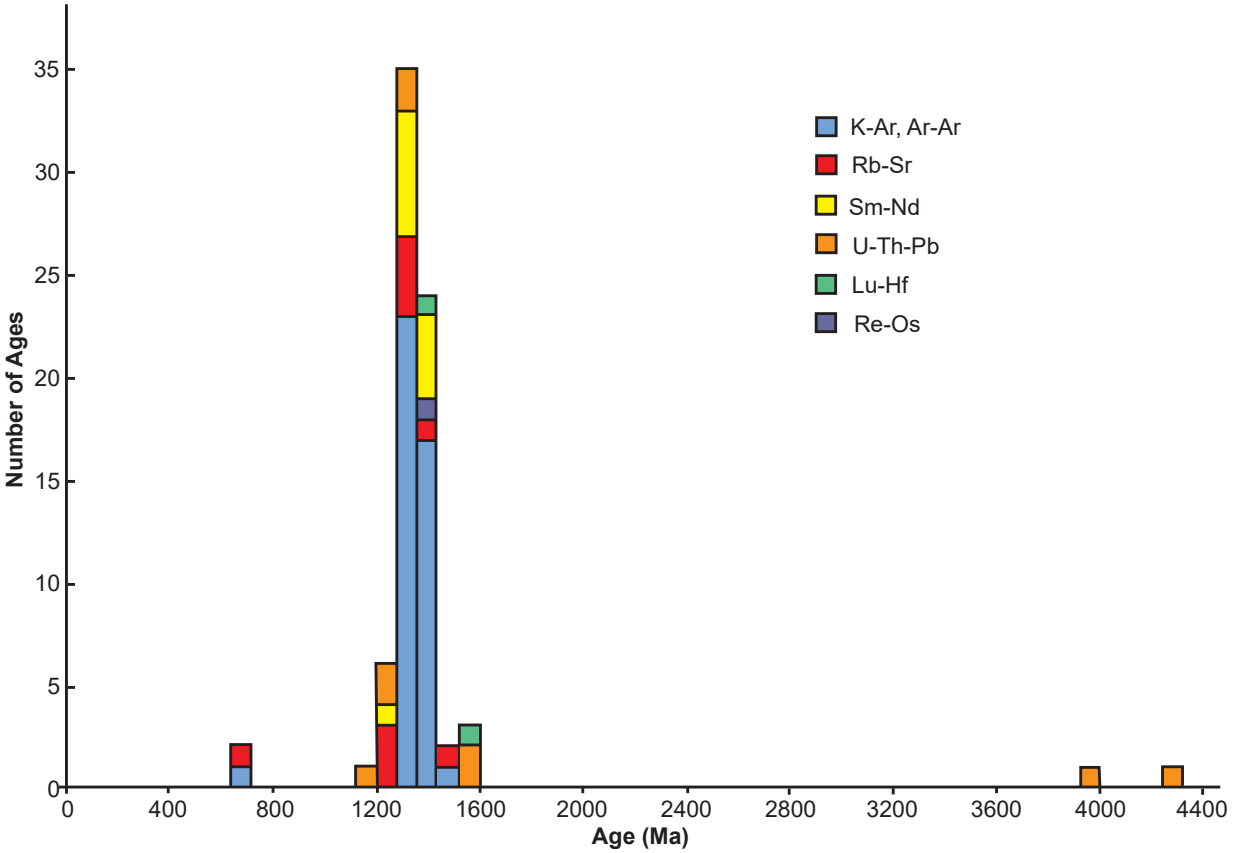

Fig. 16. Frequency (number of ages) versus radioisotope ages histogram diagram for all the nakhlites listed in table 2, color-coded according to the radioisotope methods utilized to obtain them.

ages, twenty-four (24) U-Th-Pb ages, nine Lu-Hf ages and one Re-Os age. There are also adjacent much smaller frequency peaks in the 80–160Ma range (twenty-four ages), in the 320–400Ma range (twenty-five ages) and in the 560–640Ma range (thirteen ages), consisting of K-Ar, Ar-Ar, Rb-Sr, Sm-Nd, U-Th-Pb, and Lu-Hf ages.

While there is good agreement between the 123 determinations by all six methods in the major 160–240Ma peak, the determinations were obtained using different samples. For example, the twenty-nine (29) K-Ar and Ar-Ar ages were obtained primarily using plagioclase grains, sometimes whole rocks, and rarely whole rocks and mineral separates. And while these are mostly isochron ages, a few were K-Ar model or Ar-Ar plateau ages. On the other hand, all the thirty-four (34) Rb-Sr, twenty-six (26) Sm-Nd and nine Lu-Hf ages are isochron ages and all were obtained using whole rocks and mineral separates. The one Re-Os isochron age was obtained using whole rock samples. However, while all the twenty-four (24) U-Th-Pb determinations resulted in sixteen U-Pb isochron ages, five Pb-Pb ages and three Th-Pb isochron ages, they were obtained using whole rocks and mineral separates (nine determinations), baddeleyite grains (twelve determinations), and phosphate grains (three determinations). There is thus such good agreement between all six major methods, even using different target samples, although it could be argued that the isotopic compositions of the baddeleyite and phosphate grains would have been incorporated into the crushed whole rock samples where the U-Th-Pb method was used on both targets from the same meteorites.

The only other cluster of radioisotope ages are all U-Th-Pb ages in the 4000–4560Ma range (thirteen U-Th-Pb ages or 5% of the 251 available determined ages) with a small peak of six ages in the 4080–4160Ma range, all six are Pb-Pb isochron ages (fig. 15). Of the thirteen U-Th-Pb ages in the overall 4000–4560Ma cluster, two are U-Pb isochron ages and eleven are Pb-Pb isochron ages, but all were obtained from whole rock samples and mineral separates, primarily plagioclase and pyroxene, but sometimes included oxides and/or phosphates, and/or leachates or residues. On the other hand, the U-Th-Pb ages obtained from phosphate and baddeleyite grains, and from including phosphates with the whole rock and other minerals when plotting isochron ages, all (but one) fall within the 80–640Ma range as do all fifty (50) Rb-Sr isochron ages obtained from whole rocks and mineral separates. Otherwise, there is a sporadic spread of a few K-Ar, Ar-Ar, Sm-Nd, and U-Th-Pb ages in the 800–3520Ma range.

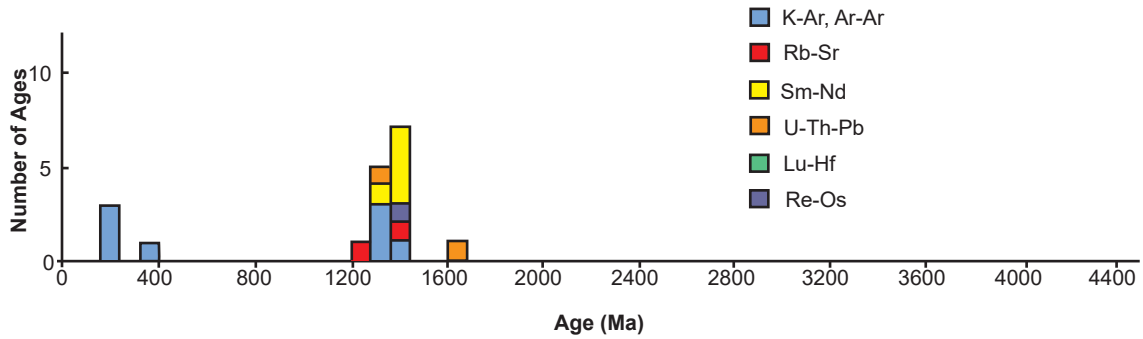

Fig. 17. Frequency versus radioisotope ages histogram diagram for the two chassignites listed in table 3, color-coded according to the radioisotope methods utilized to obtain them.

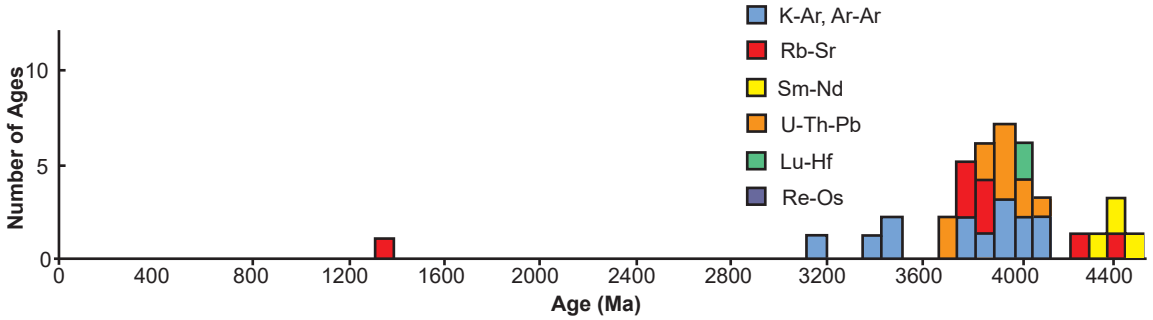

Fig. 18. Frequency versus radioisotope ages histogram diagram for the orthopyroxenite ALH84001 listed in table 4, color-coded according to the radioisotope methods utilized to obtain them.

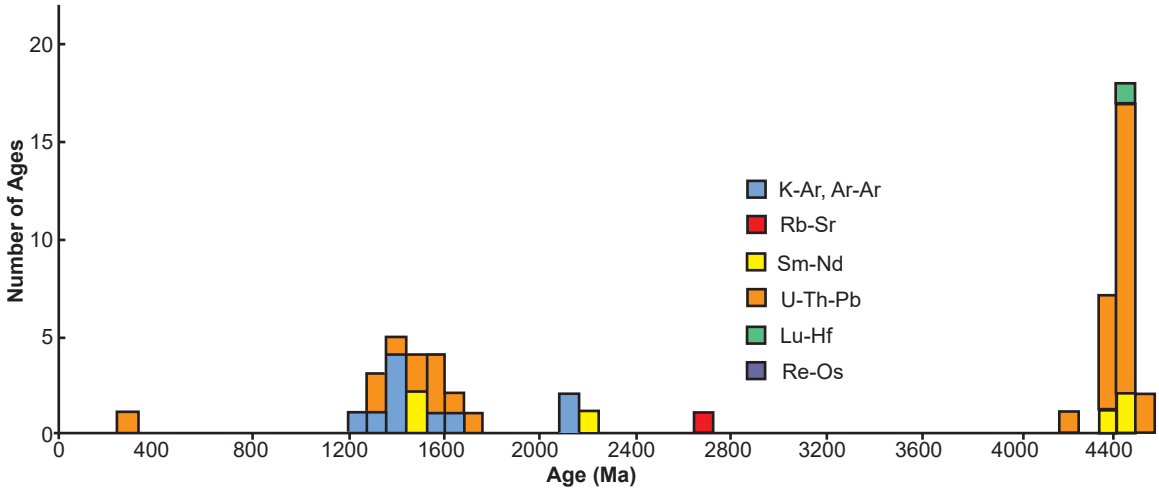

Fig. 19. Frequency versus radioisotope ages histogram diagram for the polymict regolith breccias listed in table 5, color-coded according to the radioisotope methods utilized to obtain them.

The most "dated" shergottite is the basaltic shergottite Zagami with forty-eight (48) radioisotope ages (or 19% of the total of 251 radioisotope ages in table 1), comprising twelve Ar-Ar age determinations (ten of which were obtained using feldspar grains), eleven Rb-Sr ages, ten Sm-Nd ages, and two Lu-Hf ages (all obtained using whole and mineral separates, and sometimes leachates and residues), and thirteen U-Th-Pb ages (eight obtained using whole rocks and mineral separates and/or leachates and residues, three obtained on baddeleyite grains, and one obtained on phosphate grains). Thirty-seven or 77% of these forty-eight radioisotope ages fall in the peak 160–240Ma range, including eleven of the twelve Ar-Ar age determinations, all eleven Rb-Sr ages, six of the ten Sm-Nd ages, seven of the thirteen U-Th-Pb ages and the two Lu-Hf ages. Three U-Th-Pb ages are >4000Ma, one Ar-Ar age is 242Ma, while the remaining seven radioisotope ages (Sm-Nd and U-Th-Pb ages) are <160Ma. Thus, the radioisotope age determinations on Zagami reflect the overall pattern of radioisotope ages for the forty-five (45) shergottite meteorites listed in table 1 and plotted on fig. 15, namely, the major peak in

the 160–240 Ma range comprising radioisotope age determined by all five major methods, and a very minor peak of a few U-Th-Pb isochron ages at >4000 Ma.

It is also worth noting that there is often general agreement between the different methods used on the same basaltic shergottite. For example, all four radioisotope determinations (three Rb-Sr and one Sm-Nd) using whole rocks and mineral separates for EETA790001B are in very close overlapping agreement within the error margins at 169±23 to 185±25 Ma, as are the Rb-Sr and Sm-Nd radioisotope determinations using whole rocks, mineral separates, leachates and residues for NWA5990 at 389±12 Ma and 402±22 Ma (table 1). Similarly, the nine radioisotope determinations on NWA1460 (one K-Ar and four Ar-Ar using plagioclase grains, and two Rb-Sr and two Sm-Nd using whole rock, minerals separates and sometimes leachates) all are in very close overlapping agreement within the error margins at 336±15 Ma to 360±6 Ma (table 1). Furthermore, the four radioisotope determinations on NWA3171 (two Ar-Ar on plagioclase grains, one Sm-Nd on whole rocks and mineral separates and one U-Pb on baddeleyite grains) all yielded isochron ages in close agreement within the error margins from 171±129 to 232±7 Ma, and the four radioisotope determinations on NWA4468 (one Ar-Ar on the whole rock, and one Rb-Sr, one Sm-Nd, and one Lu-Hf all using whole rocks and minerals separates, plus leachates and residues) all yielded isochron ages in close agreement within the error margins from 150±29 Ma to 188±17 Ma (table 1). And finally, the six radioisotope determinations on LAR06319 (one Ar-Ar on the whole rock, one Rb-Sr, two Sm-Nd and two Lu-Hf all using whole rocks and minerals separates, plus leachates and residues) all also yielded isochron ages in close agreement within the error margins from 163±13 Ma to 207±14 Ma, and the five radioisotope determinations on NWA856 (two Rb-Sr, two Sm-Nd and one U-Pb) all yield isochron ages in close agreement within the error margins from 150±32 Ma to 186±15 Ma (table 1). This same pattern is also seen in two olivine-phyric shergottites (Dho019 and Tissint) and in one poikilitic (lherzolitic) shergottite (Y000097).

In contrast, as with the forty-eight (48) radioisotope determinations on basaltic shergottite Zagami of which three U-Pb and Pb-Pb isochron ages are >4000 Ma compared with all the other forty-five (45) Ar-Ar, Rb-Sr, Sm-Nd, Lu-Hf, and U-Th-Pb radioisotope ages in the range 70±35 Ma to 261±16 Ma, among the twenty-eight (28) radioisotope determinations on the type basaltic shergottite Shergotty, one Pb-Pb isochron age is 4100 Ma compared with all the other twenty-seven (27) K-Ar, Ar-Ar, Rb-Sr, Sm-Nd, Lu-Hf, and U-Th-Pb radioisotope ages in the range from 147±20 to 600±20 Ma (table 1). A similar pattern can be seen among the fifteen radioisotope determinations on the Los Angeles basaltic shergottite with one Pb-Pb isochron age of 4100 Ma and the other fourteen Ar-Ar, Rb-Sr, Sm-Nd, Lu-Hf, and U-Pb isochron ages in the range from 158±15 Ma to 329±12 Ma (table 1). And whereas two other basaltic shergottites (QUE94201 and display the same pattern, only one olivine-phyric does but no poikilitic (lherzolitic) shergottites do (table 1).

Nakhlites

Seventy-nine (79) radioisotope ages have been determined on twelve (12) nakhlites and are spread between 640 and 4320 Ma (table 2, and in fig. 16, where it should be noted the vertical frequency scale is a third of that for the shergottites in fig. 15). However, seventy-five (75) or 95% of those radioisotope ages cluster in the range between 1120 and 1600 Ma. Furthermore, the major peak within that cluster consists of fifty-nine (59) radioisotope ages (or almost 75% of the seventy-nine radioisotope ages) spans the range of 1280–1440 Ma—thirty-five (35) radioisotope ages (or over 44%) in the range 1280–1360 Ma and another twenty-four (24) radioisotope ages (or over 30%) in the range 1360–1440 Ma. That major 1280–1440 Ma peak encompasses forty (40) K-Ar and Ar-Ar radioisotope ages, five Rb-Sr radioisotope ages, ten (10) Sm-Nd radioisotope ages, and two U-Th-Pb radioisotope ages, plus one Lu-Hf and one Re-Os radioisotope age. Thus there is good agreement between all six major radioisotope dating methods.

The lower radioisotope age outlier in the 640–720 Ma range consists of one Ar-Ar and one Rb-Sr determination on iddingsite in the Lafayette nakhlite. Iddingsite is a hydrothermal alteration product of olivine, so it is not surprising that its radioisotope dates reflect disturbance of the K-Ar and Rb-Sr radioisotope systems. In contrast, the upper radioisotope age outlier consists of two U-Th-Pb determinations on the NWA998 nakhlite (table 2). These are a Pb-Pb isochron age of 4290 Ma obtained from five points consisting of pyroxene, plagioclase, olivine and opaques, and a Pb-Pb model age of 3954 Ma obtained as the mean of spot analyses of a large apatite (phosphate) grain.

The most "dated" nakhlite is the type Nakhla meteorite with twenty-one (21) radioisotope ages (or almost 27% of the seventy-nine radioisotope ages in table 2). All twenty-one of these radioisotope ages are within the major 1280–1440 Ma peak in fig. 16, comprising twelve (12) K-Ar and Ar-Ar, three Rb-Sr, three Sm-Nd, and two U-Th-Pb radioisotope ages, plus one Re-Os radioisotope age. Thus there

is excellent agreement between all these five major radioisotope dating methods.

Chassignites

Only two chassignites have been radioisotope dated—Chassigny (eleven radioisotope ages) and NWA2737 (seven radioisotope ages) (table 3 and fig. 17). These eighteen radioisotope ages are spread between 160 and 1680Ma. However, twelve (12) or almost 67% of those radioisotope ages cluster in the range in the major peak in the range between 1280 and 1440Ma, exactly the same radioisotope age range as the major peak in the nakhlite data (fig. 16). This major peak in the chassignite data consists of five radioisotope ages in the range 1280–1360Ma (three Ar-Ar, one Sm-Nd, and one U-Th-Pb) and seven radioisotope ages in the range 1360–1440Ma (one K-Ar, one Rb-Sr, three Sm-Nd and one Re-Os). Thus again there is good agreement between all five of the major radioisotope dating methods used.

Ten of the eleven radioisotope ages determined for Chassigny are within that 1280–1440Ma major peak, one Rb-Sr age of 1260Ma just falling below that peak. All were obtained on either whole rock samples (K-Ar and Ar-Ar) or whole rocks and mineral separates of plagioclase, pyroxene, olivine and opaques and/or leachates and residues (Rb-Sr, Sm-Nd, U-Th-Pb, and Re-Os). In contrast, only the two Sm-Nd radioisotope ages for NWA2737 fall within the 1360–1440Ma range within that major peak. Its three Ar-Ar age determinations fall within the 160–240Ma range and its one K-Ar determination falls within the 320–400Ma range (fig. 16). All the K-Ar, Ar-Ar and Sm-Nd determinations were obtained using whole rock samples. The only U-Th-Pb determination on NWA2737 was obtained analyzing baddeleyite grains which yielded a high outlier U-Pb isochron age of 1640Ma and thus clearly indicates disturbance of the U-Pb isotope system when the baddeleyite formed.

Orthopyroxenite

Only the one orthopyroxenite ALH84001 has been found thus far. However, forty (40) radioisotope age determinations have been made on it and its constituent minerals—twenty-two (22) obtained using whole rocks and/or mineral separates of plagioclase, pyroxene, and chromite, and leachates and residues, twelve (12) obtained on carbonates or using carbonate leachates, and six (6) obtained on phosphate grains (table 4). These forty (40) radioisotope ages are spread between 1360 and 4640Ma, although one Rb-Sr radioisotope age of 1410Ma determined on carbonates is an outlier (fig. 18). All the other thirty-nine (39) radioisotope ages are spread from 3200Ma to 4640Ma, although four radioisotope ages in the 3200–3600Ma range are outliers to the two main >3840Ma clusters. Those four outliers are a K-Ar model age for a whole rock sample, and three Ar-Ar ages obtained using carbonates.

The two main clusters are in the ranges of 3840–4240Ma and 4320–4640Ma (fig. 18). The cluster from 3840 Ma to 4240Ma is the dominant cluster with a broad peak from 3920Ma to 4160Ma. That peak consists of five radioisotope ages in the 3840–3920Ma range (one K-Ar and one Rb-Sr determinations using whole rocks and/or silicate mineral separates, and one Ar-Ar and two Rb-Sr determinations using carbonates and leachates), six radioisotope ages in the 3920–4000Ma range (one Ar-Ar determination using silicate mineral separates, three Rb-Sr determinations using leachates of carbonates, and two U-Th-Pb determinations on phosphate grains), seven radioisotope ages in the 4000–4080Ma range (one K-Ar, two Ar-Ar and one U-Th-Pb determinations using whole rocks and/or silicate mineral separates, two U-Th-Pb determinations using leachates of carbonates, and one U-Th-Pb determination on phosphate grains), and six radioisotope ages in the 4080–4160Ma range (two Ar-Ar determinations using feldspar separates, two Lu-Hf determinations, two U-Th-Pb determinations using whole rock and mineral separates). In contrast, the minor cluster from 4320Ma to 4560Ma consists of two Rb-Sr and four Sm-Nd radioisotope ages determined using whole rocks, silicate mineral separates, and/or leachates and residues. The peak within that cluster is three radioisotope ages (one Rb-Sr and two Sm-Nd) in the 4480–4560Ma range. The oldest determination in that cluster is actually the Sm-Nd radioisotope age 4568±88Ma which within its error margins coincides with the claimed age for Mars (like the earth) of 4.57Ga.

Generally there is good agreement between the five major radioisotope dating methods used on this meteorite, although there might be a hint of patterns. Among the determination methods used on the whole rocks, silicate mineral separates and/or leachates and residues, the K-Ar and Ar-Ar ages are generally slightly lower than the Rb-Sr ages which are slightly lower than the Sm-Nd ages, while the Lu-Hf and U-Th-Pb ages are generally the same as one another and also many of the Ar-Ar ages (table 4). On the other hand, among the determination methods used on carbonates and carbonate leachates, the Ar-Ar, Rb-Sr, and U-Th-Pb ages are generally similar, except where several Ar-Ar and Rb-Sr ages are lower, suggesting these radioisotope systems are sometimes disturbed, which makes sense if the carbonates are secondary minerals, that is, formed later than the silicates minerals in this meteorite.

Similarly, the phosphate grains yield a wide range in the six U-Th-Pb ages from 3770 Ma to 4220 Ma, much less than the two Rb-Sr and two Sm-Nd ages of 4500–4568 determined on whole rocks and silicate mineral separates, again suggestive that these phosphate grains in this meteorite are secondary, that is, formed later than the silicates minerals.

Polymict Regolith Breccias

Only three polymict regolith breccia meteorites have been radioisotope dated, and then primarily NWA7034 and NWA7533, which are regarded as paired meteorites. Thus far, thirty-three (33) radioisotope age determinations have been made on NWA7034—on K-Ar, seven Ar-Ar, two Rb-Sr, and four Sm-Nd determinations using whole rocks, mineral separates and/or leachates and residues, and also sixteen (16) U-Th-Pb determinations on zircon and/baddeleyite grains and three U-Th-Pb determinations on phosphate grains, primarily apatite (table 5). For NWA7533 fifteen (15) U-Th-Pb radioisotope determinations have been made on zircon and sometimes also baddeleyite grains, often within the breccia's igneous clasts, and one U-Th-Pb radioisotope determination on apatite grains in the breccia's igneous clasts, as well as one Ar-Ar radioisotope determination on feldspar grains and one Sm-Nd radioisotope determination on apatite grains, both in the breccia's igneous clasts, plus a Lu-Hf radioisotope determination on six igneous clasts and two zircon grains within them (table 5). The only other radioisotope determination has been Sm-Nd on apatite grains in NWA8171.

The spread in the resultant fifty-three (53) radioisotope ages is 300±1 Ma to 4486±2 Ma (table 5 and fig. 19). However, there are obviously two clusters of radioisotope ages, the major cluster having a major peak and the other cluster having a minor and broader peak.

The major cluster is in the range of 4160–4560 Ma and consists of twenty-eight (28) radioisotope ages. The major peak within that cluster is at 4400–4080 Ma and consists of two Sm-Nd isochron ages determined using whole rocks, mineral separates, leachates and residues, a Lu-Hf isochron age determined on six igneous clasts and two zircons, and fifteen (15) various U-Th-Pb radioisotope determinations on zircon and baddeleyite grains (table 5). Immediately adjacent to that major peak are seven radioisotope ages in the range 3920–4000 Ma, one Sm-Nd isochron age and six various U-Th-Pb ages, these determined respectively using whole rocks, pyroxene and a leachate, and on zircon and baddeleyite grains.

The minor cluster with the broader peak is in the range 1200–1720 Ma and consists of twenty (20) radioisotope ages. The highest part of that broad peak is at 1360–1440 Ma and consists of five radioisotope ages—four Ar-Ar determinations on feldspars or a whole rock, and one U-Pb isochron determination on zircons. Immediately adjacent are four radioisotope ages in the 1440–1520 Ma range (two Sm-Nd radioisotope determinations on apatite grains and two U-Th-Pb radioisotope determinations, one on zircon and one on apatite grains), and four radioisotope ages in the 1520-1600 Ma range (one K-Ar model age for a whole rock and three U-Th-Pb determinations, two on zircon and one on apatite grains).

The 300 ± 1 Ma date is an extreme outlier (fig. 19), being the youngest U-Pb concordia age for a suite of zircon grains in NWA7533 (table 5) which Costa et al. (2020) regarded as detrital zircon grains and thus not representative of the igneous clasts in the breccia. And finally, between the two clusters are four radioisotope ages—an Ar-Ar plateau age of 2120 Ma for plagioclase, two Rb-Sr isochron ages of 2089 Ma and 2700 Ma determined using whole rocks and mineral separates, and leachates and residues, and a Sm-Nd isochron age of 2190 Ma determined on a whole rock and mineral separates. These are potentially indicative of some occasional disturbances in these radioisotope systems, especially in plagioclase if it has experienced some shock metamorphism.

The Conventional Explanation for these Radioisotope Ages

Martian Meteorite Radioisotope Ages

The majority of the shergottites are mid to late Amazonian in age according to the Martian timescale (fig. 20), with enriched shergottite crystallization ages ranging from 165 to 225 Ma (Borg, Gaffney, and DePaulo 2008; Combs et al. 2019; Ferdous et al. 2017; Lapen et al. 2009; Moser et al. 2013; Nyquist et al. 2001b; Shafer et al. 2010b; Usui et al. 2010), intermediate shergottites ranging from 150 to 346 Ma (Borg et al. 2002; Nyquist et al. 2001b, 2009), and depleted shergottite ages from 327 Ma to 2.4 Ga, including NWA7635 and NWA8159 (Brennecka, Borg, and Wadhwa 2014; Herd et al. 2017a; Lapen et al. 2017; Nyquist et al. 2001b; Shih et al. 2011a). In contrast, nakhlites and chassignites have been dated to ~1.3 Ga early Amazonian ages (figs. 16, 17, and 20) (Borg et al. 2002, 2003; Brennecka, Borg, and Wadhwa 2014; Cohen et al. 2017; Herd et al. 2017a; Lapen et al. 2017; Nyquist et al. 2001b, 2009; Righter et al. 2018).

Using Pb-Pb isotopic compositions, Bouvier, Blichert-Toft, and Albarède (2009) and Bouvier et al. (2008, 2018) proposed >4 Ga Noachian ages for all shergottites. However, other isotopic systems, such as Rb-Sr, Lu-Hf, Sm-Nd, U-Pb, and Re-Os, are concordant and yield Amazonian ages (fig.

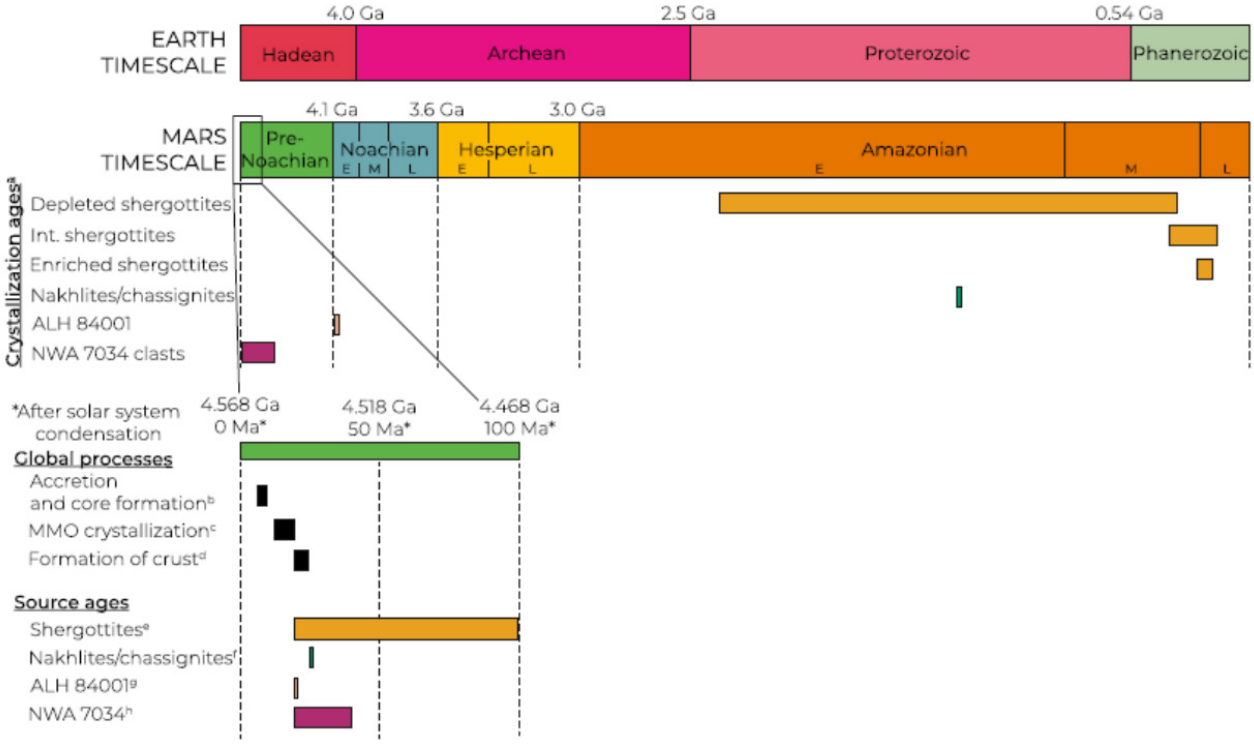

Fig. 20. Timeline of major processes in Mars' history based on Martian meteorite studies, including measured crystallization ages, interpreted source ages, and interpreted global processes (after Udry et al. 2020), as also seen in the spread of published ages in fig. 15. The designated Martian age periods are from the Hartmann and Neukum (2001) chronology with thinner lines representing different divisions of Martian periods (for example, E = early, M = mid, and L = late), as compared with earth's geologic timescale.

15). Bellucci et al. (2015b) proposed that the Pb-Pb compositions of shergottites do not represent an >4 Ga isochron age, but minor additions from an additional highly radiogenic, probably crustal reservoir on Mars. The radiogenic Pb component may be widespread and mixed into virtually every Martian meteorite (Bellucci et al. 2016; Gaffney et al. 2011). Gaffney et al. (2011) showed that maskelynite is more susceptible to Pb disturbance than other minerals. Maskelynite is a diaplectic glass formed during shock and is common in shergottites, which have Sm-Nd and Pb-Pb isochron ages that are identical within uncertainties. Gaffney, Borg, and Connelly (2007) also observed that U-Pb ages generated older apparent ages (~4.3 Ga) for shergottites that they interpreted as being erroneous. Furthermore, Niihara et al. (2012) showed that U-Pb baddeleyite ages were not reset through shock but give younger ages than bulk rock Pb-Pb data, and thus support "young" ages for shergottites. The combined evidence from independent isotopic systems (Ar-Ar, Rb-Sr, Lu-Hf, Sm-Nd, Re-Os, and U-Pb) is that the shergottites have relatively young eruption ages, between 150 and 2,400 Ma. The cause of this apparent discrepancy between whole-rock Pb-Pb in some Martian samples and the other long-lived isotope systems (Rb-Sr, Lu-Hf, Sm-Nd, and Re-Os) is yet to be resolved.

However, there are two definite Noachian lithologies known from Martian meteorites (fig. 20). The orthopyroxenite ALH 84001 has been dated with igneous crystallization age of 4.09±0.03 Ga (Lapen et al. 2010), and has younger carbonates dated at 3.95 Ga (fig. 18) (Beard et al. 2013; Borg et al. 1999). The polymict regolith breccias NWA7034/7533 have within them igneous clasts that contain the oldest dated Martian minerals, which are zircons >4300 Ma up to 4476±1 Ma (figs. 19 and 21), with a minimum source model age of 4547 Ma, suggesting the formation of an extremely old enriched and andesitic primordial crust, as the last stage of postulated magma ocean crystallization (Baziotis et al. 2018; Bellucci et al. 2018; Bouvier et al. 2018; Hu et al. 2019; Lapen et al. 2010; McCubbin et al. 2016; Nyquist et al. 2016). The fact that some alkaline clasts have crystallization ages of ~4.4 Ga show that alkaline magmatism presumably occurred early in Martian history, possibly due to early partial melting of mantle or contamination of primary magmas by the early alkali-rich Martian crust (McCubbin et al. 2016). It has been suggested also that the breccias NWA7034/7533 likely assembled by pyroclastic eruption(s) and/or impact event(s), then underwent lithification represented by a thermal event at ~1500–1100 Ma, as indicated by the cluster of those ages in figs. 19 and 21 (Bridges et al. 2017; Goderis et

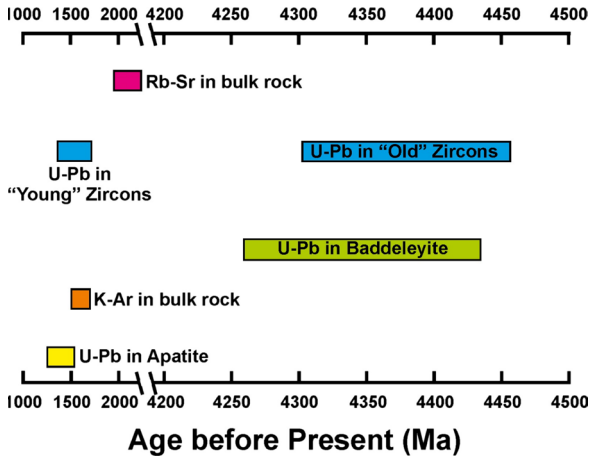

Fig. 21. Summary of ages for matrix, clast, and bulk rock of NWA 7034/7533 (after Nyquist et al. 2016) as listed in table 5. The full ranges of ages and their associated uncertainties are represented by the widths of the colored rectangles. U-Pb zircon ages (blue rectangle) are from Humayun et al. (2013), Tartèse et al. (2014), Yin et al. (2014), and Nemchin et al. (2014). U-Pb baddeleyite ages from Tartèse et al. (2014) (green rectangle). A Rb-Sr bulk-rock isochron age (Agee et al. 2013; pink rectangle), K-Ar bulk-rock age from Cartwright et al. (2014) (orange rectangle), U-Pb isochron age from apatite (Bellucci et al. 2015b; McCubbin et al. 2015; Yin et al. 2014; yellow rectangle).

al. 2016; MacArthur et al. 2019; McCubbin et al. 2016). Alternatively, Cassata et al. (2018) proposed that contact metamorphism occurred between ~1500 and 1200 Ma based on $^{40}Ar/^{39}Ar$ ages (table 5 and figs. 19 and 21), with brecciation and lithification happening at ≤225 Ma. The contact metamorphic event could coincide with a ^{37}Cl-rich fluid metamorphic event at ~1.6 Ma (Hu et al. 2019).

Identifying Martian Meteorite Igneous Lithologies

Meteorites are the only rock samples currently available from Mars. Crater-forming meteorite impact events on Mars generated sufficient energy to eject fragments of the crust at greater than the escape velocity ~5 km/s (Fritz, Artemieva, and Greshake 2005) through the atmosphere and into space through near-surface spallation (Head, Melosh, and Ivanov 2002). Fragments of these ejection events represent the Martian meteorites that have so far been recovered. Laboratory studies have determined their chemistry, mineralogy, elemental, and isotopic compositions, as well as physical properties of samples from hand-sample to the atomic scale. However, there is little to no field location context for these studied Martian meteorites. Nonetheless, using samples, evolutionary (uniformitarian) scientists claim that several fundamental planetary processes have been documented. These include the timing and nature of emplacement and formation of magmatic rocks on Mars, the nature and timing of postulated planetary accretion and differentiation, the chemical and isotopic diversity of the Martian mantle, the distribution and evolution of volatile compounds in and on Mars, environments and timing of alteration and weathering, and impact processes (Udry et al. 2020) (fig. 22).

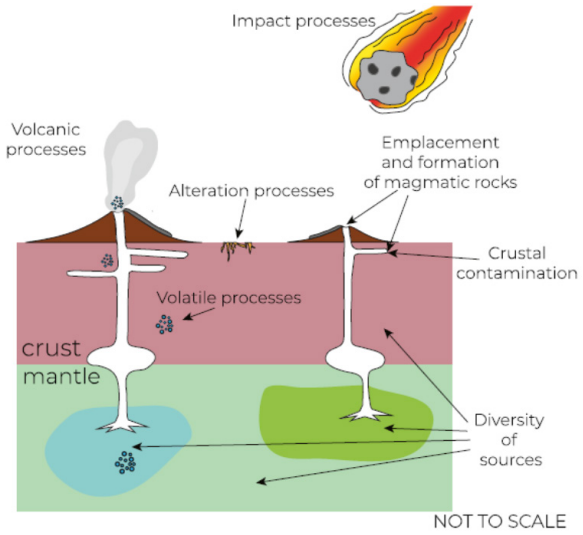

Fig. 22. Schematic diagram representing the different kinds of information that Martian meteorites can provide about the Martian surface and interior (after Udry et al. 2020). Blue bubbles represent highly volatile compounds, such as OH, H_2O, CO_2, Cl, and S. Not to scale.

The diversity in textures and mineralogies observed in Martian meteorites would appear to indicate various emplacement processes close to the surface of Mars. The increasing number of supposed ejection age determinations have allowed groupings of meteorites into different ejection sites and volcanic systems, and thus, provide more constraints on the evolution of their magmas and volcanic systems. Two examples of proposed cogenetic relationships include the nakhlite-chassignite association, where complementary igneous compositions and crystallization and ejection ages all imply that they originate from the same or a similar volcano-magmatic edifice on Mars (McCubbin et al. 2013; Udry and Day 2018). Another is represented by a group of shergottite specimens that have identical ejection ages at 1.1 Ma and similar geochemical and isotopic characteristics, perhaps representing a magmatic center active for at least 2 Ga (Lapen et al. 2017).

Based on bulk major element compositions, shergottites from enriched, intermediate, and depleted sources have been calculated to originate from mantle sources with anomalous mantle potential temperatures (~1750°C) compared to Noachian rocks from Gale crater (~1450°C), and thus represent

products from a hot mantle plume (Filiberto 2017). The large number of shergottite specimens enables a better understanding of how the different subtypes (poikilitic, gabbroic, basaltic, and olivine-phyric) were apparently emplaced in the Martian crust and surface; a schematic representation is presented in fig. 23 (Udry et al. 2020).

Olivine-phyric shergottites contain zoned olivine megacrysts that would have co-crystallized at depth within magma staging chambers, likely close to the base of the crust (based on pyroxene Ti/Al thermometry). These crystals were entrained in an ascending magma, which then either erupted at the surface or were emplaced in the near-surface hypabyssal environment. Some of the olivine-phyric shergottites are thus believed to represent the closest approximation of primary Martian mantle derived magmas, for example, Y 980459, NWA 5789, NWA 6234, and NWA1068 (Collinet et al. 2017; Gross et al. 2011, 2013; Mussel White et al. 2006; Usui, McSween, and Floss 2008).

Poikilitic shergottites are characterized by coarse-grained large low-Ca pyroxene crystals with high-Ca rims enclosing olivine and chromite chadacrysts. As with olivine-phyric shergottites, these phases likely crystallized close to the crust-mantle boundary, based on pyroxene Ti/Al thermometry (Rahib et al. 2019). Pyroxene oikocrysts were entrained and transported to shallower depths during magma ascent, at which point additional pyroxene and olivine co-crystallized, as informed by mineral composition and quantitative textural analyses (fig. 22) (Combs et al. 2019; Howarth et al. 2014, 2015; Rahib et al. 2019). The high abundance of olivine with resultant high bulk-rock MgO contents of the poikilitic shergottites clearly indicates significant accumulation of olivine during their emplacement in the crust and thus these meteorites do not represent primary mantle melts. Plagioclase, along with accessory phases, then crystallized during emplacement as shallow sills.

Basaltic and gabbroic shergottites appear to have formed from relatively evolved magmas that have undergone previous stages of olivine crystallization and fractionation and complete loss of olivine phenocrysts from the system. They are marked by pyroxene crystallization at depths, possibly within the same magma staging chambers where olivine fractionation occurred, followed by subsequent plagioclase and accessory mineral crystallization during emplacement at the surface as a flow or within the near-surface hypabyssal environment (fig. 23) (Howarth, Udry, and Day 2018). Although most shergottites show some degree of accumulation of early formed phases (olivine and pyroxene), most basaltic shergottites likely erupted onto the surface as lava flows (Liu et al. 2016).

Thus, according to their mineralogy, bulk chemistry, and isotopic compositions, the different subtypes of

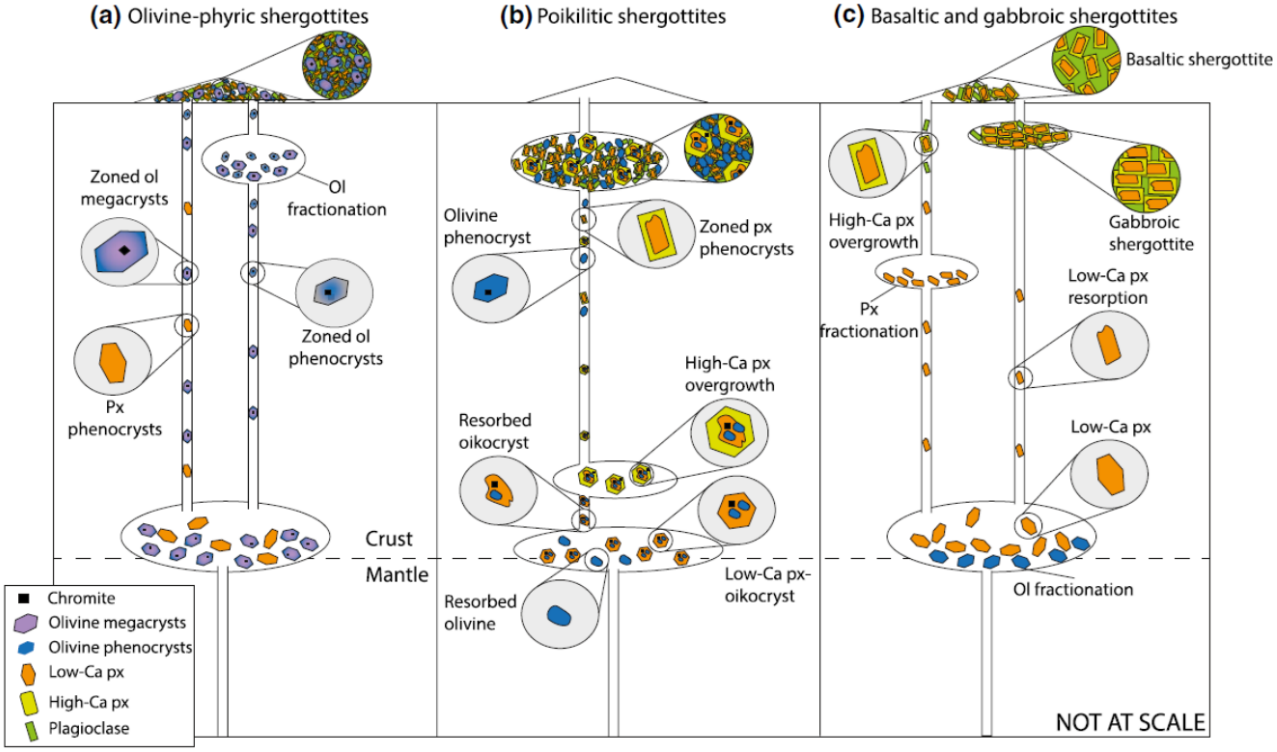

Fig. 23. Interpretation of possible emplacement scenarios for (a) olivine-phyric, (b) poikilitic, and (c) basaltic and gabbroic shergottites (after Udry et al. 2020). Note that the relative grain size of different mineral in the different types of shergottites are not at the same scale.

shergottites are likely petrogenetically linked (Rahib et al. 2019; Treiman and Filiberto 2015), signifying that different subtypes can originate from the same magmatic systems or bodies. Based on texture, isotopic composition, and mineralogy, poikilitic shergottites may have formed from fractionation of an originally olivine-phyric shergottite-like magma through fractionation of olivine within the same staging chambers at depth (Filiberto et al. 2018; Rahib et al. 2019; Udry et al. 2017). Early pulses of magma ascending from the staging chambers incorporated predominantly olivine and formed olivine-phyric shergottites at the surface, whereas later ascending magmas incorporated more pyroxene oikocrysts and formed the poikilitic shergottites at the surface (Combs et al. 2019). Basaltic shergottites may also have formed from an olivine-phyric shergottite magma, through fractionation of olivine or lack of olivine entrainment (Combs et al. 2019; Filiberto et al. 2012; Treiman and Filiberto 2015; Udry et al. 2017). Gabbroic shergottites are also likely linked to basaltic shergottites (fig. 23). For example, the gabbroic NWA 7320 originated from a common volcanic system with the basaltic shergottites, Los Angeles and NWA 856, based on similar mineralogy and isotopic composition (Udry et al. 2017). NWA 7320 represents a subvolcanic cumulate version of a basaltic shergottite that erupted at the surface. Some of the gabbroic meteorites could represent the feeder dike system that fed the lava flows represented by the basaltic shergottites. The petrogenetic link between groups of shergottites is also supported by the fact that approximately twenty depleted shergottites, including basaltic and olivine-phyric shergottites, and the augite-rich types (NWA 7635 and 8159), have ejection ages within error of 1.1Ma, suggesting that they originated from the same long-lived volcanic system, active from at least 327 to 2403Ma (Brennecka, Borg, and Wadhwa 2014; Lapen et al. 2017).

Due to lack of calibrations for Martian conditions, few geobarometers have been used to constrain the depth of crystallization of Martian meteorite phenocryst/megacryst phases. Pyroxene Ti/Al can help to constrain a range of approximate pressures of crystallization (Filiberto et al. 2010; Nekvasil et al. 2007). The application of this geobarometer to various shergottites and chassignites suggests that formation of staging chambers at the crust/mantle boundary may have been widespread on Mars, possibly leading to the formation of the various shergottite lithologies (Combs et al. 2019; Dunham et al. 2019; Filiberto 2017; Howarth, Udry, and Day 2018; Nekvasil et al. 2004; Rahib et al. 2019; Udry et al. 2017).

Minor element compositions in pyroxene in nakhlites also suggest that they could have formed at the bottom of the Martian crust (McCubbin et al. 2013; Udry and Day 2018). In contrast to shergottites, which originated from different localities, the nakhlite and chassignite meteorites have been inferred to be derived from a large igneous pile. A recent comprehensive study by Udry and Day (2018) showed that nakhlites and chassignites were likely emplaced as various lava flows and/or hypabyssal sills according to their different mineralogies, cooling rates, and qualitative and quantitative textures, similar in many ways to volcanic emplacement on earth (Balta et al. 2017; Corrigan, Velbel, and Vicenzi 2015; Daly et al. 2019b; Jambon et al. 2016; Udry and Day 2018). At least five eruptive events for the nakhlites are suggested by their $^{40}Ar/^{39}Ar$ ages that vary between 1415±7 (Y000749) to 1322±9Ma (Lafayette) (Cohen et al. 2017), with the youngest events at 1215±67Ma (Krämer Ruggiu et al. 2020) (table 2).

Radiogenic isotope data of nakhlites as a whole are similar to depleted/intermediate shergottites. However, there are distinct differences that appear to preclude or complicate genetic relationships between shergottites (including ALH 84001) and nakhlites. For example, all shergottites plot as a linear array on a $^{142}Nd/^{144}Nd$(measured) versus $^{143}Nd/^{144}Nd$(source calculated at the present day) diagram (Borg, Brennecka, and Symes 2016; Caro et al. 2008; Debaille et al. 2007; Lapen et al. 2017). Regardless of whether the linear array represents a mixing line between depleted and enriched mantle sources (Debaille et al. 2007; Lapen et al. 2017) or that the slope of the array has age significance (Borg, Brennecka, and Symes 2016), the nakhlites do not plot on this array requiring that the nakhlite mantle source has a different early evolution than shergottite sources. Based on ^{176}Lu-^{176}Hf, ^{146}Sm-^{142}Nd, ^{147}Sm-^{143}Nd, and W isotope compositions of nakhlites, Debaille et al. (2009) proposed a model of early majoritic garnet fractionation that explains the apparent decoupling of W, Hf, and Nd isotopes observed in these meteorites and not shergottites. Given that there is as yet no evidence for isotopic mixing between shergottite and nakhlite mantle sources, these reservoirs and the melts derived from them seem to have remained isolated from one another during their petrogeneses.

Based on their bulk trace element compositions, nakhlite, chassignite, and shergottite-like magmas have all been predicted to have been produced from large plume-fed systems (Day et al. 2018). In order to explain the distinct mantle sources, it has been proposed that shergottites and nakhlites represent main shield and later rejuvenated magmas from metasomatized lithosphere, respectively, in a stagnant-lid regime (Day et al. 2018). This process

is represented in fig. 24 (Udry et al. 2020). Due to eruption of a large volume of shergottite lavas during the supposed main shield period, load is emplaced unevenly on the underlying lithosphere, leading to flexure and the development of a flexural bulge outboard of the volcanic edifice. Flexural moats and bulges are observed on earth in the Hawaiian-Emperor chain volcanoes and also occur, based on gravity, in the Tharsis volcanic province on Mars (Genova et al. 2016; Sandwell et al. 2014). A previously depleted mantle is required for the source of nakhlites based on their Sr-Nd isotope systematics, which had to be metasomatized in order to induce localized partial melting through decompression during lithospheric flexure. This depleted mantle likely represents Martian lithosphere, and so the apparent cause of ^{182}W and ^{142}Nd isotope variations in nakhlites would seem to relate to the early formation of the Martian lithosphere, or by inheritance from metasomatizing partial melts from deeper mantle sources, but also could be a consequence of both processes.

Formation of Mars and Martian Mantle Reservoirs

Martian meteorites potentially allow the timing of planet-formation processes to be postulated using isotopic and elemental compositions inherited from their source reservoirs. Both earth and Mars have geochemically and isotopically distinct components, but Mars does not seem to have plate tectonics that would have facilitated mixing and dilution of primordial components (Debaille et al. 2013). Thus, Mars retains a higher resolution record of mantle heterogeneities produced during supposed early planetary differentiation. Such mantle heterogeneities were assessed using trace elements and isotopic compositions, including ^{146,147}Sm-^{142,143}Nd, ^{182}Hf-^{182}W, ^{176}Lu/^{177}Hf, U-Pb, ^{87}Rb-^{87}Sr, and ^{187}Re-^{187}Os, as well as redox conditions (Armytage et al. 2018; Bellucci et al. 2018; Brandon et al. 2012; Day et al. 2018; Debaille et al. 2007, 2008, 2009; Foley et al. 2005; Herd 2003; Herd et al. 2017a; Lapen et al. 2017; Tait and Day 2018; Wadhwa 2001). At least six different reservoirs have been proposed on Mars, including a mixture of three for shergottites and ALH 84001 (Lapen et al. 2010; 2017), one for the nakhlites and chassignites (Debaille et al. 2009), one for NWA 8159 (Bellucci et al. 2020), and at least one for some components in NWA 7034 (Armytage et al. 2018).

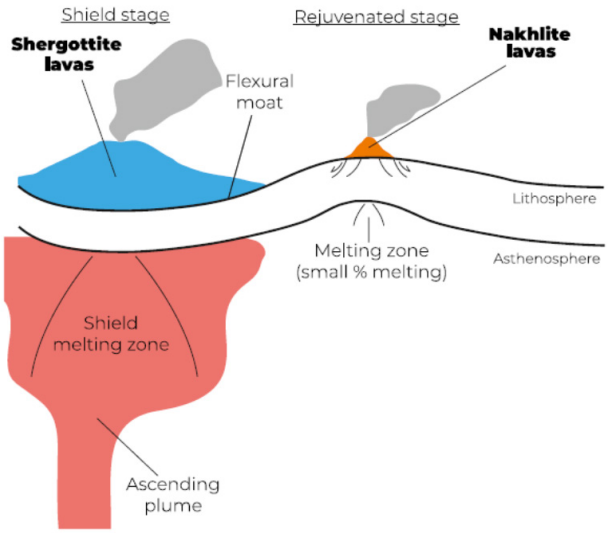

Fig. 24. Schematic diagram representing the emplacement of shergottite-like lavas versus nakhlite-like lavas based on a lithospheric flexure model (Day et al. 2018) and using a terrestrial analog from Hawaii (Bianco et al. 2005) (after Udry et al. 2020). The lithosphere above the plume is slightly thinner. Not at scale.

The mantle sources of some igneous components in the regolith breccia NWA 7034 and its paired meteorites are different from the sources of the other Martian meteorites, primarily because it is a polymict breccia with clasts of a variety of material types. Nevertheless, the isotopic composition (low ^{147}Sm/^{144}Nd and ^{176}Lu/^{177}Hf) of some clasts is consistent with an ancient LREE-enriched crust, which is distinct from the enriched shergottite source (Armytage et al. 2018; Kruijer et al. 2017; Nyquist et al. 2016). In addition, the Pb isotopic compositions of the paired regolith breccias show that a previously unknown enriched reservoir in ^{207}Pb/^{204}Pb is present in the Martian interior and is possibly crustal (Bellucci et al. 2016). Alkali basalt clasts in NWA 7034 are also highly oxidized compared to all other Martian meteorites with fO_2 of QFM+3 calculated from ilmenite-magnetite pairs (Santos et al. 2015). These clasts within NWA 7034 (and paired rocks) thus seem to provide unprecedented insights into the apparent nature of the early Martian crust and show that it was likely isotopically and chemically distinct from the sources of the other Martian meteorites.

Mars accretion and core formation is postulated to have occurred before the accretion of the earth, both estimated between 7 and 10Ma (fig. 20) (Dauphas and Pourmand 2011; Debaille et al. 2009; Foley et al. 2005; Kleine et al. 2004; Kruijer et al. 2017) after solar system condensation of calcium-aluminum-rich inclusions (CAIs) at ~4,567Ma (Amelin 2002; Connelly et al. 2012; Connelly, Bollard, and Bizzarro 2017). After a supposed initial major phase of accretion, terrestrial planets including Mars are widely believed to have undergone global and deep melting, resulting in a magma ocean (Elkins-Tanton, Parmentier, and Hess 2003). The latest estimates of the duration of crystallization of the Martian magma ocean are from 10 to 25 Ma after solar system condensation (Kruijer et al. 2017), with the

earliest estimates at 33 Ma (Borg et al. 2003), but it could have lasted up to 100 Ma (fig. 20) (Debaille et al. 2009; Elkins-Tanton, Hess, and Parmentier 2005). Following crystallization of the supposed Martian magma ocean and the formation of solid cumulates, mantle overturn apparently occurred. Mantle overturn would have been induced by the final crystallizing layers, which are inferred to have been rich in Fe and incompatible elements forming near the top of the Martian magma ocean. They would thus have been denser compared to earlier-crystallizing layers so they would therefore have sunk into the mantle (Elkins-Tanton, Parmentier, and Hess 2003). The solid cumulates that were formed during initial crystallization would then have moved within the mantle during overturn.

Large-scale mantle reservoirs, including the different sources of Martian meteorites, likely formed during supposed silicate differentiation associated with Martian mantle ocean solidification and overturn (Bouvier et al. 2018; Debaille et al. 2008, 2009; Kruijer et al. 2017). Combined W and Nd isotopic compositions of shergottites, ALH 84001, and NWA 7034, suggest a single differentiation event between 25 and 40 Ma after solar system condensation that established the mantle sources for the meteorites (Kruijer et al. 2017). Formation of components recorded in these rocks need not have been contemporaneous, nor do all enriched shergottite components need to be identical on this basis (Kruijer et al. 2017). The cumulate components of the Martian mantle ocean likely represent the depleted component(s), whereas it is postulated that the enriched component(s) are likely the last dregs of Martian magma ocean crystallization (Borg and Draper 2003; Debaille et al. 2008; Lapen et al. 2010; Moriwaki et al. 2020).

Mixing of the two could have formed the intermediate reservoir (Borg et al. 2003). The depleted shergottite reservoir might also be locally heterogeneous based on U/Pb and Sm/Nd ratios (Foley et al. 2005) and coupled Lu/Hf and Sm/Nd source systematics (Lapen et al. 2017), possibly due to later events than the Martian magma ocean, including further mixing of enriched and depleted sources or local remelting (Tait and Day 2018), or as produced directly from the Martian magma ocean crystallization processes (Debaille et al. 2008). Differentiation histories were likely different between shergottites and nakhlites/chassignites based on the ^{182}Hf-^{182}W and ^{146}Sm-^{142}Nd systems (Bellucci et al. 2018), due to possible mantle overturn (Dauphas and Pourmand 2011; Debaille et al. 2009; Foley et al. 2005). While nakhlites potentially record the mantle overturn (Debaille et al. 2009), it would be a complex heritage, with metasomatism of a depleted mantle source during plume impingement required to explain their gross geochemical characteristics (Day et al. 2018), as the nakhlite depleted source was likely metasomatized subsequently by fluids. The nakhlite mantle source likely formed before the shergottite source and might have formed during the first 10-25 Ma after CAI condensation (Borg and Drake 2005; Debaille et al. 2009; Foley et al. 2005) and have different ^{182}W than shergottites. The source of ALH 84001 also apparently formed early at ~20 Ma after CAI condensation (Kruijer et al. 2017). This source is related to, and perhaps identical with, the enriched shergottite source end-member (Lapen et al. 2010).

It is postulated that solid-state Martian magma ocean overturn and associated decompression melting could have formed the Martian crust between 20 and 100 Ma after the supposed solar system condensation (Bouvier et al. 2018; Debaille et al. 2008; Kruijer et al. 2017). The more recent estimate of crustal formation (~4,547 Ma) was calculated using the oldest zircons found in NWA 7034. This age implies that an enriched andesitic-like crust formed extremely early in Mars history at the last stages of magma ocean crystallization (Bellucci et al. 2018; McCubbin et al. 2016; Nyquist et al. 2016). The source of NWA 7034 could have formed up to ~40 Ma after CAI condensation, but as NWA 7034 is a polymict breccia, it might have originated from several sources (Kruijer et al. 2017).

Furthermore, the similarity in W-Nd isotopic composition between NWA 7034, ALH 84001, and enriched shergottites suggests that Mars is relatively simple in terms of W and Nd isotopic reservoirs. Little compositional mixing has apparently occurred throughout the entire geologic history of Mars (Blichert-Toft et al. 1999) and thus the shergottite sources have not significantly changed since their formation due to the absence of vigorous convection (Debaille et al. 2013), in particular, because of the lack of toroidal flow associated with transform boundaries (Kiefer 2003).

Possible Source Craters

To locate the possible source location of meteorites at the surface, crater features need to fit meteorite features, including the age of ejection and crystallization, the minerals present, and their modal abundances (Treiman 1995). For most meteorites, we expect their source craters to be young craters in Amazonian terrains. In addition, Bowling et al. (2020) recently showed that the size of crater can be linked to "dwell times" (time spent by meteorites at high pressure during impact) determined by the high pressure mineralogy observed in meteorites. Less than 10% of the Martian surface is younger

than 1 Ga (Hartmann and Neukum 2001), including Tharsis, Amazonis Planitia, and Elysium (fig. 25). The higher elevation of some of these areas, and thus lower density of the atmosphere, leads to easier ejection of fragments to space. Oblique and rayed craters at these locations, which represent young and high ejection velocities craters with preserved impactites, are likely the best candidates (Artemieva and Ivanov 2004; Fritz, Artemieva and Greshake 2005; Tornabene et al. 2006).

Several techniques have been attempted to try to determine meteorite source craters (Herd et al. 2024), including remote sensing spectral matching (Hamilton et al. 2003; Ody et al. 2015), combined with crater counting (Mouginis-Mark et al. 1992; Werner, Ody, and Poulet 2014), as well as impact modeling (Herd et al. 2017b, 2018). Notably, spectral matching is hindered by dust coverage, especially for the Amazonian igneous terrains (Lang et al. 2009). Modeling using a shock physics code has simulated dwell times and peak pressures of ejection of Mars-like basaltic target and constrains preimpact burial depth (Bowling et al. 2020). A crater diameter range can be inferred from this model (Herd et al. 2018). Fewer than 20 well-preserved potential source craters with diameters larger than 2.5 km in igneous terrains of Amazonian ages were identified as possible sources for four representative meteorites, Zagami, Tissint, Chassigny, and NWA8159 (Herd et al. 2018). A subset of these are currently being mapped in detail to further assess their likelihood as source craters (Hamilton et al. 2020).

Several source craters have been proposed for each group of Martian meteorites, but none have been confirmed. Even if where they were ejected from was able to be constrained, it is difficult to determine their field context. Terrains proposed by Hamilton et al. (2003) match the mineralogy of some Martian meteorites, but are not consistent with meteorite ages nor associated with young source craters. Similarly, Lang et al. (2009) proposed that lava flows in Arsia Mons show bulk compositions similar to shergottites, but these have discrepancies in mineralogy. Some craters were selected by Werner, Ody, and Poulet (2014) and Ody et al. (2015) as source craters for shergottites, including Mojave crater. However, they assumed that shergottites are Noachian in age. Nakhlite source craters were proposed at Syrtis Major, Tharsis, and Zumba and Gratteri craters, located south of Tharsis (Hamilton et al. 2003; Harvey and Hamilton 2005; Mouginis-Mark et al. 1992; Tornabene et al. 2006). Six <3 km diameter rayed craters dated at 11 Ma were identified as possible sources of nakhlites (Kereszturi and Chatzitheodoridis 2016). Daly et al. (2019a) showed that nakhlites have undergone shock metamorphism

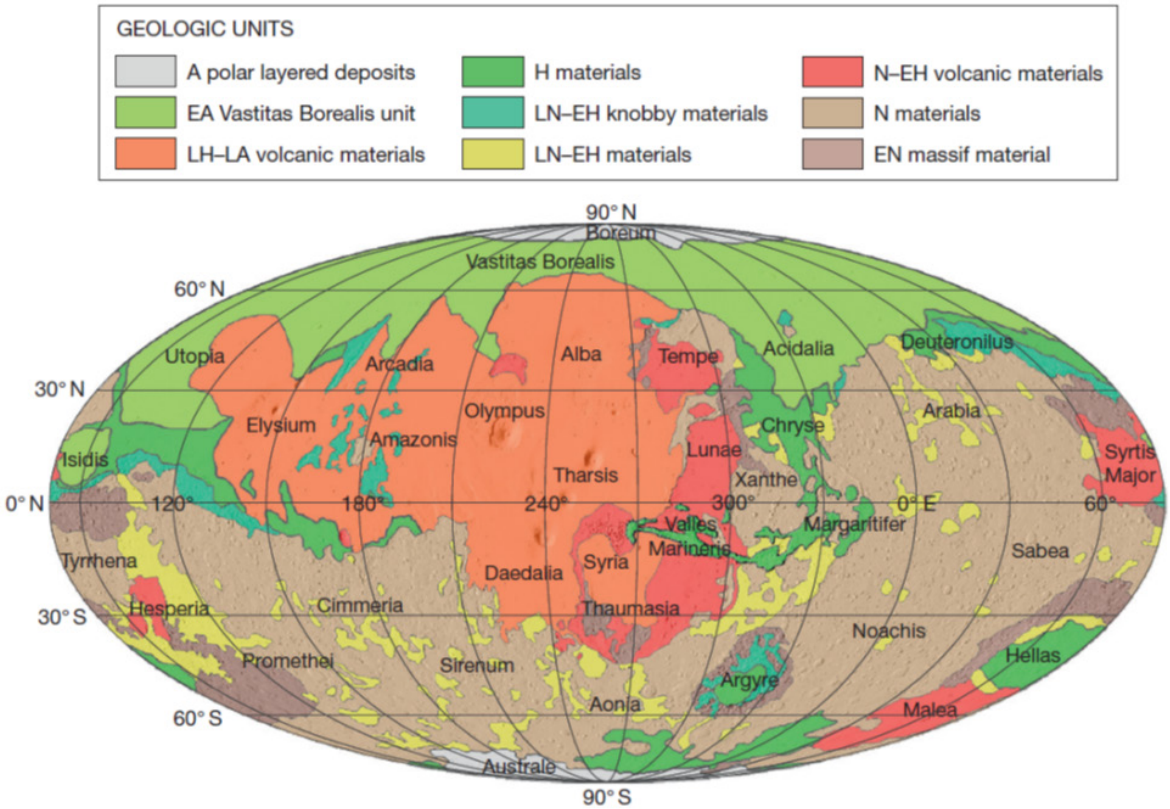

Fig. 25. Generalized geologic map of Mars (after Nimmo and Tanaka 2005). The ages of units are abbreviated as early (E) and late (L) Noachian (N), Hesperian (H), and Amazonian (A).

before 633Ma (time of aqueous alteration) and that the 11Ma nakhlite source crater should have formed close to the impact occurring before 633Ma. Nakhlites might also originate at a shield volcano flexural bulge (Day et al. 2018), but as of now, no craters in this geological context have been identified as the potential nakhlite source crater. Wittmann et al. (2015) proposed that the polymict regolith breccia NWA 7533 and paired meteorites (including NWA 7034) originated from the 6.9km diameter, ~5Ma old Gratteri crater. Until better crater counting calibration is completed the source craters for Martian meteorites will be difficult to constrain (Udry et al. 2020).

An Overview of the Geology and Geologic History of Mars

Finally, it is helpful to provide the context for the radioisotope "ages" for these Martian meteorites an overview of the geology and geologic history of Mars as conventionally determined and understood (Carr and Head 2010; McSween and McLennan 2014; Nimmo and Tanaka 2005; Tanaka et al. 2014; Udry, Ostwald, and Usui 2025). A generalized geologic map of the planet is shown in fig. 25 (Nimmo and Tanaka, 2005), as compiled by numerous Mars-surveying spacecraft. The ages and distributions of units, along with the names of major named features, are illustrated. An overview of the apparent geological activity on Mars as a function of conventional geologic time is portrayed in fig. 26 (Carr and Head 2010). And in fig. 27 (Udry, Ostwald and Usui 2025) an overview of the proposed geologic history of Mars is compared with the determined meteorite crystallization ages. However, it should be immediately evident from fig. 27 that Martian meteorites are not representative of the Martian crust, as most Martain meteorites are younger than 2.4 Ga, much younger than the average Mars crust. Furthermore, most of Mars' surface (~75%) is apparently older than 3.4 Ga (Tanaka et al. 2014).

Mars Global Surveyor gravity and topography data suggest an average crustal thickness of ~50 km, comprising 3–6% of the silicate portion of Mars (Wieczorek and Zuber 2004). The most noticeable physiographic feature is a global dichotomy in topography, crustal structure, and ages of geologic units (fig. 25). The dichotomy boundary follows approximately a great circle tilted ~30° to the equator. Its origin is unknown, but it is speculated to have formed as a result of a giant impact early in Mars history (Reese, Orth, and Solomatov 2010). South of this boundary are ancient (Noachian era), heavily cratered terrains with elevations higher than the global average. These highlands also contain the huge impact basins, Hellas and Argyre (fig. 25). North of the divide are younger (Hesperian-Amazonian), less cratered plains with lower than average elevations. The younger northern lowlands are layered sedimentary and volcanic deposits covering an ancient (Noachian) basement, comparable in age to the highlands (Frey et al. 2002). Magmatic centers hosting enormous volcanoes are represented by Tharsis and Elysium (fig. 25). Martian tectonics are dominated by Tharsis, which is surrounded by a flexural moat, radial rifts, and concentric compressional ridges. Valles Marineris, a 4000km long rift valley, extends to the east from Tharsis to the northern lowlands (fig. 25). Significantly, Mars lacks any observational evidence of plate tectonics or crustal recycling into the mantle. However, magnetic lineations discovered by Mars Global Surveyor may imply ancient crustal spreading. Superimposed on both highlands and lowlands are erosional and deposition features of apparent fluvial, glacial, and eolian origin, as well as blankets of regolith and fine red dust. Layered strata composed of H_2O and CO_2 ices mixed with dust occur at both poles (fig. 25).

Mars apparently accreted early and rapidly within 5–10Ma after the first solids supposedly formed in the solar system (Kruijer et al. 2017), then differentiated early into crust, mantle and core within a few supposed tens of millions of years of postulated solar system formation, as apparently shown by isotopic compositions in the different meteorite classes (Debaille et al. 2007). Most subsequent geologic activity was confined to the first 1.5 billion years of its history (fig. 26). Observable Martian stratigraphy is divided into the Noachian (4.1 to 3.7Ga), the Hesperian (3.7 to 3.0Ga), and the Amazonian (<3.0Ga) systems, with ages inferred from crater density measurements (Carr and Head 2010; Hartmann 2005; Hartmann and Neukum 2001). Some uncertainty in the ages of these proposed systems derives from imprecise knowledge of the production rate of impact craters on Mars through time.

The pre-Noachian era ended with the formation of the Hellas basin, which has been adopted as the base of the Noachian era (fig. 26), and which occurred at around 4.1 to 3.8Ga. Little is known of the pre-Noachian era except that early in Martian history multiple large basins formed, likely due to numerous large basin-forming impacts that probably included one that formed the global dichotomy, and it was characterized by a magnetic field due to the Martian dynamo possibly being present both before and after basin formation (Mittelholz et al. 2020).

The southern highlands and the basement under the northern lowlands are of Noachian age (Nimmo and Tanaka 2005) (fig. 25). The Noachian era, which ended at around 3.7Ga, was characterized by high

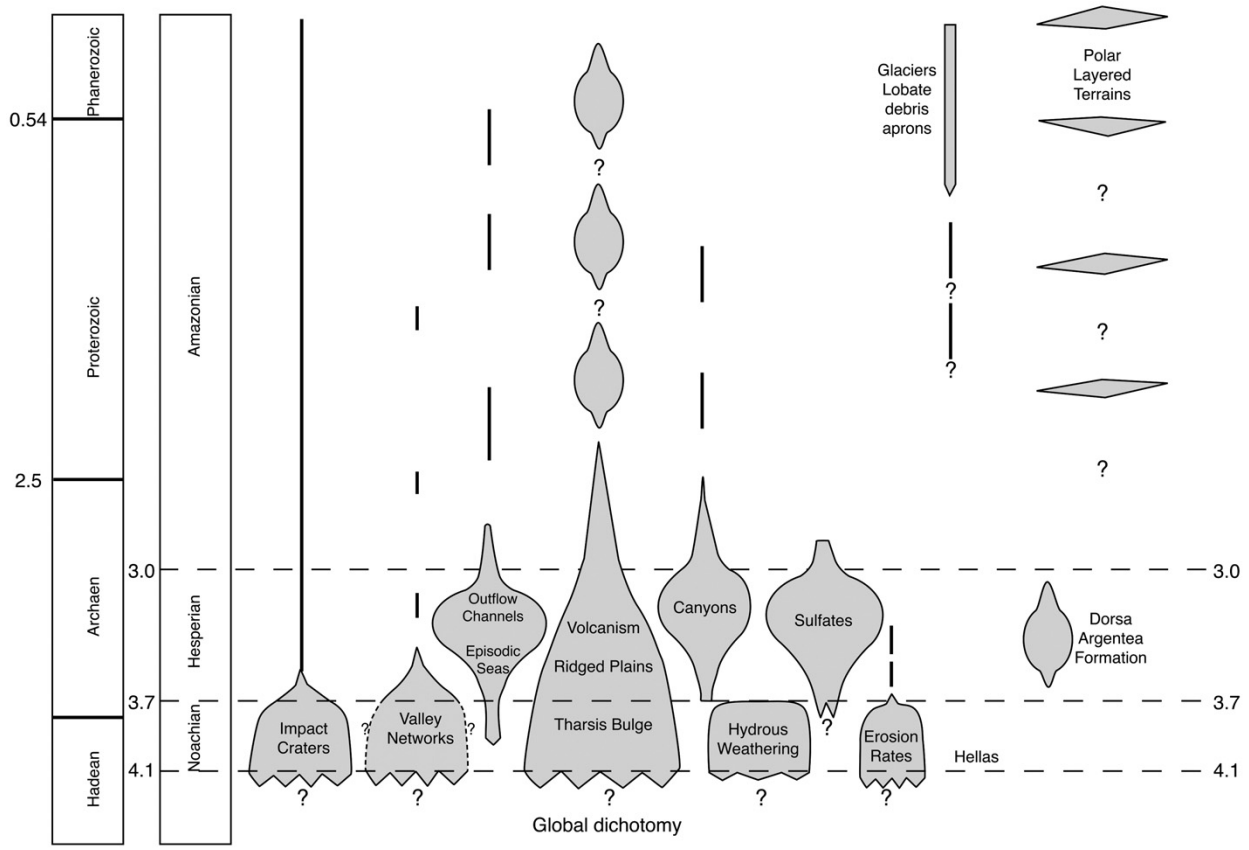

Fig. 26. Geological activity as a function of time on Mars (after Carr and Head 2010). Shown are the relative importance of different processes (impact cratering, volcanism), the time and relative rates of formation of various features and units (valley networks, Dorsa Argentea Formation), and types and rates of weathering, as a function of time. The approximate boundaries of the major time periods of Mars history are shown (Hartmann and Neukum 2001), and are compared to similar major time subdivisions in earth history (shown far left).

rates of cratering, erosion, and valley formation (Carr and Head 2010) (fig. 26). Most of Tharsis formed during this period, and surface conditions were at least episodic such as to cause widespread production of hydrous weathering products such as phyllosilicates. The Martian surface underwent weathering and water-rock interactions, as shown especially by the presence of clastic and chemically precipitated sedimentary rocks on the surface. Minerals formed from low-temperature alteration processes, including carbonates, clays, evaporites (so called), and salts (Ehlmann and Edwards 2014) (fig. 27). Extensive sulfate deposits accumulated late in the period and into the subsequent Hesperian. The clays commonly found during the Noachian era are widespread across the planet, indicating that early Mars likely had surface liquids (mostly water) with neutral pH conditions. Average erosion rates, though high compared with later epochs, appear to have fallen short of the lowest average terrestrial rates and though valley networks are common, they form an immature system that had only a modest effect in shaping the landscape. The dendritic channels on these ancient terranes might seem to suggest that warm, wet conditions necessary for perceived fluvial activity may have occurred only occasionally, particularly late in the Noachian, such as might occur if caused by large impacts, volcanic eruptions, or postulated spin-axis/orbital induced climate change.

A major change apparently occurred at the end of the Noachian era. The rates of impact, valley formation, weathering, and erosion all dropped precipitously (fig. 26). Observations suggest that the change at the end of the Noachian suppressed most aqueous activity at the surface other than large floods, and resulted in growth of a thick cryosphere. However, the presence of discrete sulfate rich deposits and sulfate concentrations in soils suggests that water activity did not decline to zero, and sulfates, carbonates and salts were likely more common until the end of the Hesperian era even as the production of clay minerals declined (fig.27). Silica (representing hydrothermal products), lava flows, igneous intrusions, and impactites are more common in Hesperian and Amazonian terrains (Ehlmann and Edwards 2014), likely because they are better preserved than those of Noachian ages.

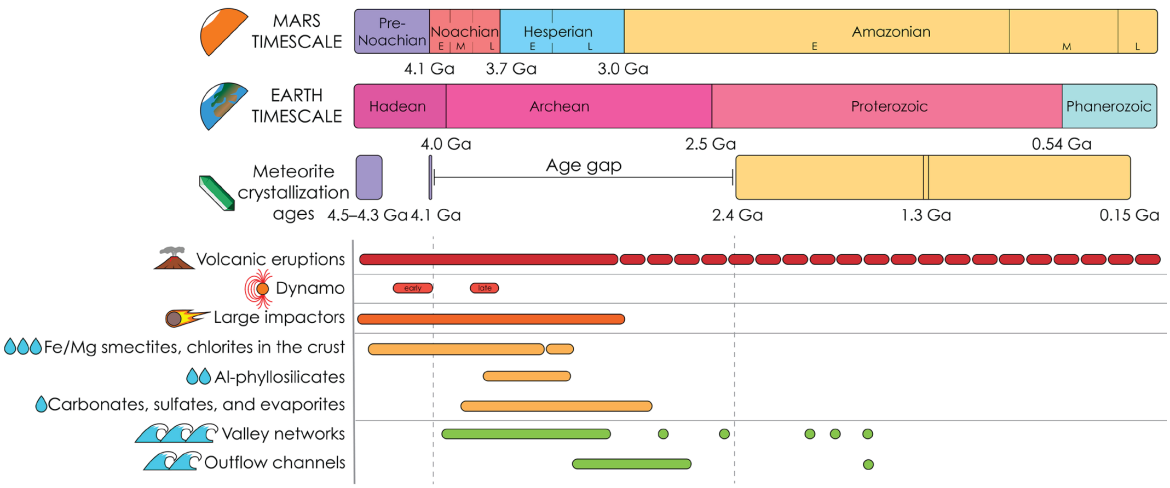

Fig. 27. An overview of the proposed geologic history of Mars compared with the determined meteorite crystallization ages (after Udry et al. 2025). Mars and Earth timescales with colors used by Tanaka et al. (2014), as well as meteorite crystallization ages, with a gap in age of meteorites between 4.1 and 2.4 Ga (Udry et al. 2020). The different processes are described in Carr and Head (2010), Ehlmann and Edwards (2014), Mittelholz et al. (2020), and Grady (2020). E = early, M = middle, L = late.

During Hesperian time, volcanism seems to have continued at a relatively high average rate, particularly in the first half, when towering volcanoes were constructed on the Tharsis and Elysium plateaus, and at least 30% of the planet was volcanically resurfaced. Large water floods apparently formed episodically, particularly in the latter parts of the Hesperian era, possibly leaving behind large bodies of water in the northern lowlands. The Valles Marineris and other canyons formed. Outflow channels episodically debouched sediments onto the northern lowlands, forming a veneer called the Vastitas Borealis Formation.

After the end of the Hesperian era at around 3 Ga the pace of geologic activity appears to have slowed further (figs. 26 and 27). In the subsequent Amazonian era, volcanic, tectonic, and fluvial sedimentation processes waned and eolian processes apparently dominated. The main era of water flooding was over, although small floods appear to have occurred episodically until geologically recent times. Canyon development apparently was largely restricted to formation of large landslides. Erosion and weathering rates remained extremely low.

The average rate of volcanism during the Amazonian era (<3 Ga) seems to have been approximately a factor of ten lower than in the Hesperian era and the sporadic volcanism was likely confined largely to volcanic provinces such as Tharsis and Elysium (Herd et al. 2024), where some relatively young volcanic flows continued to erupt (figs. 26 and 27). Magmatic processes appear to have been similar to those observed on the earth in intraplate contexts (Udry et al. 2020). However, Martian magma compositions appear to have evolved throughout Martian geologic time (Payré, Udry, and Fraeman 2024) and Martian global chemistry shows temporal trends (McSween et al. 2023). Low-Ca pyroxenes and olivine appear to be in higher concentrations in older terrains, and there seems to be a global decrease in K and other alkali elements with time, possibly due to different levels of partial melting and/or fractional crystallization, or the change of mantle source compositions over time (Ehlmann and Edwards 2014; McSween et al. 2023). Mars' crust contains evolved rocks (that is, high silica content), as observed in meteorites and at the surface by orbiters and rovers (Payré, Udry, and Fraeman 2024). Such evolved rocks appear to have been more common during the Noachian and Hesperian eras than during the Amazonian era.

The most distinctive characteristic of the Amazonian era appears to be the formation of features that have been attributed to the presence, accumulation, and movement of ice (Carr and Head 2010). Included are the polar layered deposits (fig. 25), latitude-dependent ice-rich veneers at high latitudes, glacial deposits on the flanks of tropical volcanoes, and a variety of landforms in the 30–55° latitude belts indicative of the accumulation of ice and glacial flow, including lobate debris aprons, lineated valley fill and concentric crater fill (fig. 26). Gullies on steep mid-latitude slopes seem to have formed in the latest Amazonian. The rate and latitude of formation of the ice-related features and the gullies varied as supposed changes in orbital parameters apparently affected the ice stability relation. By the Late Amazonian, Mars seems to have become the arctic desert that it is today.

A Biblical Perspective on these Radioisotope Ages

Any postulated naturalistic or uniformitarian history for the formation of Mars as the source of these meteorites, and of course for the solar system itself, is completely superseded by the divinely provided biblical account of the six normal days of God creating supernaturally during the Creation Week. The very first description of the earth in Genesis 1:2 is that it "was formless and void, and darkness was over the face of the deep." The inference is that the matter that became the solid earth originally was formless and unstructured and enveloped in water. However, early on creation Day Three, God said, "Let the waters below the heavens be gathered into one place and let the dry land appear." Since the dry land almost certainly refers to the continental crust, by this point it seems safe to assume that the earth's internal structure of core, mantle, and crust was already present. The Genesis 1 text reveals further that on Day Four God made the sun and the moon to provide light on the earth during the day and night respectively (Genesis 1:14–16). We are not specifically told that the rest of the solar system was also created on Day Four, but God did make the stars also on that day, and all the lights were placed in the expanse of the heavens to be for signs and seasons. From this description it is not unreasonable to conclude that the rest of the solar system was made by God on Day Four, including the other planets such as Mars. Furthermore, each entity God created and made during these six normal days of the Creation Week was formed exceedingly rapidly within the time and space of each normal day, so by the end of Day Four planets, moons and asteroids were completely formed entities, including those with iron-nickel cores, ultramafic mantles, and basaltic crusts, all the necessary supposed silicate-metal fractionation and crust-mantle differentiation happening exceedingly rapidly within hours, and thus not requiring the millions of years postulated by uniformitarians.

Created "Primordial" Isotopic Endowments

Given the general conventional consensus that the asteroids and at least the rocky planets including the earth and Mars consist of residual material from the formation of the solar system, Snelling (2014a, b, e, 2015b, d) proposed that the accepted coincident 4.55–4.57 Ga ages for the earth and many meteorites could be due to the earth and the parent asteroids having been created by God from the same primordial material, which He had created on Day One, as already proposed by Faulkner (1999, 2013). His proposal is based on the usages in Genesis 1 of the Hebrew words *āśâ* (meaning to do or to make) and *bārā'* (meaning to create). Because it is indisputably evident that *āśâ* is commonly used to refer to the act of fashioning something out of already-existing material (for example, the creation of man in Genesis 1:26; cf. 2:7), Faulkner (2013) contends that, apart from any contextual clues to suggest that it must bear the sense of creation out of nothing, there is a distinct possibility that the making of the astronomical bodies was instead a matter of fashioning them from material previously created on Day One. Just as the description of the earth in Genesis 1:2 is of something unfinished that God returned to over the next several days to shape and prepare, perhaps the matter that would become the astronomical bodies was likewise created on Day One but was shaped on Day Four, whereupon God brought forth their light to the earth.

Thus the simplest unifying assumption would therefore be that all such primordial material may have had the same created initial elemental and isotopic endowment (Baumgardner, 2000). But what about those isotopes that today are the products of radioactive decay? It is noteworthy that the earth appears to have the same time-integrated Pb isotopic endowment and thus display the same Pb-Pb "age" as the meteorites plotted on the geochron (Patterson 1956). The earth's current Pb isotopic endowment was represented on that geochron by the Pb isotopic composition of a modern oceanic sediment sample, which would appear to contain the time-integrated Pb isotopic endowment from the earth's beginning which was then processed through the earth's subsequent rock cycle (Tyler 1990). But is it plausible to conclude that the presently measured levels of parent U isotopes and daughter Pb isotopes both in the meteorites and in the earth correspond to the initial created isotope values *plus* the approximate 600 million years' worth of accelerated radioisotope decay during the Flood as has previously been suggested (Snelling 2014a, b, e, 2015b, d)? While the possibility could be considered that the created initial ratios of parent to daughter elements were different for the earth compared to those created for other solar system objects, that seems unwarranted if God made all the solar system objects (planets, moons, and asteroids) from the same primordial material He had created on Day One, which is consistent with them all having a common Designer. Thus, the reasoning behind that suggestion is that otherwise it would not have been possible to plot the meteorites and the earth on the same Pb-Pb geochron, or meteorites and groups of meteorites would not have yielded the same Pb-Pb, U-Pb, Rb-Sr, Sm-Nd, Lu-Hf, and Re-Os isochron ages as shown by previous studies (Snelling 2014a, b, e, 2015b, d).

More specifically it has been proposed that God created *some* of all the isotopes of each element at the beginning in the primordial material, including

those isotopes that subsequently only formed by radioisotope decay as daughter isotopes from parent isotopes, regardless of when radioisotope decay started. In other words, when God made the primordial material He included in it ^{206}Pb, ^{207}Pb, and ^{208}Pb atoms along with ^{238}U, ^{235}U, and ^{232}Th atoms. However, those primordial ^{206}Pb, ^{207}Pb, and ^{208}Pb atoms would not have been derived from radioisotope decay of ^{238}U, ^{235}U, and ^{232}Th atoms, respectively. It is reasonable to posit that God did create ^{206}Pb, ^{207}Pb, and ^{208}Pb atoms along with ^{238}U, ^{235}U, and ^{232}Th atoms, given that when He created the "primordial material" it likely had to have some initial isotopic ratios. Whether it will be possible to develop a model for those initial isotope ratios that will explain the current radioisotope data must be the goal of future research. In any case, initial isotope ratios in the primordial material need not have been in secular equilibrium, because these initial ratios are solely the ratios in what are now the daughter Pb isotopes, without any of the other isotopes in the ^{238}U, ^{235}U, and ^{232}Th decay "chains" being relevant. (However, the tendency if a large amount of accelerated decay has occurred would be to approach secular equilibrium.) Indeed, even the conventional scientific community has assumed the initial material of the solar system had the "primeval" Pb isotopic ratios as measured in the troilite (iron sulfide) in the Canyon Diablo iron meteorite, without reference to any of the intermediate daughters (Faure and Mensing 2005). This is consistent with God creating a fully-functioning universe, as typified by Him creating fruit trees already bearing fruit in fully-functioning soil on prepared land, all during Day Three, and the sun, planets, moons, asteroids and stars fully-functioning in their ordained positions and roles on Day Four.

However, zircons would seem to pose a profound challenge for this hypothesis, in that they strongly exclude Pb atoms when they crystallize from a melt. For this reason, ^{206}Pb, ^{207}Pb, and ^{208}Pb atoms found today within zircon crystals most logically would be the product of nuclear decay of the ^{238}U, ^{235}U, and ^{232}Th, isotopes that are still present in the crystals, subsequent to the crystallization of the zircons. Such an inference is consistent with the near *absence* of ^{204}Pb, which is not a product of U or Th decay. The reality of nuclear decay as the explanation for the ^{206}Pb, ^{207}Pb, and ^{208}Pb in these zircons is further supported by the presence of radiogenic ^{4}He, often at significant levels, as documented in the RATE investigations of zircons with a U-Pb age of 1.5 Ga (Vardiman, Snelling, and Chaffin 2005). It is difficult to imagine a scenario not involving radioactive decay whereby such high concentrations of ^{4}He might occur inside these crystals. In addition to the daughter products ^{206}Pb, ^{207}Pb, ^{208}Pb, and ^{4}He together with the parent isotopes ^{238}U, ^{235}U, and ^{232}Th, there is the physical evidence of nuclear decay in the form of radiohalos, fission tracks and alpha recoil tracks. Thus, to posit that God included ^{206}Pb, ^{207}Pb, and ^{208}Pb atoms along with ^{238}U, ^{235}U, and ^{232}Th atoms in the primordial material out of which He formed the solar system in ratios that commonly yield a radioisotope age of 4.55–4.57 Ga in meteorites and that the primordial ^{206}Pb, ^{207}Pb, and ^{208}Pb atoms are not derived from radioisotope decay of ^{238}U, ^{235}U, and ^{232}Th atoms, respectively, would seem difficult to defend in light of these zircon data. However, that line of reasoning from the zircon data presupposes the zircons in the earth's earliest crustal rocks crystallized from melts, when instead it is plausible based on the description in the Genesis text that those crustal rocks were directly created on Day One with primordial isotopic ratios, including even Pb isotopes in their zircon grains. Furthermore, the proposed hypothesis is that the radioisotopic ratios we measure today are the sum of those primordial ratios *plus* the ratios resulting from at least 600 million years' worth of accelerated radioisotope decay that occurred during the Flood for which we have impeccable evidence (Vardiman, Snelling, and Chaffin 2005).

It is true that the conventional geochronology community recognizes that the earth's mantle today, and thus in the past, has within it various geochemical reservoirs with distinctive isotopic signatures that reflect stirring and mixing in the mantle during the earth's history due primarily to plate tectonics recycling crustal and mantle materials (Rollinson and Pease 2021; Snelling 2000, 2005c). And it is well known that this is the case because recent basalt lavas yield very old radioisotope "ages" due to sourcing these mantle reservoirs, for example, the Pb-Pb radioisotope "ages" of 1-2 billion years form recent ocean island basalts (Snelling 2000 and references therein). Similarly, based on the isotopic analyses of Martian meteorites it is well documented that the Martian mantle also has geochemical reservoirs with distinctive isotopic signatures (Armytage et al. 2018; Bellucci et al. 2020; Debaille et al. 2009; Lapen et al., 2010, 2017; Udry et al. 2020). While those geochemical reservoirs do not appear to be well mixed, likely due to plate tectonics not having occurred on Mars, magma compositions of erupted Marian lavas appear to have evolved during Mars' geologic history possibly due to different levels of partial melting and/or fractional crystallization, or the change of mantle source compositions over time (Ehlmann and Edwards 2014; McSween et al. 2023; Payré, Udry, and Fraeman 2024; Udry et al. 2020).

Nevertheless, while it might appear difficult to account for all these isotopic signatures as being

due to a large initial isotopic abundance of daughter products and subsequent mixing of geochemical reservoirs on Mars, in the case of the earth there was a major mixing of geochemical reservoirs during the Flood cataclysm while at least 600 million years' worth of accelerated radioisotope decay was occurring concurrently. Yet it is suggested here that since it appears that Mars' geology was affected by the Flood cataclysm (see below), then Mars may also have experienced the same accompanying accelerated radioisotope decay that likewise consequently changed its primordial isotopic ratios.

When Did Accelerated Radioactive Decay Occur?

At what point in time radioactive decay began is unclear from Scripture, and is still a matter of debate among creationists. The RATE project considered the possibility of a large amount of accelerated radioisotope decay occurring during the Creation Week, as radioisotope decay may not be regarded as decay in the sense of deterioration of matter (Vardiman, Snelling, and Chaffin 2005). It is instead a transmutation process, by which one element is changed into another. The daughter element is certainly not inferior to the parent element. However, it is the ionizing radiation given off by radioactive decay as we know it today which is harmful that causes concern as to whether the radioisotope decay processes met the standard of God's declaration of His completed creation being "very good" (Genesis 1:31). Thus, it could be argued that, at the very least, from halfway through Day Three to the end of the Creation Week no radioisotope decay occurred to damage in any way God's "very good" creation.

In the context of the decay evident today due to the operation of the second law of thermodynamics, Anderson (2013) contended that there is no real biblical evidence to suggest that the second law was inoperable prior to the curse, and so argued that rather the second law was in effect from the beginning of creation. He thus also suggested that the tendency toward entropy implicit in the second law was never of a kind that conflicted with God's declaration that the creation was "very good," or that eventuated in the death of any sentient creature. On the other hand, it could be argued that radioisotope decay is more than the operation of the second law of thermodynamics, because the additional outcome is the ionizing radiation produced which is harmful to life's biological and chemical makeup. Indeed, if billions of years of accelerated radioisotope decay had occurred during the early part of the Creation Week, as considered a possibility by the RATE team (Vardiman, Snelling, and Chaffin 2005), it must have occurred prior to God's creation of plants on Day Three. Any enormous burst of ionizing radiation subsequent to then would surely have been detrimental to all life on the earth, for example, the fish, birds and animals of Days Five and Six. It is for this reason that many creationists are not comfortable theologically with postulating that accelerated radioisotope decay happened during the Creation Week, so maybe there was no radioisotope decay at all until it was started as part of the curse.

Yet it might be argued that this postulation of no radioisotope decay before the curse involves a logical fallacy. After all, gravity operated in God's "very good" creation before the curse, but gravity can cause bad things to happen, such as animals and people falling and breaking bones. However, in comparison, who would argue that water is bad just because animals and people can drown in water? It is thus contended here that comparing radioisotope decay with gravity is not comparing equivalents. That is, suggesting that just as gravity has always been "very good" in creation from the beginning to hold everything together, then there is nothing inherently "bad" about radioisotope decay in God's "very good" creation. As already stated, the radioactive decay of radioisotopes today produces ionizing radiation that causes damage to living tissues and thus would conflict with God's declaration that His creation was "very good". On the other hand, it could be argued that the topsoil, fruits and vegetables in the Garden of Eden need not have contained these radioactive isotopes, nor were they originally in living tissues, and in particular Adam and Eve's bodies. To be sure, potassium is needed in bones and for other uses in living things, but there are stable isotopes of potassium, so perhaps God did not incorporate radioactive ^{40}K in the original created kinds. Hence, it might be inferred that the existence of radioactive decay may not have been a concern in the original creation before the curse. However, this does not consider that the rocks beneath the topsoil would have contained radioisotopes, as measured today in the earliest crustal rocks, and any decay of those radioisotopes during the Creation Week would have produced ionizing radiation that penetrated through the topsoil to impinge on the living tissues God created on Days Three, Five, and Six. Thus, the RATE team concluded that any accelerated nuclear decay in those crustal rocks must have occurred prior to the creation of the plants on Day Three (Vardiman, Snelling, and Chaffin 2005). Nevertheless, it is assumed here that there was no radioisotope decay before the curse.

There is a lack of any definitive evidence of patterns of different isochron ages yielded by the different radioisotope systems in the groups of Martian meteorites in this study, as well as in the thirty-eight (38) chondrite, basaltic achondrite (eucrite), and primitive and other achondrite meteorites, and

groups of meteorites previously studied (Snelling 2014a, b, e, 2015b, d), that matches the pattern found during the RATE project (Snelling 2005c; Vardiman, Snelling, and Chaffin 2005). Just why this is the case is a subject for further study. Nevertheless, this lack of any definitive evidence of patterns of different isochron ages would seem to suggest that all these meteorites, their parent asteroids and the planet Mars did not experience any episode of accelerated radioisotope decay, either at the time of the creation of the primordial material on Day One or at the time of their formation on Day Four. This could then be taken to infer that no accelerated radioisotope decay occurred anywhere in the solar system during the Creation Week, including on the earth. Such a conclusion is based on the assumption that the mechanism of small changes to the binding forces in the nuclei of the parent radioisotopes proposed as the cause of a past episode of accelerated radioisotope decay (Vardiman, Snelling, and Chaffin 2005) would thus have affected every atom making up the earth, and by logical extension every atom of the universe at the same time, because God appears to have created the physical laws governing the universe to operate consistently through time and space.

So how might we correlate the physical histories of the earth, the Moon, and Mars? Since they all seem to display nearly the same total amount of nuclear decay of the longer half-life isotopes such as ^{238}U, assuming that all radioisotope "ages" are only due to nuclear decay, it could be tentatively and cautiously assumed that U-Pb dating does indeed provide correct relative dates for these three bodies. If that assumption is valid, what specific conclusions might be reached? For example, what radioisotope age should correspond to Day Three on earth after the dry land had appeared and God had created plants and fruit trees bearing fruit? If there was negligible or no nuclear decay from the time God created plants on Day Three and the Flood, then all igneous rocks that today display a radioisotope age greater than about 600 Ma, which is the approximate radioisotope age for the onset of the Flood, must have formed prior to the end of Day Three! This is consistent with the findings of the RATE team that at least 600 Ma worth of accelerated nuclear decay occurred during the Flood.

That inference has profound implications. For the earth, it means that zircons with more than about 600 Ma worth of radiogenic daughter products crystallized prior to sometime during Day Three. This, of course, includes zircons in all the granites that today form the basement rocks of the continents. Relative to such zircons in rocks from the Moon and Mars with U-Pb ages greater than 600 Ma, it likewise means that these rocks date to Creation Day Three or before. That might imply the planetary history of Mars referred to as Noachian, Hesperian, and Amazonian all unfolded prior to the end of Day Three. It might similarly imply the so-called Late Heavy Bombardment of the Moon and other inner solar system bodies likewise occurred prior to the end of Day Three. However, other considerations (see below) might instead correlate the Martian Noachian and Hesperian eras, and the impact cratering, with the biblical Flood cataclysm on the earth.

But what about the possible conclusion that the sun, moon, and stars were not created by God until Day Four? Note that the focus of the text of Genesis 1:14–19 is on lights in the expanse of the heavens, a greater light to rule the day and a lesser light to rule the night. Together with the stars, the text says that God placed them in the expanse of the heavens to give light on the earth, to govern the day and the night, and to separate the light from the darkness. The focus is not just on the physical bodies themselves but on the light they give forth. If, as mentioned earlier, the primordial matter from which the earth, moon, sun, and planets were made all had the same initial elemental and isotopic composition and was possibly present beginning on Day One, the question immediately arises as to where all this material that was to become the sun, moon, and planets was "warehoused" during Days One, Two, and Three if these bodies did not come into existence until Day Four. However, the text does seem to exclude the possibility that these bodies were created by God on Day One. Thus, the alternative is that when God made the sun, moon and planets on Day Four He created more of the same primordial material, which He had used to create the earth on Day One, rather than having "warehoused" primordial material to then use. The text simply tell us He made (or fashioned) the sun, moon and stars on Day Four.

On the other hand, if the assumption is true that no accelerated radioisotope decay occurred anywhere in the solar system during the Creation Week, and it is consistent with God's work of providentially maintaining the universe after He created it, then why is there evidence of an episode of accelerated radioisotope decay in the earth, but not in these parent asteroids and their meteorite fragments, or apparently on Mars as indicated by these Martian meteorites? Indeed, these asteroidal and Martian meteorites do not have in them unequivocal physical evidence that they have experienced ~4.5 Ga worth or less of nuclear decay commensurate with their radioisotope ages. The answer would seem to be that the accelerated radioisotope decay only occurred subsequent to the end of the Creation Week during the catastrophic global Flood event on the earth, and that the parent asteroids of the asteroidal meteorites

as well as Mars and these Martian meteorites were not similarly affected. However, if the earth's atoms were affected by accelerated radioisotope decay during the Flood, then surely every other atom in the universe would have been similarly affected. And could the Flood not have had solar system wide consequences that left evidence of it, including on Mars? However, God is not bound by the physical laws He put in place at creation, as He can change them at any time anywhere or everywhere. After all, when Jesus Christ the Creator locally suspended the law of gravity as He walked on the surface of the stormy waters of the Sea of Galilee, the law of gravity was still operating at the same time to keep the disciples in their boat, their boat on the water, and the earth in space in orbit around the sun. Thus God could have made small changes to the binding forces of the nuclei of only the earth's atoms during the Flood to cause accelerated radioisotope decay only on the earth, while leaving the atoms making up the rest of the solar system and universe untouched. Perhaps the reason God initiated accelerated radioisotope decay on the earth was to generate the heat necessary to initiate and drive the catastrophic plate tectonics which reshaped the earth's surface during the Flood (Baumgardner 2003). So if catastrophic plate tectonics or a similar process occurred on other rocky plantes like Mars, then He could have similarly used accelerated radioisotope decay to generate the heat to drive tectonic processes there.

Another reason for arguing that accelerated radioisotope decay occurred in earth's rocks only during the Flood is that so far we have only found that most of the earth's rocks contain the physical evidence of the at least 600 million years' worth of radioisotope decay (as calculated using today's measured decay rates), which equates to approximately the same time period postulated by uniformitarians during which the geologic record of the Flood accumulated (Snelling 2009, 2022). This physical evidence of radioisotope decay in earth's rocks is provided by radiohalos and fission tracks (Snelling 2005a, b). However, some of the zircons in the Fenton Hill granodiorite, which have a U-Pb age of 1.5 Ga, contained 80% of the 1.5 Ga worth of radiogenic helium, in other words, 1,200 million years' worth (Humphreys 2005). So could this imply more than 600 million years' worth of accelerated nuclear decay occurred during the Flood, perhaps some of it just prior to the Flood to generate the heat needed to initiate the breaking up of the fountains of the great deep? Thus far such equivalent physical evidence of radioisotope decay has not been found in lunar rocks or Martian meteorites. Each fully-formed U radiohalo, no matter where in earth's geologic record it occurs or the supposed age of its host rock, only represents up to 100 million or so years' worth of U decay. So even if U radiohalos are in a Precambrian (pre- Flood or Creation Week) granite they still only record up to 100 million or so years' worth of U decay that occurred during the Flood (Snelling 2023). At the same time during the Flood new granites containing U radiohalos were forming in plutons which had intruded into fossil-bearing (and therefore Flood-deposited) sedimentary strata. On the other hand, at least 600 million years' worth of fission tracks are found in zircon grains in tuff beds near the base of the strata record of the Flood matching the U-Pb radioisotope ages of those same zircon grains (Snelling 2005b).

The Tentative Postulated Implications

This still does not fully explain why there is such a spread of radioisotope "ages" from 4.03 Ga to the present in the earth's rocks, or why the radioisotope "ages" of the oldest earth rock (the Acasta Gneiss, Canada) (Bowring, Williams, and Compston 1989; Stern and Bleeker 1998) and the oldest mineral in an earth rock (a zircon grain in the Jack Hills sandstone, Western Australia) (Valley et al. 2014; Wilde at al. 2001) are 4.03 Ga and 4.4 Ga respectively rather than 4.56 Ga, the supposed age of the earth. The answer *might* be that the earth's rocks, subsequent to their creation on Day One with their primordial isotopic endowment, first suffered from the processes of mixing of those isotopes and thus apparent "resetting" of what would be today conventionally regarded as radioisotope "clocks" in the mantle and crust during the Day Three "Great Upheaval" when God formed the dry land. Then the earth's rocks further suffered from mixing of isotopes and resetting of the conventional radioisotope "clocks" in the earth's mantle and crust as a consequence of the catastrophic plate tectonics during the Flood (Austin et al. 1994), as well as from the concurrent accelerated radioisotope decay during the Flood (Snelling 2000, 2005c). These mixing processes would not just have affected isochron ages. The mixing and adding or removing of parent and/or daughter isotopes produces mixing lines that are then interpreted as isochrons, but the same mixing, adding and/or subtracting of parent and/or daughter isotopes would also have reset the radioisotope model ages. In these ways the radioisotope "clocks" would have been reset in earth's rocks during various stages of both the Day Three "Great Upheaval" and the Flood, just as they were when pre-Flood crustal rocks (with older radioisotope ages) were melted to form granite magmas, which when they crystallized had their radioisotope "clocks" reset to record the younger granite formation ages. This is in stark contrast to the earlier suggestion that if there was

negligible or no nuclear decay between the time God created plants on Day Three and the Flood, then all igneous rocks that today display a radioisotope age greater than about 600 Ma, which is the approximate radioisotope age for the onset of the Flood, must have formed prior to the end of Day Three.

By comparison, the Day Three "Great Upheaval" which the Scriptures describe as occurring on the earth would not have affected other bodies in the solar system, including Mars which was the source of the meteorites in this study, because the Genesis 1 text stipulates that the planets including Mars were not created until Day Four. Thus we can be dogmatic that this Day Three "Great Upheaval" event was earth-specific, as it was designed to produce the continental crust and the dry land on the earth in readiness for the subsequent creation of plants, birds, animals, and man.

However, when Mars was formed on Day Four its formation may have included incredibly rapid silicate-metal fractionation and mantle-crust differentiation with accompanying redistribution of its created primordial elemental and isotopic endowment, the previously created parent and (what uniformitarians now interpret as) daughter isotopes, as likely happened inside the earth on Days One and Two (Baumgardner 2000). In any case, so far our observations of the surface of Mars via orbiters and rovers, plus studies of the Martian meteorites, do not indicate any "granitic" composition continental crust on Mars akin to that which formed on the earth on Day Three (figs. 25–27). Instead the crust is basaltic, equivalent to earth's oceanic crust, apart from the veneer of water-deposited sedimentary rock layers in some terrains.

Nevertheless, we do find evidence on Mars that might correlate with the global Flood cataclysm on the earth. Such evidence includes the surface water flows and episodic seas that deposited sedimentary layers of carbonates, sulfates and so-called evaporites, and eroded canyons and valley networks, accompanied by major volcanism, large impact cratering and hydrous weathering (fig. 26 and 27). On Mars the relevant geologic eras are the Noachian and Hesperian, the former name perhaps a conventional "tongue-in-cheek" hint of correlation with Noah's Flood on the earth. However, those Martian geologic eras are "dated" at between 4.1 and 3.0 Ga, which according to earth's geologic timescale is late Hadean to terminal mid-Archean (figs. 26 and 27). Then since the 3.0 Ga end of the Hesperian era on Mars in the Amazonian era to the present geologic activity has been minor by comparison to that in the Noachian and Hesperian eras, with just sporadic isolated volcanism and the minor development of polar layered terrains and glacial lobate debris aprons (fig. 26).

If the elevated geologic activity on Mars in the Noachian and Hesperian eras correlates with the biblical global Flood cataclysm on the earth, then it is immediately obvious the respective radioisotope dates do not correlate. On Mars the radioisotope dates for the Noachian and Hesperian eras are 3.0–4.1 Ga, whereas on the earth most Flood geologists date the Flood cataclysm to younger than 0.6 Ga (600 Ma), that is, most of the Phanerozoic era (see fig, 27). Is this apparent disparity in the radioisotope dates of significance? Yes, it could be consistent with Mars not having experienced the Day Three Great Upheaval which only occurred on the earth because Mars had not yet been created until Day Four. Thus Mars did not experience any adjustments to its created radioisotope endowment until when the global Flood cataclysm occurred on the earth accompanied by accelerated nuclear decay. In contrast, the earth's created radioisotope endowment potentially experienced mixing and adjusting during the Day Three Great Upheaval that made the Day Three to late Creation Week and pre-Flood radioisotope "ages" progressively younger as different mantle geochemical reservoirs were "tapped into" by magma generation and eruption of lavas. Then earth's radioisotope "ages" became progressively even younger due to the accelerated radioisotope decay accompanying the Flood cataclysm. In this scenario with progressive geologic processes over time stirring both the earth's and Mars' mantles the relative radioisotope "dates" became younger due to the accelerated radioisotope decay during the global Flood cataclysm on both the earth and Mars.

As indicated above, the major geological activity of the Noachian and Hesperian eras on Mars included giant impact cratering, so how does that correlate with the earth's global Flood cataclysm? There are just a few large impact craters on the earth, and of the 200 or so definitively identified and recognized terrestrial impact craters only about five have been categorically claimed to be Precambrian (Koeberl, Shulz, and Huber 2024; Osinski et al. 2022). That means, in spite of the recognized vagaries of "dating" terrestrial impact craters as indicated by the wide ranges of claimed "dates" for them, the vast majority of them correlate with the terrestrial global Flood cataclysm.

However, on both Mars and the earth's Moon the many large impact craters have been "dated" as being 3.1–4.0 Ga and thus are correlated with one another (Carr and Head 2010; Koeberl, Shulz, and Huber 2024; Udry et al. 2020). Faulkner (2014) has thus suggested that, due to such claimed "dates" for the lunar impact craters so early in the Moon's history, the impact cratering must have occurred on Day Four of the Creation Week soon after the Moon was

created. And due to their correlation with Martian impact craters this hypothesis would include the impact cratering on Mars also occurring on Day Four. However, it is maintained here that there could not have been any such impact cratering on creation Day Four to mar God's "very good" creation, as declared by God in Genesis 1:31. Why would God have created earth's Moon and Mars on Day Four and then have immediately caused them to be disfigured by such impact cratering? Theologically it makes no sense. And yet the Day Four cratering hypothesis is based on the inflated vagaries of "dating" those craters on the Moon and Mars based on remote sensing and the radioisotope "dating" of a few scattered lunar samples. It makes more sense to correlate the Martian impact craters in the Noachian and Hesperian eras (Udry et al. 2020) with the earth's global Flood cataclysm which was accompanied by accelerated radioisotope decay that inflated the resultant radioisotope "ages". Thus the lunar impact craters and the Moon's accompanying and subsequent geologic activity might likewise correlate with the earth's global Flood cataclysm and its accompanying accelerated radioisotope decay that would likewise have inflated the resultant radioisotope "ages" for lunar rocks.

Where to From Here?

As concluded previously by Snelling (2014a, b, e, 2015b, d) from his studies of 16 chondrite meteorites, 12 basaltic achondrites (eucrites), 10 primitive and other achondrites, and groups of chondrites, stony achondrites and irons, based on the assumptions made conventionally the 4.55–4.57 Ga radioisotope "ages" are likely not their true real-time ages. Those 4.55–4.57 Ga radioisotope "ages" were obtained primarily by Pb-Pb, U-Pb, and Re-Os isochron dating, supported by some Rb-Sr and Lu-Hf isochron dating, of whole-rock samples of those meteorites and some various constituent minerals and fractions**.** but also by the Mn-Cr and Hf-W radioisotope methods directly calibrated against Pb-Pb meteorite ages. Similarly, the spread of radioisotope "ages" obtained by the K-Ar, Ar-Ar, Rb-Sr, Sm-Nd, U-Th-Pb, Lu-Hf, and Re-Os methods (primarily isochrons) for these Martian meteorites based on the assumptions made conventionally in the use of the radioisotope dating methods are likely not their true real-time ages. The assumptions on which the radioisotope dating methods are based conventionally are simply unprovable, and in the light of the possibility of an inherited primordial geochemical signature, subsequent resetting of radioisotope "clocks" due to impact cratering of asteroids, and the evidence in earth rocks for past accelerated radioisotope decay, mixing of isotopes and resetting of radioisotope "clocks," these assumptions are unreasonable (Snelling 2000, 2005c; Vardiman, Snelling, and Chaffin 2005).

However, we still need to develop a coherent and comprehensive explanation of what these radioisotope compositions in both meteorites and earth rocks really represent and mean within our biblical young-age creation-Flood framework for earth and universe history. We have some further possible clues, as discussed here. A few Martian meteorites have retained radioisotope "ages", primarily U-Th-Pb and Sm-Nd (figs. 15, 16, 18 and 19), that appear to coincide with the planet's earliest history. Some pre–4.1 Ga radioisotope "ages" might record the planet's initial primordial (created) isotopic endowment, though partially modified by impact cratering and igneous activity (fig. 27). However, others of those radioisotope "ages" are Noachian and early Hesperian and are coincident with giant impact catering and major geologic activity on the Martian surface, including water outflows and deposition of sedimentary layers (figs. 26 and 27) that possibly correlates with the biblical global Flood cataclysm on the earth. Furthermore, most of the Martian meteorites yield younger radioisotope "ages" by all methods (figs. 15–19) appear to record subsequent sporadic melting in pockets of the Martian mantle and eruptive igneous activity, as well as surface weathering, which span the subsequent largely dormant Martian geologic activity (figs. 26 and 27).

So, if Mars was also affected by earth's global Flood cataclysm accompanied by accelerated radioisotope decay that occurred throughout the solar system, then the spread of relative radioisotope "ages" might still be reflective of Martian mantle stirring due to accelerated radioisotope decay during the Flood cataclysm and its aftermath. And if Mars was affected by earth's global Flood cataclysm and accompanying accelerated radioisotope decay, then earth's Moon would have been similarly affected. Thus, the giant impact cratering and massive basalt outpourings on the lunar surface that are also claimed to have occurred very early in the Moon's history may likewise correlate with earth's global Flood cataclysm and accompanying accelerated radioisotope decay. Therefore, the radioisotope "ages" of lunar meteorites and rocks need to be investigated in the context of the Moon's geology to determine or confirm whether the Moon was affected like Mars by that aspect of the Flood catastrophe or not, and that there is thus a similar "disconnect" between the "old" Martian and lunar Flood cataclysm's radioisotope "ages" and the "much younger" radioisotope "ages" of the rocks produced during the earth's Flood cataclysm and accompanying accelerated radioisotope decay. As already noted, this "disconnect" in radioisotope "ages" could well be due to only the earth experiencing the

creation Day Three Great Upheaval before Mars and earth's Moon were created on Day Four.

Additionally, the radioisotope dating data for many more earth rocks from all levels of the geologic record need to be collated and examined. If accelerated radioisotope decay only occurred during the Flood, then it might be expected that the radioisotope "ages" of pre-Flood (mostly Precambrian) strata determined by the different methods would be noticeably discordant (as found by Snelling 2005c), whereas the radioisotope "ages" of the strata formed during the Flood (mostly Phanerozoic) would be mostly concordant (Snelling 2005b). This difference might be expected due to the pre-Flood rocks having already been formed with their initial primordial (created) isotopic endowment and then being stirred and changed by the Day Three Great Upheaval before their radioisotope "clocks" started at the curse and then were accelerated by different amounts according to the atomic weights or decay constants (half-lives) of the parent radioisotopes at the onset of the accelerated radioisotope decay during the Flood, which continued for the full duration of the Flood event. In contrast, the Flood rocks would have had their radioisotopes mixed by plate subduction, mantle plumes and the mantle stirring due to the Flood's catastrophic plate tectonics (Austin et al. 1994; Baumgardner 2003) and then reset when those rocks were progressively formed. Thus their radioisotope "clocks" only started at different times during the accelerated radioisotope decay of the Flood event, and consequently progressively-formed Flood rocks experienced progressively less accelerated radioisotope decay than pre-Flood rocks, thus yielding progressively "younger" radioisotope "ages". It may take the collation and examination of huge radioisotope dating data sets of as many different earth rocks as possible from all levels of the geologic record to enable any firm conclusions to be made.

Whatever the radioisotope dating data for the earth's rocks may reveal, it is already well-established that there are so many problems with the radioisotope dating methods which render them totally unreliable in providing anything more than relative time markers for the different stages in the earth's history (Snelling 2000; Dickin 2005; Faure and Mensing 2005). Indeed, the investigations of determinations of the decay constants of each of the parent radioisotopes universally calibrated against the U decay constants (Snelling 2014c, d, 2015a, c, 2016) and the problems with the U decay constants and the U-Th-Pb dating methods (Snelling 2017a, b, 2018, 2019) further document the numerous uncertainties in the crucial assumptions underlying these claimed timekeepers that the conventional uniformitarian worldview relies on. Therefore, even though these Martian meteorites yield consistent radioisotope "ages" beginning around 4.55–4.57 Ga similar to the earth's claimed "age" and then spread through subsequent progressively younger apparent Martian geologic activity, these cannot be their true real-time ages, which according to the biblical paradigm are only about 6,000 and less real-time years.

Conclusions

More than sixty Martian meteorites (shergottites, nakhlites, chassignites, orthopyroxenite and polymict regolith breccias) are of igneous origin and have been radioisotope dated using the K-Ar, Ar-Ar, Rb-Sr, Sm-Nd, U-Th-Pb, Lu-Hf, and Re-Os methods. They have yielded some 3.0–4.57 Ga radioisotope "ages" that coincide with the postulated formation of Mars and the subsequent giant impact cratering, massive volcanism and water outflows that deposited sedimentary layers and carved canyons during the Martian Noachian and Hesperian eras. Other younger <3.0 Ga Amazonian era radioisotope "ages" are sporadically distributed, coinciding with minor, scattered, lingering igneous activity. The radioisotope "ages" are generally concordant, so they provide no definitive evidence of accelerated radioisotope decay having occurred during and since the formation of the Martian igneous rocks from which these meteorites came.

In the naturalistic paradigm Mars was formed at the same time as the earth formed from the solar nebula. However, in His eyewitness biblical account God specifically tells us that He created the earth on Day One of the Creation Week, and Mars, the other planets, their moons and earth's Moon were subsequently created along with the stars on Day Four. It has been suggested the Hebrew of the Genesis text allows for God to have made "primordial material" on Day One from which He made the earth on Day One and then all the non-earth components of the solar system on Day Four. Thus today's measured radioisotope compositions of these Martian meteorites may reflect in part a geochemical and isotopic signature of that "primordial material" consisting of atoms of all elemental isotopes created by God including parent isotopes and their now daughter isotopes that were at their creation not derived by radioactive decay. It is postulated here that radioisotope decay did not occur during the Creation Week because God declared at the end of Day Six that everything He had made was "very good" (Genesis 1:31). Thus radioisotope decay with its emitted ionizing radiation which damages the cells of plants, animals and humans would only have commenced when God cursed the ground. Similarly, it is postulated here that the impact cratering of

earth, its Moon, Mars and the other planets would likewise not have occurred during the Creation Week to damage God's "very good" creation.

It would appear that the giant impact cratering, massive volcanism and water outflows that deposited sedimentary layers and carved canyons during the Martian Noachian and Hesperian eras (3.0–4.1 Ga) might correlate with the global Flood cataclysm on the earth. In the subsequent Martian Amazonian era (<3.0 Ga) geologic activity was minor, localized and sporadic, as recorded in many of the Martian meteorites. However, there is thus a glaring major "disconnect" between the radioisotope "ages" for these 3.0–4.1 Ga major geologic events and rocks on Mars, and the radioisotope "ages" of <0.6 Ga (600 Ma) for rocks formed during the earth's global Flood cataclysm. It is postulated here that this "disconnect" in radioisotope "ages" is due to the earth having suffered from the Day Three Great Upheaval in which the primordial isotopic endowment was mixed and redistributed producing younger radioisotope "ages" in the resultant rocks, whereas Mars being subsequently created on Day Four was not affected and so maintained its primordial mantle isotopic endowment. Then when earth's global Flood cataclysm occurred with its accompanying accelerated radioisotope decay and stirring of mantle reservoirs due to plate subduction and mantle plumes during catastrophic plate tectonics, Mars was also affected with giant impact cratering and massive volcanism, in which its mantle reservoirs were stirred and their isotopic endowment mixed, and water outflows that deposited sedimentary layers and carved canyons. However, whereas the radioisotope "clocks" in the earth's rocks were accelerated from their pre-Flood settings through some 600 million years, the Martian rocks' radioisotope "clocks" would appear to have been mixed, reset and accelerated through some 4 billion years from their pre-Flood settings.

This scenario potentially has implications for earth's Moon, since it also did not suffer from the Day Three Great Upheaval and early in it supposed geologic history it also suffered from giant impact cratering and massive volcanism, which thus could also correlate with the earth's global Flood cataclysm. Thus, the radioisotope "ages" of lunar meteorites and rocks need to be investigated in the context of the same possible history of geologic activity that included solar-system-wide accelerated radioisotope decay during the Flood cataclysm. In any case, even though these Martian meteorites yield consistent radioisotope "ages" beginning around 4.55–4.57 Ga similar to the earth's claimed "age" and then spread through subsequent progressively younger apparent Martian geologic activity, these cannot be their true real-time ages, which according to the biblical paradigm are only about 6,000 and less real-time years.

References

Agee, Carl B., Nicole V. Wilson, Francis M. McCubbin, Karen Ziegler, Victor J. Polyak, Zachary D. Sharp, Yemane Asmerom, et al. 2013. "Unique Meteorite from Early Amazonian Mars: Water-Rich Basaltic Breccia Northwest Africa 7034." *Science* 339, no. 6121 (3 January): 780–785.

Amelin, Yuri, Alexander N. Krot, Ian D Hutcheon, and Alexander A. Ulyanov. 2002. "Lead Isotopic Ages of Chondrules and Calcium-Aluminum-Rich Inclusions." *Science* 297, no. 5587 (6 September): 1678–1683.

Amelin, Yuri, Angela Kaltenbach, Tsuyoshi Iizuka, Claudine H. Stirling, Trevor R. Ireland, Michail Petaev, and Stein B. Jacobsen. 2010. "U-Pb Chronology of the Solar System's Oldest Solids with Variable $^{238}U/^{235}U$." *Earth and Planetary Science Letters* 300, nos. 3–4 (1 December): 343–350.

Anand, Mahesh, Ray Burgess, Vera Fernandes, and M.M. Grady. 2006. "Ar-Ar Age and Halogen Characteristics of Nakhlite MIL 03346: Records of Crustal Processes on Mars." *Meteoritics and Planetary Science* 41: A16.

Anders, Edward, Charles K. Shearer, Jr., James J. Papike, Jeffrey F. Bell, Simon Clemett, Richard N. Zare, David. S McKay, Kathie Thomas-Keprta, Christopher S. Romanek, Everett K. Gibson, Jr., and Hojatollah Vali, Jr. 1996. "Evaluating the Evidence for Past Life on Mars." *Science* 274, no. 5295 (20 December): 2119–2125.

Anderson, Lee A., Jr. 2013. "Thoughts on the Goodness of Creation: In what Sense was Creation 'Perfect'?" *Answers Research Journal* 6: 391–397.

Andreasen, Rasmus, Minako Righter, Thomas J. Lapen, Anthony J. Irving, Kunihiko Nishiizumi, A.J. Timothy Jull, and Marc W. Caffee. 2014. "Lead-Lead Isotope Systematics and Terrestrial and Ejection Ages of Early Amazonian Depleted Shergotitte Northwest Africa 7635." *Lunar and Planetary Science Conference* 45: #2865.

Armytage, Rosalind M.G., Vinciane Debaille, Alan D. Brandon, and Carl B. Agee. 2018. "A Complex History of Silicate Differentiation of Mars from Nd and Hf Isotopes in Crustal Breccia NWA 7034." *Earth and Planetary Science Letters* 502 (15 November): 274–283.

Artemieva, Natalia, and Boris A. Ivanov. 2004. "Launch of Martian Meteorites in Oblique Impacts." *Icarus* 171, no. 1 (September): 84–101.

Ash, Richard D., S.F. Knott, and Grenville Turner. 1996. "A 4-Gyr Shock Age for a Martian Meteorite and Implications for the Cratering History of Mars." *Nature* 380, no. 6569 (7 March): 58–59.

Ashwal, Lewis D., Jeffrey L. Warner, and Charles A. Wood. 1982. "SNC Meteorites: Evidence Against an Asteroidal Origin." *Journal of Geophysical Research* 8, no. S01 (15 November): A393–A400.

Austin, Steven A., John R. Baumgardner, D. Russell Humphreys, Andrew A. Snelling, Larry Vardiman, and Kurt P. Wise. 1994. "Catastrophic Plate Tectonics: A Global Flood Model of Earth History." In *Proceedings of the Third International Conference on Creationism*. Edited by Robert E. Walsh, 609–621. Pittsburgh, Pennsylvania: Creation Science Fellowship.

Balta, J. Brian, Matthew E. Sanborn, Arya Udry, Meenakshi Wadhwa, and Harry Y. McSween, Jr. 2015. "Petrology and Trace Element Geochemistry of Tissint, the Newest

Shergottite Fall." *Meteoritics* and *Planetary Science* 50, no. 1 (January): 63–85.

Balta, J. Brian, Matthew E. Sanborn, Rhiannon G. Mayne, Meenakshi Wadhwa, Harry Y. McSween, Jr., and Samuel D. Crossley. 2017. "Northwest Africa 5790: A Previously Unsampled Portion of the Upper Part of the Nakhlite Pile." *Meteoritics* and *Planetary Science* 52, no. 1 (January): 36–59.

Barber, David J., and Edward R. D. Scott. 2003. "Transmission Electron Microscopy of Minerals in the Martian Meteorite Allan Hills 84001." *Meteoritics and Planetary Science* 38, no. 6 (June): 831–848.

Barrat, Jean-Alix, and Claire Bollinger. 2010. "Geochemistry of the Martian Meteorite ALH 84001, Revisited." *Meteoritics and Planetary Science* 45, no. 4 (April): 495–512.

Basu Sarbadhikari, Amit, James M. D. Day, Yang Liu, Douglas Rumble III, and Lawrence A. Taylor. 2009. "Petrogenesis of Olivine-Phyric Shergottite Larkman Nunatak 06319: Implications for Enriched Components in Martian Basalts." *Geochimica et Cosmochimica Acta* 73, no. 7 (April): 2190–2214.

Basu Sarbadhikari, A., E.V.S.S.K. Babu, and T. Vijaya Kumar. 2017. "Chemical Layering in the Upper Mantle of Mars: Evidence from Olivine-Hosted Melt Inclusions in Tissint." *Meteoritics* and *Planetary Science* 51, no. 2 (February): 1–17

Baumgardner, John R. 2000. "Distribution of Radioactive Isotopes in the Earth." In *Radioisotopes and the Age of the Earth: A Young-Earth Creationist Research Initiative*. Edited by Larry Vardiman, Andrew A. Snelling, and Eugene F. Chaffin, 49–94. El Cajon, California: Institute for Creation Research, and St. Joseph, Missouri: Creation Research Society. http://www.icr.org/rate/.

Baumgardner, John R. 2003. "Catastrophic Plate Tectonics: The Physics Behind the Flood." In *Proceedings of the Fifth International Conference on Creationism*. Edited by Robert L. Ivey, Jr., 113–126. Pittsburgh, Pennsylvania: Creation Science Fellowship.

Baziotis, Ioannis, Paul D. Asimow, Jinping Hu, Ludovic Ferrière, Chi Ma, Ana Cernok, Mahesh Anand, and Dan Topa. 2018. "High Pressure Minerals in the Chateau-Renard (L6) Ordinary Chondrite: Implications for Collisions on its Parent Body." *Scientific Reports* 8: Article number 9851. https://doi.org/10.1038/s41598-018-28191-6

Beard, Brian L., James M. Ludois, Thomas J. Lapen, and Clark M. Johnson. 2013. "Pre-4.0 Billion Year Weathering on Mars Constrained by Rb-Sr Geochronology on Meteorite ALH84001". *Earth and Planetary Science Letters* 361 (1 January): 173–182.

Beck Pierre, Jean-Alix Barrat, Philippe Gillet, Meenakshi Wadhwa, Ian A. Franchi, R.C. Greenwood, M. Bohn, J. Cotten, B. van de Moortèle, and B. Reynard. 2006. "Petrography and Geochemistry of the Chassignite Northwest Africa 2737 (NWA 2737)." *Geochimica et Cosmochimica Acta* 70, no. 8 (15 April): 2127–2139.

Bellucci Jeremy J., Alexander A. Nemchin, Martin J. Whitehouse, Joshua F. Snape, Philip A. Bland, and Gretchen K. Benedix. 2015a. "The Pb Isotopic Evolution of the Martian Mantle Constrained by Initial Pb in Martian Meteorites." *Journal of Geophysical Research: Planets* 120, no. 12 (December): 2224–2240.

Bellucci, Jeremy J., Alexander A. Nemchin, Martin J. Whitehouse, Munir Humayun, Roger H. Hewins, and Briggitte Zanda. 2015b. "Pb-isotopic Evidence for an Early, Enriched Crust on Mars." *Earth and Planetary Science Letters* 410 (15 January): 34–41.

Bellucci, Jeremy J., Alexander A. Nemchin, Martin J. Whitehouse, Joshua F. Snape, R.B. Keilman, Philip A. Bland, and Gretchen K. Benedix. 2016. "A Pb Isotopic Resolution to the Martian Meteorite Age Paradox." *Earth and Planetary Science Letters* 433 (1 January): 241–248.

Bellucci, Jeremy J., Alexander A. Nemchin, Martin J. Whitehouse, Joshua F. Snape, Philip A. Bland, Gretchen K. Benedix, and J. Roszjar. 2018. "Pb Evolution in the Martian Mantle." *Earth and Planetary Science Letters* 485 (1 March): 79–87.

Bellucci, Jeremy J., Christopher D.K. Herd, Martin J. Whitehouse, Alexander A. Nemchin, G.G. Kenny, and R.E. Merle. 2020. "Insights into the Chemical Diversity of the Martian Mantle from the Pb Isotope Systematics of Shergottite Northwest Africa 8159." *Chemical Geology* 545 (5 July): Article number 119638. https://doi.org/10.1016/j.chemgeo.2020.119638.

Berkley, J.L, Klaus Keil, and Martin Prinz. 1980. "Comparative Petrology and Origin of Governador Valadares and Other Nakhlites." *Proceedings of the Eleventh Lunar and Planetary Science Conference* 2: 1089–1102.

Bianco, Todd Anthony, Garrett Ito, Janet M. Becker, and Michael O. Garcia 2005. "Secondary Hawaiian Volcanism Formed by Flexural Arch Decompression." *Geochemistry, Geophysics, Geosystems* 6, no. 8 (August): Q08009, 1–24. https://doi.org/10.1029/2005gc000945.

Blichert-Toft, Janne, James D. Gleason, Philippe Télouk, and Francis Albarède. 1999. "The Lu-Hf Isotope Geochemistry of Shergottites and the Evolution of the Martian Mantle-Crust System." *Earth and Planetary Science Letters* 173, nos. 1–2 (November): 25–39.

Blichert-Toft, Janne, Audrey Bouvier, Jeffrey D. Vervoort, Philippe Gillet, and Francis Albarède. 2007 "Old Shergottites and Young Impact Ages." *Meteoritics and Planetary Science* 42: A20.

Bogard, Donald D., and Liaquat Husain. 1977. "A New 1.3 Aeon-Young Achondrite." *Geophysical Research Letters* 4, no. 2 (February): 69–71.

Bogard, Donald D., Liaquat Husain, and Laurence E. Nyquist. 1979 "^{40}Ar-^{39}Ar Age of the Shergotty Achondrite and Implications for its Post-Shock Thermal History." *Geochimica et Cosmochimica Acta* 43, no. 7 (July): 1047–1056.

Bogard, Donald D., and Daniel H. Garrison. 1999. "Argon-39-Argon-40 'Ages' and Trapped Argon in Martian Shergottites, Chassigny, and Allan Hills 84001." *Meteoritics and Planetary Science* 34, no. 3 (May): 451–473.

Bogard, Donald D., Daniel H. Garrison, and Timothy J. McCoy. 2000. "Chronology and Petrology of Silicates from IIE Iron Meteorites: Evidence of a Complex Parent Body Evolution." *Geochimica et Cosmochimica Acta* 64, no. 12 (June): 2133–2154.

Bogard, Donald D., and Daniel H. Garrison. 2006. "Ar-Ar Dating of Martian Chassignites, NWA2737 and Chassigny, and Nakhlite MIL03346." *Lunar and Planetary Science Conference* 37: #1108.

Bogard, Donald D., and Jisun Park. 2007. "Ar-Ar Age of NWA-1460 and Evidence For Young Formation Ages of the Shergottites." *Lunar and Planetary Science Conference* 37: #1096.

Bogard, Donald D., and Daniel H. Garrison. 2008. "^{39}Ar–^{40}Ar Age and Thermal History of Martian Dunite NWA 2737." *Earth and Planetary Science Letters* 273, nos. 3–4 (15 September): 386–392.

Bogard, Donald D., and Jisun Park. 2008. "^{39}Ar-^{40}Ar Dating of the Zagami Martian Shergottite and Implications for Magma Origin of Excess ^{40}Ar." *Meteoritics and Planetary Science* 43, no. 7 (July): 1113–1126.

Bogard Donald D., Jisun Park, and Daniel H. Garrison. 2009. "^{39}Ar-^{40}Ar 'Ages' and Origin of Excess ^{40}Ar in Martian Shergottites." *Meteoritics and Planetary Science* 44, no. 6 (June): 905–923.

Bogard, Donald D. 2011. "K–Ar Ages of Meteorites: Clues to Parent-Body Thermal Histories." *Chemie der Erde–Geochemistry* 71, no. 3 (August): 207–226.

Borg, Lars E., Laurence E. Nyquist, Larry A. Taylor, Henry Wiesmann, and Chi-Yu Shih. 1997. "Constraints on Martian Differentiation Processes from Rb-Sr and Sm-Nd Isotopic Analyses of the Basaltic Shergottite QUE 94201." *Geochimica et Cosmochimica Acta* 61, no. 22 (November): 4915–4931.

Borg, Lars E., Laurence E. Nyquist, and Henry Wiesmann. 1998. "Rb-Sr Isotopic Systematics of the Lherzolitic Shergottite LEW88516." *Lunar and Planetary Science Conference* 29 #1233.

Borg, Lars E., Laurence E. Nyquist, Henry Wiesmann, and Young D. Reese. 1998a. "Samarium-Neodymium-Isotopic Systematics of the Lherzolitic Shergottite Lewis Cliff 88516." *Meteoritics and Planetary Science* 33, no. 4: A20.

Borg, Lars E., Laurence E. Nyquist, Chi-Yu Shih, Henry Wiesmann, Young D. Reese, and James N. Connelly. 1998b. "Rb-Sr Formation Age of ALH 84001 Carbonates." *Lunar and Planetary Institute Workshop on the Issue Martian Meteorites*, A7030.

Borg, Lars E., James H. Connelly, Laurence E. Nyquist, Chi-Yu Shih, Henry Wiesmann, and Young D. Reese. 1999. "The Age of the Carbonates in Martian Meteorite ALH84001." *Science* 286, no. 5437 (1 October): 90–94.

Borg, Lars E., Laurence E. Nyquist, Henry Wiesmann, Young D. Reese, and James J. Papike. 2000. "Sr-Nd Isotopic Systematics of Martian Meteorite DaG476." *Lunar and Planetary Science Conference* 31: #1036.

Borg Lars E., Laurence E. Nyquist, Young D. Reese, Henry Wiesmann, Chi-Yu Shih, M. Ivanova, M.A. Nazarov, and Lawrence A. Taylor. 2001a. "The Age of Dhofar 019 and its Relationship to the Other Martian Meteorites." *Lunar and Planetary Science Conference* 32: #1144.

Borg, Lars E., Laurence E. Nyquist, Henry Wiesmann, and Young D. Reese. 2001b. "Rubidium-Strontium and Samarium-Neodymium Isotopic Systematics of the Lherzolitic Shergottites ALH77005 and LEW88516: Constraints on the Petrogenesis of Martian Meteorites." *Meteoritics and Planetary Science* 36: A25.

Borg, Lars E., Laurence E. Nyquist, Henry Wiesmann, and Young D. Reese. 2002. "Constraints on the Petrogenesis of Martian Meteorites from the Rb-Sr and Sm-Nd Isotopic Systematics of the Lherzolitic Shergottites ALHA77005 and LEW 88516." *Geochimica et Cosmochimica Acta* 66, no. 11 (1 June): 2037–2053.

Borg, Lars E., and David S. Draper. 2003. "A Petrogenetic Model for the Origin and Compositional Variation of the Martian Basaltic Meteorites." *Meteoritics* and *Planetary Science* 38, no. 12 (December): 1713–1731.

Borg, Lars E., Laurence E. Nyquist, Henry Wiesmann, Chi-Yu Shih, and Young D. Reese. 2003. "The Age of Dar al Gani 476 and the Differentiation History of the Martian Meteorites Inferred from their Radiogenic Isotopic Systematics." *Geochimica et Cosmochimica Acta* 67, no. 18 (15 September): 3519–3536.

Borg, Lars E., Yemane Asmeron, and Jennifer E. Edmunson. 2003. "Uranium-Lead Isotopic Systematics of the Martian Meteorite Zagami." *Lunar and Planetary Science Conference* 34: #1107.

Borg, Lars E., and Michael J. Drake. 2005. "A Review of Meteorite Evidence for the Timing of Magmatism and of Surface or Near-Surface Liquid Water on Mars." *Journal of Geophysical Research: Planets* 110, no. E12 (December): E12S03. doi:10.1029/2005JE002402.

Borg, Lars E., Jennifer E. Edmunson, and Yemane Asmerom. 2005. "Constraints on the U-Pb Isotopic Systematics of Mars Inferred from a Combined U-Pb, Rb-Sr, and Sm-Nd Isotopic Study of the Martian Meteorite Zagami." *Geochimica et Cosmochimica Acta* 69, no. 24 (15 December): 5819–5830.

Borg, Lars E., Amy M. Gaffney, and Donald J. DePaolo. 2008. "Preliminary Age of Martian Meteorite Northwest Africa 4468 and its Relationship to other Incompatible-Element-Enriched Shergottites." *Lunar and Planetary Science Conference* 39: #1851.

Borg, Lars E., Gregory A. Brennecka, and Steven J.K. Symes. 2016. "Accretion Timescale and Impact History of Mars Deduced from the Isotopic Systematics of Martian Meteorites." *Geochimica et Cosmochimica Acta* 175 (15 February): 150–167.

Bouvier, Audrey, Janne Blichert-Toft, Jeffrey D. Vervoort, and Francis Albarède. 2005a. "The Age of Zagami and Other Shergottites." *Meteoritics and Planetary Science* 40: A23.

Bouvier, Audrey, Janne Blichert-Toft, Jeffrey D. Vervoort, and Francis Albarède. 2005b. "The Age of SNC Meteorites and the Antiquity of the Martian Surface." *Earth and Planetary Science Letters* 240, no. 2 (1 December): 221– 233.

Bouvier, Audrey, Janne Blichert-Toft, Jeffrey D. Vervoort, Philippe Gillet, and Francis Albarède. 2008. "The Case for Old Basaltic Shergottites." *Earth and Planetary Science Letters* 266, nos. 1–2 (1 February): 105–124.

Bouvier, Audrey, Janne Blichert-Toft, and Francis Albarède. 2009. "Martian Meteorite Chronology and the Evolution of the Interior of Mars." *Earth and Planetary Science Letters* 280, nos. 1–4 (15 April): 285–295.

Bouvier, Laura C., Maria M. Costa, James N. Connelly, Ninna K. Jensen, Daniel Wielandt, Michael Storey, Alexander A. Nemchin, et al. 2018. "Evidence for Extremely Rapid Magma Ocean Crystallization and Crust Formation on Mars." *Nature* 558, no. 7711 (June): 586–589.

Bowling, T.J., B.C. Johnson, S.E. Wiggins, Erin L. Walton, H. Jay Melosh, and T.G. Sharp. 2020. "Dwell Time at High Pressure of Meteorites during Impact Ejection from Mars." *Icarus* 343 (June): 113689. https://doi.org/10.1016/j.icarus.2020.113689.

Bowring, Samuel A., Ian S. Williams, and William Compston. 1989. "3.96 Ga Gneisses from the Slave Province, Northwest-Territories, Canada." *Geology* 17, no. 11 (November): 971–975.

Bradley, J.P., R.P. Harvey, and Harry Y. McSween, Jr. 1996. "Magnetite Whiskers and Platelets in the ALH84001

Martian Meteorite: Evidence of Vapor Phase Growth." *Geochimica et Cosmochimica Acta* 60, no. 24 (December): 5149–5155.

Brandon Alan D., Richard J. Walker, J.W. Morgan, and G.G. Goles. 2000. "Re-Os Isotopic Evidence for Early Differentiation of the Martian Mantle." *Geochimica et Cosmochimica Acta* 64, no. 23 (1 December): 4083–4095.

Brandon Alan D., Larry E. Nyquist, Chi-Yu Shih, and Henry Wiesmann. 2004. "Rb-Sr and Sm-Nd Isotope Systematics of Shergottite NWA 856: Crystallization Age and Implications for Alteration of Hot Desert SNC Meteorites." *Lunar and Planetary Science Conference* 35: #1931.

Brandon, Alan D., Igor S. Puchtel, Richard J. Walker, James M.D. Day, Anthony J. Irving, and Lawrence A. Taylor. 2012. "Evolution of the Martian Mantle Inferred from the ^{187}Re-^{187}Os Isotope and Highly Siderophile Element Abundance Systematics of Shergottite Meteorites." *Geochimica et Cosmochimica Acta* 76 (1 January): 206–235.

Brearley, A. J., and R. H. Jones. 1998. "Chondritic Meteorites." In *Planetary Materials*. Edited by James J. Papike. *Reviews in Mineralogy* 36: 3.1–3.398. Washington DC: Mineralogical Society of America.

Brennecka, Gregory A., Lars E. Borg, Steven J.K. Symes, and Meenakshi Wadhwa. 2013. "The Age of Tissint: Sm-Nd and Rb-Sr Isotope systematics of a Martian Meteorite." *Lunar and Planetary Science Conference* 44: #1786.

Brennecka, Gregory A., Lars E. Borg, and Meenakshi Wadhwa. 2014. "Insights into the Martian Mantle: The Age and Isotopics of the Meteorite Fall Tissint." *Meteoritics and Planetary Science* 49, no. 3 (March): 412–418.

Bridges, J.C., L.J. Hicks, C. Bedford, and S.P. Schwenzer, J. MacArthur, and P.H. Edwards. 2017. "Igneous Differentiation of the Martian Crust." *First British Planetary Science Congress*: 764–904.

Burgess Ray, Greg Holland, Vera Fernandes, and Grenville Turner. 2000. "New Ar-Ar Data on Nakhla Minerals." *Goldschmidt Conference Abstracts* 5, no. 2: 266.

Cannon, Kevin M., John F. Mustard, and Carl B. Agee. 2015. "Evidence for a Widespread Basaltic Breccia Component in the Martian Low-Albedo Regions from the Reflectance Spectrum of Northwest Africa 7034." *Icarus* 252 (15 May): 150–153.

Carlson, Richard W., and Anthony J. Irving. 2004. "Pb-Hf-Sr-Nd Isotopic Systematics and Age of Nakhlite NWA 998." *Lunar and Planetary Science Conference* 35: #1442.

Carlson, Richard W., and Maud Boyet. 2009. "Short-Lived Radionuclides as Monitors of Early Crust-Mantle Differentiation on the Terrestrial Planets." *Earth and Planetary Science Letters* 279, nos. 3–4 (30 March): 147–156.

Caro, Guillaume, Bernard Bourdon, Alex N. Halliday, and Ghylaine Quitté. 2008. "Super-Chondritic Sm/Nd Ratios in Mars, the Earth and the Moon." *Nature* 452, no. 7185 (20 March): 336–339.

Carr, Michael H., and James W. Head III. 2010. "Geologic History of Mars." *Earth and Planetary Science Letters* 294, nos. 3–4 (1 June)**:** 185–203.

Cartwright J.A., Ulrich Ott, S. Hermann, and Carl B. Agee. 2013. "NWA 7034 Contains Martian Atmospheric Noble Gases." *Lunar and Planetary Science Conference* 44: #2314.

Cartwright J.A., Ulrich Ott, S. Hermann, and Carl B. Agee. 2014. "Modern Atmospheric Signatures in 4.4Ga Martian Meteorite NWA 7034." *Earth and Planetary Science Letters* 400 (15 August): 77–87.

Cassata, William S., David L. Shuster, Paul R. Renee, and Benjamin P. Weiss. 2010. "Evidence for Shock Heating and Constraints on Martian Surface Temperatures Revealed ^{40}Ar/^{39}Ar Thermochronometry of Martian Meteorites." *Geochimica et Cosmochimica Acta* 74, no. 23 (1 December): 6900–6920.

Cassata, William S., and Lars E. Borg. 2016. "A New Approach to Cosmogenic Corrections in ^{40}Ar/^{39}Ar Chronometry: Implications for the Ages of Martian Meteorites." *Geochimica et Cosmochimica Acta* 187: 279–293.

Cassata, William S., Benjamin E. Cohen, Darren F. Mark, Reto Trappitsch, Carolyn A. Crow, Joshua Wimpenny, Martin R. Lee, and Caroline L. Smith. 2018. "Chronology of Martian Breccia NWA 7034 and the Formation of the Martian Crustal Dichotomy." *Science Advances* 4, no. 5 (23 May): eaap8306. https://doi.org/10.1126/sciadv.aap8306.

Chen, J.H., and Gerald J. Wasserburg. 1986. "Formation Ages and Evolution of Shergotty and its Parent Planet from U-Th-Pb Systemics." *Geochimica et Cosmochimica Acta* 50, no. 6 (June): 955–968.

Chen, J.H., and Gerald J. Wasserburg. 1993. "LEW88516 and SNC Meteorites." *Lunar and Planetary Science Conference* 24: 275–276.

Chen, Yang, Yang Liu, Yunbin Guan, John M. Eiler, Chi Ma, George R. Rossman, and Lawrence A. Taylor. 2015. "Evidence in Tissint for Recent Subsurface Water on Mars." *Earth and Planetary Science Letters* 425 (1 September): 55–63.

Cohen, Benjamin E., Darren F. Mark, William S. Cassata, Martin R. Lee, Tim Tomkinson, and Caroline L. Smith. 2017. "Taking the Pulse of Mars via Dating of a Plume-Fed Volcano." *Nature Communications* 8: Article number 640.

Cohen, Benjamin E., Darren F. Mark, William S. Cassata, Lara M. Kalnins, Martin R. Lee, Caroline L. Smith, and David L. Shuster. 2023. "Synchronising Rock Clocks of Mars' History: Resolving the Shergottite ^{40}Ar/^{39}Ar Age Paradox." *Earth and Planetary Science Letters* 621 (1 November): Article number 118373. https://doi.org/10.1016/j.epsl.2023.118373.

Collinet, Max, Bernard Charlier, Olivier Namur, Martin Oeser, Etienne Médard, and Stefan Weyer. 2017. "Crystallization History of Enriched Shergottites from Fe and Mg Isotope Fractionation in Olivine Megacrysts." *Geochimica et Cosmochimica Acta* 207 (15 June): 277–297.

Combs, Logan M., Arya Udry, Geoffrey H. Howarth, Minako Righter, Thomas J. Lapen, Juliane Gross, Daniel K. Ross, Rachel R. Rahib, and James M.D. Day. 2019. "Petrology of the Enriched Poikilitic Shergottite Northwest Africa 10169: Insight into the Martian Interior." *Geochimica et Cosmochimica Acta* 266 (1 December): 435–462.

Connelly, James N., Martin Bizzarro, Alexander N. Krot, Åke Nordlund, Daniel Wielandt, and Marina A. Ivanova. 2012. "The Absolute Chronology and Thermal Processing of Solids in the Solar Protoplanetary Disk." *Science* 338, no. 6170 (2 November): 651–655.

Connelly, James N., J. Bollard, and Martin Bizzarro. 2017. "Pb–Pb Chronometry and the Early Solar System." *Geochimica et Cosmochimica Acta* 201 (15 March): 345–363.

Corrigan, Catherine M., Michael A. Velbel, and Edward P. Vicenzi. 2015. "Modal Abundances of Pyroxene, Olivine, and Mesostasis in Nakhlites: Heterogeneity, Variation, and Implications for Nakhlite Emplacement." *Meteoritics and Planetary Science* 50, no. 9 (September): 1497–1511.

Costa, Maria M., Ninna K. Jensen, Laura C. Bouvier, James N. Connelly, Takashi Mikouchi, M.S.A. Horstwood, J.P. Suuronen, et al. 2020. "The Internal Structure and Geodynamics of Mars Inferred from a 4.2-Gyr Zircon Record." *Proceedings of the National Academy of Sciences USA* 117, no. 49 (November 16): 30973–30979.

Cronin, John R., Sandra Pizzarello, and Dale P. Cruikshank. 1988. "Organic Matter in Carbonaceous Chondrites, Planetary Satellites, Asteroids and Comets." In *Meteorites and the Early Solar System*. Edited by J.F. Kerridge and M.S. Matthews, 819–857. Tucson, Arizona: University of Arizona Press.

Dalrymple, G. Brent. 1991. *The Age of the Earth*. Stanford, California: Stanford University Press.

Dalrymple, G. Brent. 2004. *Ancient Earth, Ancient Skies*. Stanford, California: Stanford University Press.

Daly, Luke, Martin R. Lee, Sandra Piazolo, Sammy Griffin, M. Bazargan, Fabrizio Campanale, Peter Chung, et al. 2019a. "Boom Boom Pow: Shock-Facilitated Aqueous Alteration and Evidence for Two Shock Events in the Martian Nakhlite Meteorites." *Science Advances* 5, no. 9 (4 September): eaaw5549. https://doi.org/10.1126/sciadv.aaw5549.

Daly, Luke, Sandra Piazolo, Martin R. Lee, Sammy Griffin, Peter Chung, Fabrizio Campanale, Benjamin E. Cohen, Lydia J. Hallis, Patrick W. Trimby, Raphael Baumgartner, Lucy V. Forman, and Gretchen K. Benedix. 2019b. "Understanding the Emplacement of Martian Volcanic Rocks using Petrofabrics of the Nakhlite Meteorites." *Earth and Planetary Science Letters* 520 (15 August): 220–230.

Darling, James R., Desmond E. Moser, Ivan R. Barker, Kimberly T. Tait, Kevin R. Chamberlain, Axel K. Schmitt, and Brendt C. Hyde. 2016. "Variable Microstructural Response of Baddeleyite to Shock Metamorphism in Young Basaltic Shergottite NWA 5298 and Improved U–Pb Dating of Solar System Events." *Earth and Planetary Science Letters* 444 (15 June): 1–12.

Dauphas, Nicolas, and Ali Pourmand. 2011. "Hf-W-Th Evidence for Rapid Growth of Mars and its Status as a Planetary Embryo." *Nature* 473, no. 7348 (26 May): 489–492.

Day, James M.D., Lawrence A. Taylor, Christine Floss, and Harry Y. McSween, Jr. 2006. "Petrology and Chemistry of MIL 03346 and its Significance in Understanding the Petrogenesis of Nakhlites on Mars." *Meteoritics and Planetary Science* 41, no. 4 (April): 581–606.

Day, James M.D., Kimberly T. Tait, Arya Udry, Frédéric Moynier, Yang Liu, and Clive R. Neal. 2018. "Martian Magmatism from Plume Metasomatized Mantle." *Nature Communications* 9 (22 November): 4799. https://doi.org/10.1038/s41467-018-07191-0.

Debaille, Vinciane, Alan D. Brandon, Qing-Zhu Yin, and Stein B. Jacobsen. 2007. "Coupled ^{142}Nd-^{143}Nd Evidence for a Protracted Magma Ocean in Mars." *Nature* 450 (22 November): 525–528.

Debaille, Vinciane, Qing-Zhu Yin, Alan D. Brandon, and Stein B. Jacobsen. 2008. "Martian Mantle Mineralogy Investigated by the ^{176}Lu-^{176}Hf and ^{147}Sm-^{143}Nd Systematics of Shergottites." *Earth and Planetary Science Letters* 269, nos. 1–2 (15 May): 186–199.

Debaille, Vinciane, Alan D. Brandon, Craig O'Neill, Qing-Zhu Yin, and Stein B. Jacobsen. 2009. "Early Martian Mantle Overturn Inferred from Isotopic Composition of Nakhlite Meteorites." *Nature Geoscience* 2 (20 July): 548–552.

Debaille, Vinciane, Craig O'Neill, Alan D. Brandon, Pierre Haenecour, Qing-Zhu Yin, Nadine Mattielli, and Allan H. Treiman. 2013. "Stagnant-Lid Tectonics in Early Earth Revealed by ^{142}Nd Variations in Late Archean Rocks." *Earth and Planetary Science Letters* 373 (1 July): 83–92.

Dickin, Alan P. 2005. *Radiogenic Isotope Geology*. 2nd ed. Cambridge, United Kingdom: Cambridge University Press.

Dunham, Emilie T., J. Brian Balta, Meenakshi Wadhwa, Thomas G. Sharp, and Harry Y. McSween, Jr. 2019. "Petrology and Geochemistry of Olivine-Phyric Shergottites LAR 12095 and LAR 12240: Implications for their Petrogenetic History on Mars." *Meteoritics and Planetary Science* 54, no. 4 (April): 811–835.

Ehlmann, Bethany L., and Christopher S. Edwards. 2014. "Mineralogy of the Martian Surface." *Annual Reviews in Earth and Planetary Science* 42 (May): 291–315.

Elkins-Tanton, Linda T., E.M. Parmentier, and Paul C. Hess. 2003. "Magma Ocean Fractional Crystallization and Cumulate Overturn in Terrestrial Planets: Implications for Mars." *Meteoritics and Planetary Science* 38, no. 12 (December): 1753–1771.

Elkins-Tanton, Linda T., Paul C. Hess, and E.M. Parmentier. 2005. "Possible Formation of Ancient Crust on Mars through Magma Ocean Processes." *Journal of Geophysical Research: Planets* 110, no. E12 (December): E12S01. https://doi.org/10.1029/2005JE002480.

Eugster, Otto, E. Polnau, and Dario Terribilini. 1997. "Ejection Age of Martian Lherzolite Yamato 793605, Chassigny, and Shergotty and Formation Age of Shergotty Maskelynite." *Meteoritics and Planetary Science* 32, no. 4: A40.

Eugster, Otto, H. Busemann, S. Lorenzetti, and Dario Terribilini. 2002. "Ejection Ages from Krypton-81-Krypton-83 Dating and Pre-Atmospheric Sizes of Martian Meteorites." *Meteoritics and Planetary Science* 37, no. 10 (October): 1345–1360.

Faulkner, Danny R. 1999. "A Biblically-Based Cratering Theory." *Creation Ex Nihilo Technical Journal* 13, no. 1 (April): 100–104.

Faulkner, Danny R. 2013. "A Proposal for a New Solution to the Light Travel Time Problem." *Answers Research Journal* 6 (July 24): 279–284. https://answersresearchjournal.org/solution-light-travel-time-problem/.

Faulkner, Danny R. 2014. "Interpreting Craters in Terms of the Day Four Cratering Hypothesis." *Answers Research Journal* 7: 11–25, Interpreting Craters Via Day-Four https://answersresearchjournal.org/craters-day-four-cratering-hypothesis/.

Faure, Gunter, and Teresa M. Mensing. 2005. *Isotopes: Principles and Applications*. 3rd ed. Hoboken, New Jersey: John Wiley & Sons.

Ferdous, J., Alan D. Brandon, A.H. Peslier, and Z. Pirotte. 2017. "Evaluating Crustal Contributions to Enriched Shergottites from the Petrology, Trace Elements, and Rb-Sr and Sm-Nd Isotope Systematics of Northwest Africa 856." *Geochimica et Cosmochimica Acta* 211 (15 August): 280–306.

Filiberto, Justin, Donald S. Mussel White, Juliane Gross, Katherine Burgess, Loan Le, and Allan H. Treiman. 2010. "Experimental Petrology, Crystallization History, and Parental Magma Characteristics of Olivine-Phyric

Shergottite NWA 1068: Implications for the Petrogenesis of 'Enriched' Olivine-Phyric Shergottites." *Meteoritics and Planetary Science* 45, no. 8 (August): 1258–1270.

Filiberto, Justin, Emily Chin, James M.D. Day, Ian A. Franchi, Richard C. Greenwood, Juliane Gross, Sarah C. Penniston-Dorland, Susanne P. Schwenzer, and Allan H. Treiman. 2012. "Geochemistry of Intermediate Olivine-Phyric Shergottite Northwest Africa 6234, with Similarities to Basaltic Shergottite Northwest Africa 480 and Olivine-Phyric Shergottite Northwest Africa 2990." *Meteoritics and Planetary Science* 47, no. 8 (August): 1256–1273.

Filiberto, Justin, Juliane Gross, J. Trela, and Eric C. Ferré. 2014. "Gabbroic Shergottite Northwest Africa 6963: An Intrusive Sample of Mars." *American Mineralogist* 99, no. 4 (April 1): 601–606.

Filiberto, Justin, Juliana Gross, and Francis M. McCubbin. 2016. "Constraints on the Water, Chlorine, and Fluorine Content of the Martian Mantle." *Meteoritics and Planetary Science* 51, no. 11 (10 March): 2023–2035.

Filiberto, Justin. 2017. "Geochemistry of Martian Basalts with Constraints on Magma Genesis." *Chemical Geology* 466 (5 September): 1–14.

Filiberto, Justin, Juliane Gross, Arya Udry, Jarek Trela, Axel Wittmann, Kevin M. Cannon, Sarah Penniston-Dorland, Richard Ash, Victoria E. Hamilton, Andrea L. Meado, Paul Carpenter, Bradley L. Jolliff, and Eric C. Ferré. 2018. "Shergottite Northwest Africa 6963: A Pyroxene-Cumulate Martian Gabbro." *Journal of Geophysical Research: Planets* 123, no. 7 (July): 1823–1841.

Floran, R.J., Martin Prinz, P.F. Hlava, Klaus Keil, C.E. Nehru, and J.R. Hinthorne. 1978. "The Chassigny Meteorite: A Cumulate Dunite with Hydrous Amphibole-Bearing Melt Inclusions." *Geochimica et Cosmochimica Acta* 42, no. 8 (August): 1213–1229.

Foley, Catherine Nicole, Meenakshi Wadhwa, Lars E. Borg, Philip E. Janney, Rebekah Hines, and Timothy L. Grove. 2005. "The Early Differentiation History of Mars from ^{182}W-^{142}Nd Isotope Systematics in the SNC Meteorites." *Geochimica et Cosmochimica Acta* 69, no. 18 (September): 4557–4571.

Franchi, Ian A., I.P. Wright, A.S. Sexton, and C.T. Pillinger. 1999. "The Oxygen-Isotopic Composition of Earth and Mars." *Meteoritics and Planetary Science* 34, no. 4 (July): 657–661.

Frey, Herbert V., James H. Roark, Kelly M. Shockey, Erin L. Frey, and Susan E.H. Sakimoto. 2002. "Ancient Lowland on Mars." *Geophysical Research Letters* 29, no. 10 (15 May): 22-1–22-4. https://doi.org/10.1029/2001GL013832.

Fritz Jörg, Natalia Artemieva, and Ansgar Greshake. 2005. "Ejection of Martian Meteorites." *Meteoritics and Planetary Science* 40, nos. 9–10 (October): 1393–1411.

Gaffney, Amy M., Lars E. Borg, and James N. Connelly. 2007. "Uranium-Lead Isotope Systematics of Mars Inferred from the Basaltic Shergottite QUE 94201." *Geochimica et Cosmochimica Acta* 71, no.10 (15 October): 5016–5031.

Gaffney, Amy M., Lars E. Borg, Yemane Asmerom, Charles K. Shearer, Jr., and Paul V. Burger. 2011. "Disturbance of Isotope Systematics During Experimental Shock and Thermal Metamorphism of a Lunar Basalt with Implications for Martian Meteorite Chronology." *Meteoritics and Planetary Science* 46, no. 1 (January): 35–52.

Gale, N.H., J.W. Arden, and R. Hutchison. 1975. "The Chronology of the Nakhla Achondritic Meteorite." *Earth and Planetary Science Letters* 26, no. 2 (June): 195–206.

Garrison, Daniel H., and Donald D. Bogard. 2001. "Argon-39 and Argon-40 'Ages' and Trapped Argon for Three Martian Shergottites." *Meteoritics and Planetary Science* 36: A62–A63.

Geiss, Johannes, and David C. Hess. 1958. "Argon-Potassium Ages and the Isotopic Composition of Argon from Meteorites." *The Astrophysical Journal* 127 (January): 224–236.

Genova, Antonio, Sander Goossens, Frank G. Lemoine, Erwan Mazarico, Gregory A. Neumann, David E, Smith, and Maria T. Zuber. 2016. "Seasonal and Static Gravity Field of Mars from MGS, Mars Odyssey and MRO Radio Science." *Icarus* 272 (1 July): 228–245.

Goderis, Steven, Alan D. Brandon, Bernhard Mayer, and Munir Humayun. 2016. "Ancient Impactor Components Preserved and Reworked in Martian Regolith Breccia Northwest Africa 7034." *Geochimica et Cosmochimica Acta* 191 (15 October): 203–215.

Goodrich, Cyrena A. 2002. "Olivine-Phyric Martian Basalts: A New Type of Shergottite." *Meteoritics and Planetary Science* 37, no. S12: B31–B34.

Grady, Monica M. 2020. "Exploring Mars with Returned Samples." *Space Science Reviews* 216 (6 May): Article number 51. https://doi.org/10.1007/s11214-020-00676-9.

Griffin, S., L. Daly, Martin R. Lee, S. Piazolo, P.W. Trimby, L.V. Forman, P. Chung, B.E. Cohen, R. Baumgartner, and Gretchen K. Benedix. 2019. "New Insights into the Magmatic and Shock History of the Nakhlite Meteorites from Electron Backscatter Diffraction." *Lunar and Planetary Science Conference* 50: #1845.

Gross, Juliane, Allan H. Treiman, Justin Filiberto, and Christopher D.K. Herd. 2011. "Primitive Olivine-Phyric Shergottite NWA 5789: Petrography, Mineral Chemistry, and Cooling History Imply a Magma Similar to Yamato-980459." *Meteoritics and Planetary Science* 46, no. 1 (January): 116–133.

Gross, Juliane, Justin Filiberto, Christopher D.K. Herd, Mohit Melwani Daswani, Susanne P. Schwenzer, and Allan H. Treiman. 2013. "Petrography, Mineral Chemistry, and Crystallization History of Olivine-Phyric Shergottite NWA 6234: A New Melt Composition." *Meteoritics and Planetary Science* 48, no. 5 (May): 854–871.

Grosshans, T.E., Thomas J. Lapen, Rasmus Andreasen, and Anthony J. Irving. 2013. "Lu-Hf and Sm-Nd Ages and Source Compositions for Depleted Shergottite Tissint." *Lunar and Planetary Science Conference* 44: #2872.

Halevy, Itay, Woodward W. Fischer, and John M. Eiler. 2011. "Carbonates in the Martian Meteorite Allan Hills 84001 Formed at 18±4°C in a Near-Surface Aqueous Environment." *Proceedings of the National Academy of Sciences of the United States of America* 108, no. 41 (October 3): 16895–16899.

Hamilton, Victoria E., Philip R. Christensen, Harry Y. McSween, Jr., and Joshua L. Bandfield. 2003. "Searching for the Source Regions of Martian Meteorites using MGS TES: Integrating Martian Meteorites into the Global Distribution of Igneous Materials on Mars." *Meteoritics and Planetary Science* 38, no. 6 (June): 871–885.

Hamilton, J.S., Christopher D.K. Herd, Erin L. Walton, and Livio L. Tornabene. 2020. "Prioritizing Candidate Source Craters for Martian Meteorites." *Lunar and Planetary Science Conference* 51: #2607.

Hartmann, William K., and Gerhard Neukum. 2001. "Cratering Chronology and the Evolution of Mars." *Space Science Reviews* 96 (April): 165–194.

Hartmann, William K. 2005. "Martian Cratering 8: Isochron Refinement and the Chronology of Mars." *Icarus* 174, no. 2 (April): 294–320.

Harvey, R.P., and Victoria E. Hamilton. 2005. "Syrtis Major as the Source Region of the Nakhlite/Chassigny Group of Martian Meteorites: Implications for the Geological History of Mars." *Lunar and Planetary Science Conference* 36: #1019.

He, Qi, Long Xiao, J. Brian Balta, Ioannis Baziotis, Weibiao Hsu, and Yunbin Guan. 2015. "Petrography and Geochemistry of the Enriched Basaltic Shergottite Northwest Africa 2975." *Meteoritics and Planetary Science* 50, no. 12 (December): 2024–2044.

Head, James N., H. Jay Melosh, and Boris A. Ivanov. 2002. "Martian Meteorite Launch: High-Speed Ejecta from Small Craters." *Science* 298, no. 5599 (7 November): 1752–1756.

Herd, Christopher D.K. 2003. "The Oxygen Fugacity of Olivine-Phyric Martian Basalts and the Components within the Mantle and Crust of Mars." *Meteoritics and Planetary Science* 38, no. 12 (December): 1793–1805.

Herd, Christopher D.K., A. Simonetti, and N.D. Peterson. 2007. "In Situ U–Pb Geochronology of Martian Baddeleyite by Laser Ablation MC-ICP-MS." *Lunar and Planetary Science Conference* 38: #1664.

Herd, Christopher D.K., Erin L. Walton, Carl B. Agee, Nele Muttik, Karen Ziegler, Charles K. Shearer, Jr., Aaron S. Bell, et al. 2017a. "The Northwest Africa 8159 Martian Meteorite: Expanding the Martian Sample Suite to the Early Amazonian." *Geochimica et Cosmochimica Acta* 218 (1 December): 1–26.

Herd, Christopher D.K., Livio L. Tornabene, T.J. Bowling, Erin L. Walton, T.G. Sharp, and H. Jay Melosh. 2017b. "New Insights into Source Craters for the Martian Meteorites." *Meteoritics and Planetary Science* 52, no. S1: #6334.

Herd, Christopher D. K., Livio L. Tornabene, T.J. Bowling, Erin L. Walton, Thomas G. Sharp, H. Jay Melosh, Jarret S. Hamilton, C.E. Viviano, and Bethany L. Ehlmann. 2018. "Linking Martian Meteorites to their Source Craters: New Insights." *Lunar and Planetary Science Conference* 49: #2266.

Herd, Christopher D. K., Jarret S. Hamilton, Erin L. Walton, Livio L. Tornabene, Anthony Lagain, Gretchen K. Benedix, Alex I. Sheen, H. Jay Melosh, Brandon C. Johnson, Sean E. Wiggins, Thomas G. Sharp, and James R. Darling. 2024. "The Source Craters of the Martian Meteorites: Implications for the Igneous Evolution of Mars." *Science Advances* 10, no. 33 (16 August): eadn2378. https://doi.org/10.1126/sciadv.adn2378.

Hewins, Roger H., Briggitte Zanda, Munir Humayun, Alexander A. Nemchin, Jean-Pierre Lorand, Sylvain Pont, Damien Deldicque, et al. 2017. "Regolith Breccia Northwest Africa 7533: Mineralogy and Petrology with Implications for Early Mars." *Meteoritics and Planetary Science* 52, no. 1 (January): 89–124.

Hewins, Roger H., Briggitte Zanda, Sylvain Pont, and P.-M. Zanetta. 2019. "Northwest Africa 10414, a Pigeonite Cumulate Shergottite." *Meteoritics and Planetary Science* 54, no. 9 (September): 2132–2148.

Hewins, Roger H., Munir Humayun, Jean-Alix Barrat, Briggitte Zanda, Jean-Pierre Lorand, Sylvain Pont, N. Assayag, P. Cartigny, S. Yang, and V. Sautter. 2020. "Northwest Africa 8694, a Ferroan Chassignite: Bridging the Gap Between Nakhlites and Chassignites." *Geochimica et Cosmochimica Acta* 282 (1 August): 201–226.

Howarth, Geoffrey H., John F. Pernet-Fisher, J. Brian Balta, Peter H. Barry, Robert J. Bodnar, and Lawrence A. Taylor. 2014. "Two-Stage Polybaric Formation of the New Enriched, Pyroxene-Oikocrystic, Lherzolitic Shergottite, NWA 7397." *Meteoritics and Planetary Science* 49, no. 10 (October): 1812–1830.

Howarth, Geoffrey H., John F. Pernet-Fisher, Robert J. Bodnar, and Lawrence A. Taylor. 2015. "Evidence for the Exsolution of Cl-rich fluids in Martian Magmas: Apatite Petrogenesis in the Enriched Lherzolitic Shergottite Northwest Africa 7755." *Geochimica et Cosmochimica Acta* 166 (1 October): 234–248.

Howarth, Geoffrey H., Arya Udry, and James M.D. Day. 2018. "Petrogenesis of Basaltic Shergottite Northwest Africa 8657: Implications for fO_2 Correlations and Element Redistribution During Shock Melting in Shergottites." *Meteoritics and Planetary Science* 53, no. 2 (February): 249–267.

Hu, S. Sen, Yangting Lin, Jianchao Zhang, Jialong Hao, Weifan Xing, Ting Zhang, Wei Yang, and Hitesh Changela. 2019. "Ancient Geologic Events on Mars Revealed by Zircons and Apatites from the Martian Regolith Breccia NWA 7034." *Meteoritics and Planetary Science* 54, no. 4 (April): 850–879.

Humayun, Munir, Alexander A. Nemchin, Briggitte Zanda, Roger H. Hewins, M. Grange, A. Kennedy, Jean-Pierre Lorand, Christa Göpel, C. Fieni, Sylvain Pont, and Damien Deldicque. 2013. "Origin and Age of the Earliest Martian Crust from Meteorite NWA 7533." *Nature* 503, no. 7477 (28 November): 513–516.

Humphreys, D. Russell. 2005. "Young Helium Diffusion Age of Zircons Supports Accelerated Nuclear Decay" In *Radioisotopes and the Age of the Earth: Results of a Young-Earth Creationist Research Initiative*. Edited by Larry Vardiman, Andrew A. Snelling, and Eugene F. Chaffin, 25–100. El Cajon, California: Institute for Creation Research, and Chino Valley, Arizona: Creation Research Society. Young Helium Diffusion Age of Zircons Supports Accelerated Nuclear Decay | The Institute for Creation Research.

Ikeda, Y. 1997. "Petrology of the Yamato 793695 Lherzolitic Shergottite." *Proceedings of the NIPR Symposium on Antarctic Meteorites* 7: 9–29.

Ilg, S., Elmar K. Jessberger, Ahmed El Goresy. 1997. "Argon-40/Argon-39 Laser Extraction Dating of Individual Maskelynites in SNC Pyroxenite Allan Hills 84001." *Meteoritics and Planetary Science* 32: A65.

Izawa, M.R.M., Kimberly T. Tait, Desmond E. Moser, Ivan R. Barker, Brendt C. Hyde, I. Nicklin, and Thomas J. Lapen. 2015. "Mineralogy, Petrology and Geochronology of Intermediate Shergottite NWA 7042." *Lunar and Planetary Science Conference* 46: #2523

Jagoutz, Emil, and Heinrich Wänke. 1986. "Sr and Nd Isotopic Systematics of Shergotty Meteorite." *Geochimica et Cosmochimica Acta* 50, no. 6 (June): 939–953.

Jagoutz, Emil. 1989. "Sr and Nd Isotopic Systematics in ALHA77005: Age of Shock Metamorphism in Shergottites and Magmatic Differentiation on Mars." *Geochimica et Cosmochimica Acta* 53, no. 9 (September): 2429–2441.

Jagoutz, Emil, 1991. "Chronology of SNC Meteorites." *Space Science Reviews* 56, nos. 1–2 (April): 13–22.

Jagoutz, Emil, A. Sorowka, J.D. Vogel, and Heinrich Wänke. 1994. "ALH84001: Alien or Progenitor of the SNC Family?" *Meteoritics* 29: 478–479.

Jagoutz, Emil. 1996. "Nd Isotopic Systematics of Chassigny." *Lunar and Planetary Science Conference* 27: 597–598.

Jagoutz, Emil, O. Bogdanovski, N. Krestina, and R. Jotter. 1999. "DAG: A New Age in the SNC Family, or the First Gathering of Relatives." *Lunar and Planetary Science Conference* 30: #1808.

Jagoutz, Emil, and R. Jotter. 2000. "New Sm-Nd Isotope Data on Nakhla Minerals." *Lunar and Planetary Science Conference* 31: #1609.

Jagoutz, Emil, Samuel Bowring, R. Jotter, and Gerlind Dreibus. 2009. "New U-Th-Pb Data on SNC Meteorite ALHA 84001." *Lunar and Planetary Science Conference* 40: #1662.

Jambon, A., Jean-Alix Barrat, V. Sautter, Philippe Gillet, Christa Göpel, M. Javoy, J.L. Joron, and M. Lesourd. 2002. "The Basaltic Shergottite Northwest Africa 856: Petrology and Chemistry." *Meteoritics and Planetary Science* 37, no. 9 (September): 1147–1164.

Jambon, A., V. Sautter, Jean-Alix Barrat, J. Gattacceca, P. Rochette, O. Boudouma, D. Badia, and B. Devouard. 2016. "Northwest Africa 5790: Revisiting Nakhlite Petrogenesis." *Geochimica et Cosmochimica Acta* 190 (1 October): 191–212.

Jensen, Ninna K., Alexander A. Nemchin, Gavin Kenny, Martin J. Whitehouse, James N. Connelly, Takashi Mikouchi, and Martin Bizzarro. 2025. "Timing of Crustal Reworking on Mars Inferred from the Lu-Hf Isotope Systematics of Igneous Clasts in NWA 7533." *Geochimica et Cosmochimica Acta* 390 (1 February): 70–85.

Jones, J.H. 1986. "A Discussion of Isotopic Systematics and Mineral Zoning in the Shergottites: Evidence for a 180 m.y. Igneous Crystallization Age." *Geochimica et Cosmochimica Acta* 50, no. 6 (June): 969–977.

Karner Jim K., James J. Papike, and Charles K. Shearer, Jr. 2003. "Olivine from Planetary Basalts: Chemical Signatures that Indicate Planetary Parentage and those that Record Igneous Setting and Process." *American Mineralogist* 88, nos. 5–6 (May–June): 806–816.

Kereszturi, A., and E. Chatzitheodoridis. 2016. "Searching for the Source Crater of Nakhlite Meteorites." *Origins of Life and Evolution of the Biospheres* 46 (28 March): 455–471.

Kiefer, Walter S. 2003. "Melting in the Martian Mantle: Shergottite Formation and Implications for Present-Day Mantle Convection on Mars." *Meteoritics and Planetary Science* 38, no. 12 (December): 1815–1832.

Kizovski, Tanya V., Kimberly T. Tait, Veronica E. Di Cecco, Lee F. White, and Desmond E. Moser. 2019. "Detailed Mineralogy and Petrology of Highly Shocked Poikilitic Shergottite Northwest Africa 6342." *Meteoritics and Planetary Science* 54, no. 4 (April): 768–784.

Kizovski, Tanya V., M.R.M. Izawa, Kimberly T. Tait, Desmond E. Moser, James M.D. Day, Brendt C. Hyde, Lee F. White, L. Kovarik, S.D. Taylor, D.E. Perea, Ivan R. Barker, and B.R. Joy. 2020. "Petrogenesis, Alteration, and Shock History of Intermediate Shergottite Northwest Africa 7042: Evidence for Hydrous Magmatism on Mars?" *Geochimica et Cosmochimica Acta* 283 (15 August): 103–123.

Kleine, Thorsten, K. Mezger, C. Münker, H. Palme, and Addi Bischoff. 2004. "^{182}Hf-^{182}W Isotope Systematics of Chondrites, Eucrites, and Martian Meteorites: Chronology of Core Formation and Early Mantle Differentiation in Vesta and Mars." *Geochimica et Cosmochimica Acta* 68, no. 13 (1 July): 2935–2946.

Knott, S.F., Richard D. Ash, and Grenville Turner. 1996. "^{40}Ar-^{39}Ar Dating of ALH84001: Evidence for the Early Bombardment of Mars." *Lunar and Planetary Science Conference* 26 (February): 765–766.

Koeberl, Christian, Toni Schulz, and Matthew S. Huber. 2024. "Precambrian Impact Structures and Ejecta on Earth: A Review." *Precambrian Research* 411 (1 September): Article number 107511. https://doi.org/10.1016/j.precamres.2024.107511.

Koike Mizuho, Yoshihiro Ota, Yuji Sano, Naoto Takahata, and Naoji Sugiura. 2014. "High-Spatial Resolution U-Pb Dating of Phosphate Minerals in Martian Meteorite Allan Hills 84001." *Geochemical Journal* 48, no. 5 (September): 423–431.

Koike, Mizuho, Ryoichi Nakada, Iori Kajitani, Tomohiro Usui, Yusuke Tamenori, Haruna Sugahara, and Atsuko Kobayashi. 2020. "In-Situ Preservation of Nitrogen-Bearing Organics in Noachian Martian Carbonates." *Nature Communications* 11 (24 April): 1–7. https://doi.org/10.1038/s41467-020-15931-4.

Korochantseva, Ekaterina V., Mario Trieloff, Alexei I. Buikin, and Jens Hopp. 2009. "Shergottites Dhofar 019, SaU 005, Shergotty, and Zagami: ^{40}Ar-^{39}Ar Chronology and Trapped Martian Atmospheric and Interior Argon." *Meteoritic and Planetary Science* 44, no. 2 (February): 293–321.

Korochantseva, Ekaterina V., Susanne P. Schwenzer, Alexei I. Buikin, Jens Hopp, Ulrich Ott, and Mario Trieloff. 2011. "^{40}Ar-^{39}Ar and Cosmic-Ray Exposure Ages of Nakhlites—Nakhla, Lafayette, Governador Valadares—and Chassigny." *Meteoritic and Planetary Science* 46, no. 9 (September): 1397–1417.

Krämer Ruggiu, L., J. Gattacceca, B. Bevouard, Arya Udry, Vinciane Debaille, P. Rochette, Jean-Pierre Lorand, et al. 2020. "Caleta el Cobre 022 Martian Meteorite: Increasing Nakhlite Diversity." *Meteoritics and Planetary Science* 55, no. 7 (July): 1539–1563.

Kring David A., Timothy D. Swindle, James D. Gleason, and Jennifer A. Grier. 1998. "Formation and Relative Ages of Maskelynite and Carbonate in ALH84001." *Geochimica et Cosmochimica Acta* 62, no. 12 (June): 2155–2166.

Krot, Alexander N., Klaus Keil, C.A. Goodrich, Edward R.D. Scott, and M.K. Weisberg. 2005. "Classification of Meteorites." In *Meteorites, Comets, and Planets*, edited Andrew M. Davis, *Treatise on Geochemistry*, edited by Heinrich D. Holland and Karl K Turekian, vol. 1, pp.83-128. Amsterdam, The Netherlands: Elsevier.

Krot, Alexander N., Klaus Keil, Edward R. D. Scott, C. A. Goodrich, and M. K. Weisberg. 2014. "Classification of Meteorites." In *Treatise on Geochemistry*. 2nd ed. Edited by Heinrich D. Holland and Karl K. Turekian. Vol. 1 *Meteorites, Comets, and Planets*, 1–63. Amsterdam, The Netherlands: Elsevier.

Kruijer, Thomas S., Thorsten Kleine, Lars E. Borg, Gregory A. Brennecka, Anthony J. Irving, Addi Bischoff, and Carl B. Agee. 2017. "The Early Differentiation of Mars Inferred from Hf–W Chronometry." *Earth and Planetary Science Letters* 474 (15 September): 345–354.

Kuebler, Karla E. 2013. "A Comparison of the Iddingsite Alteration Products in Two Terrestrial Basalts and the Allan Hills 77005 Martian Meteorite Using Raman Spectroscopy and Electron Microprobe Analyses." *Journal of Geophysical Research: Planets* 118, no. 4 (April): 803–830.

Lancet, Michael S., and Kumiko Lancet. 1971. "Cosmic-Ray and Gas Retention Ages of the Chassigny Meteorite." *Meteoritics* 6, no.2 (June): 81–86.

Lang, Nicholas P., Livio L. Tornabene, Harry Y. McSween, Jr., and Philip R. Christensen. 2009. "Tharsis-Sourced Relatively Dust-Free Lavas and their Possible Relationship to Martian Meteorites." *Journal of Volcanology and Geothermal Research* 185, nos. 1–2 (10 August): 103–115.

Langenhorst, Falko, and Ansgar Greshake. 1999. "A Transmission Electron Microscope Study of Chassigny: Evidence for Strong Shock Metamorphism." *Meteoritics and Planetary Science* 34, no. 1 (January): 43–48.

Lapen, Thomas J., Alan D. Brandon, Brian L. Beard, A. H. Peslier, C-T. A. Lee, and H. A. Dalton. 2008. "Lu-Hf Age and Isotope Systematics of the Olivine-Phyric Shergottite RBT-04262 and Implications for the Sources of Enriched Shergottites." *Lunar and Planetary Science Conference* 39: #2073.

Lapen, Thomas J., Minako Righter, Alan D. Brandon, Brian L. Beard, J.T. Shafer, and Anthony J. Irving. 2009. "Lu-Hf Isotope Systematics of NWA4468 and NWA2990: Implications for the Sources of Shergottites." *Lunar and Planetary Science Conference* 40: #2376.

Lapen, Thomas J., Minako Righter, Alan D. Brandon, Vinciane Debaille, Brian L. Beard, J.T. Shafer, and A.H. Peslier. 2010. "A Younger Age for ALH84001 and its Geochemical Link to Shergottite Sources in Mars." *Science* 328, no. 5976 (16 April): 347–351.

Lapen, Thomas J., Minako Righter, Rasmus Andreasen, Anthony J. Irving, Aaron M. Satkoski, Brian L. Beard, Kunihiko Nishiizumi, A.J. Timothy Jull, and Marc W. Caffee. 2017. "Two Billion Years of Magmatism Recorded from a Single Mars Meteorite Ejection Site." *Science Advances* 3, no.2 (1 February): e1600922. https://doi.org/10.1126/sciadv.1600922.

Lindsay, F.N., B. Turrin, G.F. Herzog, Carl C. Swisher III, and T. Emge. 2012. "$^{39}Ar/^{40}Ar$ Ages of Single Grains from Shergottite NWA 2626: Pushing the Limits of Laser Step-Heating." *Lunar and Planetary Science Conference* 43: #2836.

Lindsay, F.N., J. Osmond, J.S. Delaney, G.F. Herzog, B. Turrin, Jisun Park, and Carl C. Swisher III. 2013. "Ar/Ar Systematics of Martian Meteorite NWA 2975." *Lunar and Planetary Science Conference* 44: #2971.

Lindsay, F.N., B.D. Turrin, Christa Göpel, G.F. Herzog, Briggitte Zanda, Roger H. Hewins, Jisun Park, J.S. Delaney, and Carl C. Swisher III. 2014. "$^{40}Ar/^{39}Ar$ Ages of Martian Meteorite NWA 7533." *Meteoritics and Planetary Science* 49: #5383.

Lindsay, F.N., J.S. Delaney, B.D. Turrin, G.F. Herzog, Jisun Park, and Carl C. Swisher III. 2016. "Ar Ages of Martian Meteorite NWA 7034." *Lunar and Planetary Science Conference* 47: #3013.

Liu, Tao, Chaofeng Li, and Yangting Lin. 2011. "Rb-Sr and Sm-Nd Isotopic Systematics of the Lherzolitic Shergottite GRV 99027." *Meteoritics and Planetary Science* 46, no.5 (May): 681–689.

Liu, Yang, Ioannis P. Baziotis, Paul D. Asimow, Robert J. Bodnar, and Lawrence A. Taylor. 2016. "Mineral Chemistry of the Tissint Meteorite: Indications of Two Stage Crystallization in a Closed System." *Meteoritics and Planetary Science* 51, no. 12 (December): 2293–2315.

MacArthur, J.L., J.C. Bridges, L.J. Hicks, Ray Burgess, K.H. Joy, M.J. Branney, G.M. Hansford, et al. 2019. "Mineralogical Constraints on the Thermal History of Martian Regolith Breccia Northwest Africa 8114." *Geochimica et Cosmochimica Acta* 246 (1 February): 267–298.

Marks, E., Lars E. Borg, Amy M. Gaffney, and Donald DePaolo. 2010. "The Relationship of Northwest Africa 4468 to the Other Incompatible- Element-Enriched Shergottites Inferred from its Rb-Sr and Sm-Nd Isotopic Systematics." *Lunar and Planetary Science Conference* 41: #2064.

Marty, Bernard, Veronika S. Heber, Ansgar Grimberg, Rainer Wieler, and Jean-Alix Barrat. 2006. "Noble Gases in the Martian Meteorite Northwest Africa 2737: A New Chassignite." *Meteoritics and Planetary Science* 41: 739–748.

McCoy, Timothy J., G. Jeffrey Taylor, and Klaus Keil. 1992. "Zagami: Product of a Two-Stage Magmatic History." *Geochimica et Cosmochimica Acta* 56, no.9 (September): 3571–3582.

McCubbin, Francis M., Stephen M. Elardo, Charles C. Shearer, Jr., Alexander Smirnov, Erik H. Hauri, and David S. Draper. 2013. "A Petrogenetic Model for the Comagmatic Origin of Chassignites and Nakhlites: Inferences from Chlorine-Rich Minerals, Petrology, and Geochemistry." *Meteoritics and Planetary Science* 48, no.5 (May): 819–853.

McCubbin, Francis M., Jeremy W. Boyce, Tímea Novák-Szabó, Alison R. Santos, Romain Tartèse, Gabor Domokos, Jorge A. Vazquez, Desmond E. Moser, Douglas J. Jerolmack, and Lindsay P. Keller. 2015. "Insights into the Martian Regolith from Martian Meteorite Northwest Africa 7034." *Geological Society of America Abstracts with Programs* 47: 216.

McCubbin, Francis M., Jeremy W. Boyce, Tímea Novák-Szabó, Alison R. Santos, Romain Tartèse, Nele Muttik, Gabor Domokos, et al. 2016. "Geologic History of Martian Regolith Breccia Northwest Africa 7034: Evidence for Hydrothermal Activity and Lithologic Diversity in the Martian Crust." *Journal of Geophysical Research: Planets* 121, no.10 (October): 2120–2149.

McFarlane, Christopher R.M., and John G. Spray. 2022. "The Los Angeles Martian Diabase: Phosphate U-Th-Pb Geochronology and Mantle Source Constraints." *Geochimica et Cosmochimica Acta* 326 (1 June): 166–179.

McKay, David S., Everett K. Gibson, Jr., Kathie L. Thomas-Keprta, Hojatollah Vali, Jr., Christopher S. Romanek, Simon J. Clemett, Xavier D.F. Chillier, Claude R. Maechling, and Richard N. Zare. 1996. "Search for Past Life on Mars: Possible Relic Biogenic Activity in Martian Meteorite ALH84001." *Science* 273, no.5277 (16 August): 924–930.

McKay, G., E. Koizumi, Takashi Mikouchi, L. Le, and C. Schwandt. 2002. "Crystallization of Shergottite QUE 94201: An Experimental Study." *Lunar and Planetary Science Conference* 33: #2051.

McSween, Harry Y. Jr., Edward M. Stolper, Lawrence A. Taylor, Richard A. Muntean, G. Davis O'Kelley, James S. Eldridge, Swarajranjan Biswas, Hung T. Ngo, and Michael E. Lipschutz. 1979. "Petrogenetic Relationship Between Allan Hills 77005 and Other Achondrites." *Earth and Planetary Science Letters* 45, no. 2 (November): 275–284.

McSween, Harry Y. Jr., Lawrence A. Taylor, and Edward M. Stolper. 1979. "Allan Hills 77005: A New Meteorite Type Found in Antarctica." *Science* 204, no. 4398 (15 June): 1201–1203.

McSween, Harry Y. Jr., Don D. Eisenhour, Lawrence A. Taylor, Meenakshi Wadhwa, and Ghislaine Crozaz. 1996. "QUE94201 Shergottite: Crystallization of a Martian Basaltic Magma." *Geochimica et Cosmochimica Acta* 60, no. 22 (November): 4563–4569.

McSween Jr., Harry Y. and Allan H. Treiman. 1998. "Martian Meteorites." In *Planetary Materials*. Edited by James J. Papike. *Reviews in Mineralogy*, vol. 36, 6.1–6.53. Washington DC: Mineralogical Society of America.

McSween, Harry Y. Jr. 2002. 'The Rocks of Mars, from Far and Near." *Meteoritics and Planetary Science* 37, no. 1 (January): 7–25.

McSween, Harry Y. Jr. 2008. "Martian Meteorites as Crustal Samples." In *The Martian Surface: Composition, Mineralogy, and Physical Properties*. Edited by James F. Bell III, 383–395. Cambridge, United Kingdom: Cambridge University Press.

McSween, Harry Y. Jr., and Scott M. McLennan. 2014. "Mars." In *Treatise on Geochemistry*. 2nd ed. Edited by Heinrich D. Holland and Karl K Turekian, vol. 1 *Meteorites, Comets, and Planets*, 251–300. Amsterdam, The Netherlands: Elsevier.

McSween, Harry Y. Jr. 2015. "Petrology on Mars." *American Mineralogist* 100, nos. 11–12 (November 1): 2380–2395.

McSween, Harry Y. Jr. 2019. "The Search for Biosignatures in Martian Meteorite Allan Hills 84001." In *Advances in Astrobiology and Biogeophysics*. Edited by B. Cavalazzi and F. Westall, 167–182. Cham, Switzerland: Springer.

McSween, Harry Y. Jr., James W. Head III, A. Deane Rogers, and Mariek E. Schmidt. 2023. "Assessing Global Trends in Mars Magma Compositions Using Ground Truth." *Meteoritics and Planetary Science* 58. no. 9 (September): 1306–1317.

Mikouchi, Takashi, Eisuke Koizumi, Akira Monkawa, Yuji Ueda, and Masamichi Miyamoto. 2003. "Mineralogy and Petrology of Yamato 000593: Comparison with Other Martian Nakhlite Meteorites." *Antarctic Meteorite Research* 16: 34–57.

Mikouchi, Takashi, and Taichi Kurihara. 2008. "Mineralogy and Petrology of Paired Lherzolitic Shergottites Yamato 000027, Yamato 000047, and Yamato 000097: Another Fragment from a Martian 'Lherzolite' Block." *Polar Science* 2, no. 3 (25 September): 175–194.

Mikouchi, Takashi, J. Makishima, and T. Kurihara. 2012. "Relative Burial Depth of Nakhlites Revisited." *Lunar and Planetary Science Conference* 43: #2363.

Misawa, Keiji, Noboru Nakamura, Wayne R. Premo, and Mitsunobu Tatsumoto. 1997. "U-Th-Pb Isotopic Systematics of Lherzolitic Shergottite Yamato 793605." *Antarctic Meteorite Research* 10 (August): 95–108.

Misawa, Keiji, Chi-Yu Shih, Henry Wiesmann, and Laurence E. Nyquist. 2003. "Crystallization and Alteration Ages of the Antarctic Nakhlite Yamato 000593." *Lunar and Planetary Science Conference* 34: #1556.

Misawa, Keiji, Chi-Yu Shih, Young D. Reese, Laurence E. Nyquist, and Jean-Alix Barrat. 2005a. "Rb-Sr and Sm-Nd Isotopic Systematics of NWA 2737 Chassignite." *Meteoritic and Planetary Science* 40: A104.

Misawa, Keiji, Chi-Yu Shih, Young D. Reese, and Laurence E. Nyquist. 2005b. "Crystallization Age and Source Signature of Chassigny." *Lunar and Planetary Science Conference* 36: #1698.

Misawa, Keiji, Chi-Yu Shih, Henry Wiesmann, Daniel H. Garrison, Laurence E. Nyquist, and Donald D. Bogard. 2005c. "Rb-Sr, Sm-Nd and Ar-Ar Isotopic Systematics of Antarctic Nakhlite Yamato 000593." *Antarctic Meteorite Research* 18: 133–151.

Misawa Keiji, Kazuhiro Yamada, Noboru Nakamura, Noritoshi Morikawa, G. Kondorosi, Katsuyuki Yamashita, and Wayne R. Premo. 2006a. "Sm-Nd Isotopic Systematics of Lherzolitic Shergottite Yamato-793605." *Lunar and Planetary Science Conference* 37: #1892.

Misawa, Keiji, Chi-Yu Shih, Young Reese, Donald D. Bogard, and Laurence E. Nyquist. 2006b. "Rb–Sr, Sm–Nd and Ar–Ar Isotopic Systematics of Martian Dunite Chassigny." *Earth and Planetary Science Letters* 246: 90–101.

Misawa Keiji, Kazuhiro Yamada, Noboru Nakamura, Noritoshi Morikawa, Katsuyuki Yamashita, and Wayne R. Premo. 2006c. "Sm-Nd Isotopic Systematics of Lherzolitic Shergottite Yamato-793605." *Antarctic Meteorite Research* 19: 45–57.

Misawa, Keiji, and A. Yamaguchi. 2007. "U-Pb Ages of NWA 856 Baddeleyite." *Meteoritic and Planetary Science* 42: A108.

Misawa Keiji, Jisun Park, Chi-Yu Shih, Young D. Reese, Donald D. Bogard, and Laurence E. Nyquist. 2008. "Rb-Sr, Sm-Nd, and Ar-Ar Isotopic Systematics of Lherzolitic Shergottite Yamato 000097." *Polar Science* 2, no. 3 (25 September):163–174.

Mittelholz, A., C.L. Johnson, J.M. Feinberg, B. Langlais, and R.J. Phillips. 2020. "Timing of the Martian Dynamo: New Constraints for a Core Field 4.5 and 3.7 Ga Ago." *Science Advances* 6, no. 18 (1 May): eaba0513. https://doi.org/10.1126/sciadv.aba0513.

Mittlefehldt, David W. 1994. "ALH84001, a Cumulate Orthopyroxenite Member of the Martian Meteorite Clan." *Meteoritics* 29, no. 2 (March): 214–221.

Mittlefehldt, David W., Timothy J. McCoy, C.A. Goodrich, and A. Kracher. 1998. "Non-Chondritic Meteorites from Asteroidal Bodies." In *Planetary Materials*. Edited by James J. Papike. *Reviews in Mineralogy*, vol. 36, 4.1–4.195. Washington, DC: Mineralogical Society of America.

Mittlefehldt, David W. 2005. "Achondrites." In *Meteorites, Comets, and Planets*. Edited by Andrew M. Davis. *Treatise on Geochemistry*. Edited by Heinrich D. Holland and Karl K Turekian, vol. 1, 291–324. Amsterdam, The Netherlands: Elsevier.

Miura, Yayoi N., Keisuke Nagao, Naoji Sugiura, Hitoshi Sagawa, and Kayo Matsubara. 1995. "Orthopyroxenite ALHA84001 and Shergottite ALHA77005: Additional Evidence for a Martian Origin from Noble Gases." *Geochimica et Cosmochimica Acta* 59, no. 10 (May): 2105–2113.

Montmerle, Thierry, Jean-Charles Augereau, Marc Chaussidon, Matthieu Gounelle, Bernard Marty, and Alessandro Mordbidelli. 2006. "Solar System Formation and Early Evolution: The First 100 Million Years." *Earth, Moon, and Planets* 98: 39–95.

Morikawa, Noritoshi, Keiji Misawa, Gabor Kondorosi, Wayne R. Premo, Mitsunobu Tatsumoto, and Noboru Nakamura. 2001. "Rb-Sr Isotopic Systematics of Lherzolitic Shergottite Yamato-793605." *Antarctic Meteorite Research* 14: 47–60.

Moriwaki, Ryota, Tomohiro Usui, Justin I. Simon, John H. Jones, Tetsuya Yokoyamaa, and Minato Tobita. 2017. "Coupled Pb Isotopic and Trace Element Systematics of the Tissint Meteorite: Geochemical Signatures of the Depleted Shergottite Source Mantle." *Earth and Planetary Science Letters* 474 (September): 180–189.

Moriwaki, Ryota, Tomohiro Usui, Minato Tobita, and Tetsuya Yokoyama. 2020. "Geochemically Heterogeneous Martian Mantle Inferred from Pb Isotope Systematics of Depleted Shergottites." *Geochimica et Cosmochimica Acta* 274 (1 April): 157–171.

Morris, John D. 2007. *The Young Earth*. Rev. ed. Green Forest, Arkansas: Master Books.

Moser, Desmond E., K.R. Chamberlain, Kimberly T. Tait, A.K. Schmitt, James R. Darling, Ivan R. Barker, and Brendt C. Hyde. 2013. "Solving the Martian Meteorite Age Conundrum Using Micro-Baddeleyite and Launch-Generated Zircon." *Nature* 499, no. 7459 (24 July): 454–457.

Mouginis-Mark, P.J., Timothy J. McCoy, G.J. Taylor, and Klaus Keil. 1992. "Martian Parent Craters for the SNC Meteorites." *Journal of Geophysical Research: Planets* 97, no. E6 (25 June): 10213–10225.

Mussel White, Donald S., Heather A. Dalton, Walter S. Kiefer, and Allan H. Treiman. 2006. "Experimental Petrology of the Basaltic Shergottite Yamato-980459: Implications for the Thermal Structure of the Martian Mantle." *Meteoritics and Planetary Sciences* 41, no. 9 (September): 1271–1290.

Nakamura, Noboru, H. Komi, and H. Kagami. 1982. "Rb-Sr Isotopic and REE Abundances in the Chassigny Meteorite." *Meteoritics* 17: 257–258.

Nakamura, Noboru, Daniel M. Unruh, Mitsunobu Tatsumoto, and Robert Hutchison. 1982. "Origin and Evolution of the Nakhla Meteorite Inferred from the Sm-Nd and U-Pb Systematics and REE, Ba, Sr, Rb Abundances." *Geochimica et Cosmochimica Acta* 46: 1555–1573.

Nekvasil, Hanna, A. Dondolini, J. Horn, Justin Filiberto, H. Long, and Donald H. Lindsley. 2004. "The Origin and Evolution of Silica-Saturated Alkalic Suites: An Experimental Study." *Journal of Petrology* 45, no. 4 (April): 693–721.

Nekvasil, Hanna, Justin Filiberto, Francis M. McCubbin, and Donald H. Lindsley. 2007. "Alkalic Parental Magmas for Chassignites?" *Meteoritics and Planetary Science* 42, no. 6 (June): 979–992.

Nemchin, Alexander A., Munir Humayun, Martin J. Whitehouse, Roger H. Hewins, Jean-Pierre Lorand, A. Kennedy, M. Grange, Briggitta Zanda, C. Fieni, and Damien Deldicque. 2014. "Record of the Ancient Martian Hydrosphere and Atmosphere Preserved in Zircon from a Martian Meteorite." *Nature Geoscience* 7, no. 9 (August): 638–642.

Niihara, T., H. Kaiden, Keiji, Misawa, T. Sekine, and Takashi Mikouchi. 2012. "U-Pb Isotopic Systematics of Shock-Loaded and Annealed Baddeleyite: Implications for Crystallization Ages of Martian Meteorite Shergottites." *Earth and Planetary Science Letters* 341–344 (August): 195–210.

Nimmo, Francis, and Ken L. Tanaka. 2005. "Early Crustal Evolution of Mars." *Annual Reviews of Earth and Planetary Sciences* 33 (May): 133–161.

Norton, O. Richard. 2002. *The Cambridge Encyclopedia of Meteorites*. Cambridge, United Kigndom: Cambridge University Press.

Nyquist, Laurence E., J. Wooden, B.M. Bansal, Henry Wiesmann, G. McKay, and Donald D. Bogard. 1979. "Rb-Sr Age of the Shergotty Achondrite and Implications for Metamorphic Resetting of Isochron Ages." *Geochimica et Cosmochimica Acta* 43, no. 7 (July): 1057–1074.

Nyquist, Laurence E., Henry Wiesmann, Chi-Yu Shih, and B.M. Bansal. 1986. "Sr Isotopic Systematics of EETA79001." *Lunar and Planetary Science Conference* 17: 624–625.

Nyquist, Laurence E., B.M. Bansal, Henry Wiesmann, and Chi-Yu Shih. 1995. "'Martians' Young and Old: Zagami and ALH84001." *Lunar and Planetary Science Conference* 26: 1065–1066.

Nyquist, Laurence E., Young D. Reese, Henry Wiesmann, Chi-Yu Shih, and C. Schwandt. 2000. "Rubidium-Strontium Age of the Los Angeles Shergottite." *Meteoritics and Planetary Science* 35: A121–A122.

Nyquist, Laurence E., Young D. Reese, Henry Wiesmann, and Chi-Yu Shih. 2001a. "Age of EET79001B and Implications for Shergottite Origins." *Lunar and Planetary Science Conference* 32: #1407.

Nyquist Laurence E., Donald D. Bogard, Chi-Yu Shih, Ansgar Greshake, D. Stöffler, and Otto Eugster. 2001b. "Ages and Geologic Histories of Martian Meteorites." *Space Science Reviews* 96 (April): 105–164.

Nyquist, Laurence E., Chi-Yu Shih, and Young D. Reese. 2006. "Initial Isotopic Heterogeneities in Zagami: Evidence of a Complex Magmatic History." *Meteoritics and Planetary Science* 41 (September): A135.

Nyquist, Laurence E., Chi-Yu Shih, Young D. Reese, and Anthony J. Irving. 2006a. "Concordant Rb-Sr and Sm-Nd Ages for NWA 1460: A 340 Ma Old Basaltic Shergottite Related to Lherzolitic Shergottites." *Lunar and Planetary Science Conference* 37: #1723.

Nyquist, Laurence E., Y. Ikeda, Chi-Yu Shih, Young D. Reese, Noboru Nakamura, and H. Takeda. 2006b. "Sm-Nd Age and Nd- and Sr-Isotopic Evidence for the Petrogenesis of Dhofar 378." *Antarctic Meteorites* 30 (January 1).

Nyquist, Laurence E., 2006. "Martian Meteorite Ages and Implications for Martian Cratering History." In: *Workshop on Surface Ages and Histories: Issues in Planetary Chronology*, #6010. Houston, Texas: Lunar and Planetary Institute.

Nyquist, Laurence E., Donald D. Bogard, Chi-Yu Shih, Jisun Park, Young D. Reese, and Anthony J. Irving. 2009. "Concordant Rb–Sr, Sm–Nd, and Ar–Ar Ages for Northwest Africa 1460: A 346 Ma Old Basaltic Shergottite Related to 'Lherzolitic' Shergottites." *Geochimica et Cosmochimica Acta* 73, no. 14 (15 July): 4288–4309.

Nyquist, Laurence E, Chi-Yu Shih, and Young D. Reese. 2010. "Rb-Sr and Sm-Nd Ages of Zagami DML and Sr Isotopic Heterogeneity in Zagami." *Meteoritics and Planetary Science* 45: A154.

Nyquist Laurence E., and Chi-Yu Shih. 2013. "Peering Through a Martian Veil: ALHA 84001 Sm-Nd Age Revisited." *Lunar and Planetary Science Conference* 44: #2182..

Nyquist, Laurence E., Chi-Yu Shih, Zhan X. Peng, and Carl B. Agee. 2013. "NWA 7034 Martian Breccia: Disturbed Rb-Sr Systematics, Preliminary ~4.4 Ga Sm-Nd Age." *Meteoritics and Planetary Science* 48: #5318.

Nyquist Laurence E., Chi-Yu Shih, Francis M. McCubbin, Alison R. Santos, Charles K. Shearer, Jr., Zhan X. Peng, Paul V. Burger, and Carl B. Agee. 2016. "Rb-Sr and Sm-Nd Isotopic and REE Studies of Igneous Components in the Bulk Matrix Domain of Martian Breccia Northwest Africa 7034." *Meteoritics and Planetary Science* 51, no. 3 (March): 483–498.

Nyquist, Laurence E., Chi-Y. Shih, Jisun Park, G. F. Herzog, K. Nagao, and Takashi Mikouchi. 2018. "Radiogenic and Cosmogenic Isotopes in Los Angeles and Dhofar 378 Shergottites." *Lunar and Planetary Science Conference* 49: #1622.

Ody, Anouck Z., François Poulet, C. Quantin, J.-P. Bibring, J.L. Bishop, and M.D. Dyar. 2015. "Candidates Source Regions of Martian Meteorites as Identified by OMEGA/MEx." *Icarus* 258 (15 September): 366–383.

Osinski, Gordon R., Richard A.F. Grieve, Ludovic Ferrière, Ania Losiak, Annemarie E. Pickersgill, Aaron J. Cavosie, Shannon M. Hibbard, Patrick J.A. Hill, Juan Jaimes Bermudez, Cassandra L. Marion, Jennifer D. Newman, and Sarah L. Simpson. 2022. "Impact Earth: A Review of the Terrestrial Impact Record." *Earth-Science Reviews* 232 (September): Article number 104112. https://doi.org/10.1016/j.earscirev.2022.104112.

Ozawa, S., Trevor R. Ireland, Ahmed El Goresy, and Eiji Ohtani. 2009. "U-Pb Dating of Baddeleyite in Shergotty, Zagami and NWA 2737: Implications for Crystallization and Impact Ages of Martian Meteorites." *Meteoritics and Planetary Science* 44: A163.

Papanastassiou, D.A., and Gerald J. Wasserburg. 1974. "Evidence for Late Formation and Young Metamorphism in the Achondrite Nakhla." *Geophysical Research Letters* 1, no. 1 (May): 23–26.

Papike, James J., J.M. Karner, Charles K. Shearer, Jr., and Paul V. Burger. 2009. "Silicate Mineralogy of Martian Meteorites." *Geochimica et Cosmochimica Acta* 73: 7443–7485.

Paquet, Marine, James M.D. Day, Arya Udry, Ruan Hattingh, Ben Kumler, Rachel R. Rahib, Kimberly T. Tait, and Clive R. Neal. 2021. "Highly Siderophile Elements in Shergottite Sulfides and the Sulfur Content of the Martian Mantle." *Geochimica et Cosmochimica Acta* 293 (15 January): 379–398.

Park, Jisun, and Donald D. Bogard. 2006. "Ar-Ar Age of Shergottite Dhofar 378: Formation or Early Shock Event?" *Meteoritics and Planetary Science* 41: A138.

Park, Jisun, and Donald D. Bogard. 2007. "^{39}Ar-^{40}Ar Age of Basaltic Shergottite NWA 3171." *Meteoritics and Planetary Science* 42: A122.

Park, Jisun, Daniel Garrison, and Donald D. Bogard. 2007. "^{39}Ar-^{40}Ar Ages of Two Nakhlites, MIL 03346 and Y 000593: A Detailed Analysis." *Lunar and Planetary Science Conference* 38: #1114.

Park, Jisun, Donald D. Bogard, and Daniel H. Garrison. 2008. "^{39}Ar–^{40}Ar dating of Martian Shergottite, DaG 476." *Lunar and Planetary Science Conference* 39: #1204.

Park, Jisun, Daniel H. Garrison, and Donald D. Bogard. 2009. "^{39}Ar-^{40}Ar ages of Martian Nakhlites." *Geochimica et Cosmochimica Acta* 73, no. 7 (1 April): 2177–2189.

Park, Jisun, G.F. Herzog, Laurence E. Nyquist, F.N. Lindsay, B. Turrin, Carl C. Swisher III, J.S. Delaney, Chi-Yu Shih, T. Niihara, and Keiji Misawa. 2013a. "^{40}Ar /^{39}Ar Ages for Maskelynites and K-rich Melt from Olivine-Rich Lithology in (Kanagawa) Zagami." *Lunar and Planetary Science Conference* 44: #2556.

Park, Jisun, G.F. Herzog, Laurence E. Nyquist, Chi-Yu Shih, B. Turrin, F.N. Lindsay J.S. Delaney, Carl C. Swisher III, and Carl B. Agee. 2013b. "Ar-Ar and Rb-Sr Ages of the Tissint Olivine-Phyric Martian Shergottite." *Lunar and Planetary Science Conference* 44: #5320.

Park, Jisun, Donald D. Bogard, Laurence E. Nyquist, Daniel H. Garrison, and Takashi Mikouchi, 2013c. "Ar–Ar Ages and Trapped Ar Components in Martian Shergottites RBT 04262 and LAR 06319." *Geochimica et Cosmochimica Acta* 121 (15 November): 546–570.

Park, Jisun, G.F. Herzog, B. Turrin, F.N. Lindsay, J.S. Delaney, Carl C. Swisher III, K. Nagao, and Laurence E. Nyquist. 2014. "^{40}Ar/^{39}Ar Studies of Martian Meteorite RBT 04262 and Terrestrial Standards." *Lunar and Planetary Science Conference* 45: #1609.

Park, Jisun, Laurence E. Nyquist, G.F. Herzog, B.D. Turrin, F.N. Lindsay, J.S. Delaney, Carl C. Swisher III. 2016. "^{40}Ar/^{39}Ar Ages of Nakhlites Miller Range (MIL) 090030, 090032 and 090136." *Lunar and Planetary Science Conference* 47: #1821.

Patterson, Claire. 1956. "Age of Meteorites and the Earth." *Geochimica et Cosmochimica Acta* 10, no. 4 (October): 230–237.

Payré, Valerie, Arya Udry, and Abigail A. Fraeman. 2024. "Igneous Diversity of the Early Martian Crust." *Minerals* 14, no. 5 (25 April): 452. https://doi.org/10.3390/min14050452.

Piercy, J.D., J.C. Bridges, L.J. Hicks, J.L. MacArthur, R.C. Greenwood, and Ian A. Franchi. 2020. "Terrestrial Alteration Mineral Assemblages in the NWA 10416 Olivine Phyric Shergottite." *Geochimica et Cosmochimica Acta* 280 (1 July): 26–45.

Pieters, Carle M., Rachel L. Klima, Takahiro Hiroi, M. Darby Dyar, Melissa D. Lane, Allan H. Treiman, Sarah K. Noble, Jessica M. Sunshine, and Janice L. Bishop. 2008. "Martian Dunite NWA 2737: Integrated Spectroscopic Analyses of Brown Olivine." *Journal of Geophysical Research: Planets* 113 (June): E06004. https://doi.org/10.1029/2007JE002939.

Podosek, F.A. 1973. "Thermal History of the Nakhlites by the ^{40}Ar-^{39}Ar Method." *Earth and Planetary Science Letters* 19, no. 2 (June): 135–144.

Rahib, Rachel R., Arya Udry, Geoffrey H. Howarth, Juliane Gross, Marine Paquet, Logan M. Combs, Dara L. Laczniak, and James M.D. Day. 2019. "Mantle Source to Near-Surface Emplacement of Enriched and Intermediate Poikilitic Shergottites in Mars." *Geochimica et Cosmochimica Acta* 266 (1 December): 463–496.

Reese, C.C., C.P. Orth, and V.S. Solomatov. 2010. "Impact Origin for the Martian Crustal Dichotomy: Half Emptied or Half Filled?" *Journal of Geophysical Research: Planets* 115, no. E5: E05004. https://doi.org/10.1029/2009JE003506.

Righter, Minako, Thomas J. Lapen, Alan D. Brandon, Brian L. Beard, J.T. Shafer, and A.H. Peslier. 2009. "Lu-Hf Age and Isotope Systematics of ALH84001." *Lunar and Planetary Science Conference* 40: #2256.

Righter, Minako, Rasmus Andreasen, Thomas J. Lapen, and Anthony J. Irving. 2014. "The Age and Source Composition for Depleted Shergottite Northwest Africa 7635: A 2.3 Ga Magmatic Rock from Early Amazonian Mars." *Lunar and Planetary Science Conference* 45: #2550.

Righter, Minako, Rasmus Andreasen, and Thomas J. Lapen. 2015. "Lu-Hf and Sm-Nd Systematics of Martian Meteorites Larkman Nunatak 12011 and 12095." *Lunar and Planetary Science Conference* 46: #2889.

Righter, Minako, Thomas J. Lapen, Rasmus Andreasen, and Anthony J. Irving. 2016. "Lu-Hf and Sm-Nd Isotopic Studies of Nakhlite Northwest Africa 10153". *Lunar and Planetary Science Conference* 47: #2780.

Righter, Minako, Thomas J. Lapen, and Anthony J. Irving. 2018. "Extending the Range in Ages and Source Compositions of Shergottites: Lu-Hf and Sm-Nd Age and Isotope Systematics of Northwest Africa 4480." *Lunar and Planetary Science Conference* 49: #2609.

Rollinson, Hugh, and Victoria Pease. 2021. *Using Geochemical Data to Understand Geological Processes*. 2nd ed. Cambridge, United Kingdom: Cambridge University Press.

Roszjar J., Martin J. Whitehouse, Kentaro Terada, K. Fukuda, T. John, A. Bischoff, Y. Morishita, and H. Hiyagon. 2019. "Chemical, Microstructural and Chronological Record of Phosphates in the Ksar Ghilane 002 Enriched Shergottite." *Geochimica et Cosmochimica Acta* 245 (15 January): 385–405.

Rubin, Alan E., Paul H. Warren, James P. Greenwood, Robert S. Verish, Laurie A. Leshin, Richard L. Hervig, Robert N. Clayton, and Toshiko K. Mayeda. 2000. "Los Angeles: The Most Differentiated Basaltic Martian Meteorite." *Geology* 28, no. 11 (November 1): 1011–1014.

Sandwell, David T., R. Dietmar Müller, Walter H.F. Smith, Emmanuel Garcia, and Richard Francis. 2014. "New Global Marine Gravity Model from CryoSat-2 and Jason-1 Reveals Buried Tectonic Structure." *Science* 346, no. 6205 (3 October): 65–67.

Sano, Yuji, Kentaro Terada, Setsuo Takeno, Laurence A. Taylor, and Harry Y. McSween Jr. 2000. "Ion Microprobe Uranium-Thorium-Lead Dating of Shergotty Phosphates." *Meteoritics and Planetary Science* 35, no. 2 (March), 341–346.

Santos, Alison R., Carl B. Agee, Francis M. McCubbin, Charles K. Shearer Jr., Paul V. Burger, Romain Tartèse, and Mahesh Anand. 2015. "Petrology of Igneous Clasts in Northwest Africa 7034: Implications for the Petrologic Diversity of the Martian Crust." *Geochimica et Cosmochimica Acta* 157 (15 May): 56–85.

Sautter, V., Jean-Alix Barrat, A. Jambon, Jean-Pierre Lorand, Philippe Gillet, M. Javoy, J.L Joran, and M. Lesourd. 2002. "A New Martian Meteorite from Morocco: The Nakhlite North West Africa 817." *Earth and Planetary Science Letters* 195, nos. 3–4 (15 February): 223–238.

Scott, Edward R.D., and A.N. Krot. 2005. "Chondrites and Their Components." In *Meteorites, Comets, and Planets*. Edited by Andrew M. Davis. *Treatise on Geochemistry*. Edited by Heinrich D. Holland and Karl K Turekian. Vol. 1, 143–200. Amsterdam, The Netherlands: Elsevier.

Shafer, J.T., Alan D. Brandon, Thomas J. Lapen, Minako Righter, Brian L. Beard, and A.H. Peslier. 2009. "Lu-Hf Age of Martian Meteorite Larkman Nunatek 06319." *Lunar and Planetary Science Conference* 40: #1803.

Shafer, J.T., Alan D. Brandon, Thomas J. Lapen, Minako Righter, and A.H. Peslier. 2010a. "Sm-Nd Age and REE Systematics of Larkman Nunatak 06319: Closed System Fractional Crystallization of a Shergottite Magma." *Lunar and Planetary Science Conference* 41: #1726.

Shafer, J.T., Alan D. Brandon, Thomas J. Lapen, Minako Righter, A.H. Peslier, and Brian L. Beard. 2010b. "Trace Element Systematics and ^{147}Sm-^{143}Nd and ^{176}Lu-^{176}Hf ages of Larkman Nunatak 06319: Closed-System Fractional Crystallization of an Enriched Shergottite Magma." *Geochimica et Cosmochimica Acta* 74, no. 24 (15 December): 7307–7328.

Shang, Sheng, Hejiu Hui, Yueheng Yang, and Tianyu Chen. 2022. "Martian Hydrothermal Fluids Recorded in the Sm-Nd Isotopic Systematics of Apatite in Regolith Breccia Meteorites." *Earth and Planetary Science Letters* 581 (1 March): 117413. https://doi.org/10.1016/j.epsl.2022.117413.

Shankar N., Carl C. Swisher III, B. Turrin, and G.F. Herzog. 2008. "^{40}Ar/^{36}Ar—CO_2 Laser Incremental Heating Release Spectra for the Pasamonte Eucrite and Martian Meteorites ALHA77005, Shergotty, and Y000749." *Lunar and Planetary Science Conference* 39: #1924.

Sheen, A.I., Christopher D.K. Herd, Leanne G. Staddon, James R. Darling, Winifred H. Schwarz, and Kimberly T. Tait. 2024. "Baddeleyite Microstructural Response to Shock Metamorphism in Three Enriched Shergottites and Implications for U–Pb Geochronology." *Geochimica et Cosmochimica Acta* 366 (1 February): 267–283.

Shih, Chi-Yu, Laurence E. Nyquist, Donald D. Bogard, G.A. McKay, J.L. Wooden, B.M. Bansal, and Henry Wiesmann. 1982. "Chronology and Petrogenesis of Young Achondrites, Shergotty, Zagami, and ALHA 77005: Late Magmatism on a Geologically Active Planet." *Geochimica et Cosmochimica Acta* 46, no. 11 (November): 2323–2344.

Shih, Chi-Yu, Laurence E. Nyquist, and Henry Wiesmann. 1996. "Sm-Nd Systematics of Nakhlite Governador Valadares." *Lunar and Planetary Science Conference* 27: 1131–1132.

Shih, Chi-Yu, Laurence E. Nyquist, Young Reese, and Henry Wiesmann. 1998. "The Chronology of the Nakhlite Lafayette: Rb-Sr and Sm-Nd Isotopic Ages." *Lunar and Planetary Science Conference* 29: #1145.

Shih, Chi-Yu, Laurence E. Nyquist, and Henry Wiesmann. 1999. "Sm-Nd and Rb-Sr Systematics of Nakhlite Governador Valadares." *Meteoritics and Planetary Science* 34, no. 4 (July): 647–655.

Shih, Chi-Yu, Laurence E. Nyquist, Henry Wiesmann, and Jean-Alix Barrat. 2003. "Age and Petrogenesis of Picritic Shergottite NWA 1068: Sm-Nd and Rb-Sr Isotopic Studies." *Lunar and Planetary Science Conference* 34: #1439.

Shih, Chi-Yu, Laurence E. Nyquist, Henry Wiesmann, and Keiji Misawa. 2004. "Rb-Sr andSm-Nd Isotopic Studies of Shergottite Y980459 and a Petrogenetic Link between Depleted Shergottites and Nakhlites." *Lunar and Planetary Science Conference* 35: #1814.

Shih Chi-Yu, Laurence E. Nyquist, Henry Wiesmann, Young D. Reese, and Keiji Misawa. 2005. "Rb-Sr and Sm-Nd Dating of Olivine-Phyric Shergottite Yamato 980459: Petrogenesis of Depleted Shergottites." *Antarctic Meteorite Research* 18: 46–65.

Shih, Chi-Yu, Laurence E. Nyquist, and Young D. Reese. 2006. "Rb-Sr and Sm-Nd Isotopic Studies of Antarctic Nakhlite

MIL 03346." *Lunar and Planetary Science Conference* 37: #1701.

Shih, Chi-Yu, Laurence E. Nyquist, and Young D. Reese. 2007. "Rb-Sr and Sm-Nd Isotopic Studies of Martian Depleted Shergottites SaU 096/005." *Lunar and Planetary Science Conference* 38: #1745.

Shih, Chi-Yu, Laurence E. Nyquist, and Young D. Reese. 2009. "Rb-Sr and Sm-Nd Studies of Olivine-Phyric Shergottites RBT 04262 and LAR 06319: Isotopic Evidence for Relationship to Enriched Basaltic Shergottites." *Lunar and Planetary Science Conference* 40: #1360.

Shih, Chi-Yu, Laurence E. Nyquist, Young D. Reese, and Keiji Misawa. 2009. "Rb-Sr Isotopic Studies of Antarctic Lherzolitic Shergottite Yamato 984028." *Antarctic Meteorites* 32: 66–67.

Shih, Chi-Yu, Laurence E. Nyquist, Young D. Reese, and A. Jambon. 2010. "Sm-Nd Isotopic Studies of Two Nakhlites, NWA 5790 and Nakhla." *Lunar and Planetary Science Conference* 41: #1367.

Shih Chi-Yu, Laurence E. Nyquist, Young D. Reese, and Keiji Misawa. 2011a. "Sm-Nd and Rb–Sr Studies of Lherzolite Shergottite Yamato 984028." *Polar Science* 4, no. 4 (January): 515–529.

Shih, Chi-Yu, Laurence E. Nyquist, Young D. Reese, and Anthony J. Irving. 2011b. "Rb-Sr and Sm-Nd Ages, and Petrogenesis of Depleted Shergottite Northwest Africa 5990." *Lunar and Planetary Science Conference* 42: #1846.

Shih, Chi-Yu, Laurence E. Nyquist, Jisun Park, and Carl B. Agee. 2014. "Sm-Nd and Rb-Sr Isotopic Systematics of a Heavily Shocked Martian Meteorite Tissint and Petrogenesis of Depleted Shergottites." *Lunar and Planetary Science Conference* 45: #1184.

Snelling, Andrew A. 2000. "Geochemical Processes in the Mantle and Crust." In *Radioisotopes and the Age of the Earth: A Young-Earth Creationist Research Initiative*. Edited by Larry Vardiman, Andrew A. Snelling, and Eugene F. Chaffin, 123–304. El Cajon, California: Institute for Creation Research, and St. Joseph, Missouri: Creation Research Society. http://www.icr.org/rate/.

Snelling, Andrew A. 2005a. "Radiohalos in Granites: Evidence of Accelerated Nuclear Decay." In *Radioisotopes and the Age of the Earth: Results of a Young-Earth Creationist Research Initiative*. Edited by Larry Vardiman, Andrew A. Snelling, and Eugene F. Chaffin, 101–207. El Cajon, California: Institute for Creation Research, and Chino Valley, Arizona: Creation Research Society. http://www.icr.org/article/radiohalos-granites-evidence-for-accelerated/.

Snelling, Andrew A. 2005b. "Fission Tracks in Zircons: Evidence for Abundant Nuclear Decay." In *Radioisotopes and the Age of the Earth: Results of a Young-Earth Creationist Research Initiative*. Edited by Larry Vardiman, Andrew A. Snelling, and Eugene F. Chaffin, 209–324. El Cajon, California: Institute for Creation Research, and Chino Valley, Arizona: Creation Research Society. http://www.icr.org/article/fission-tracks-zircons-evidence-for/.

Snelling, Andrew A. 2005c. "Isochron Discordances and the Role of Inheritance and Mixing of Radioisotopes in the Mantle and Crust." In *Radioisotopes and the Age of the Earth: Results of a Young-Earth Creationist Research Initiative*. Edited by Larry Vardiman, Andrew A. Snelling, and Eugene F. Chaffin, 393–524. El Cajon, California: Institute for Creation Research, and Chino Valley, Arizona: Creation Research Society.

Snelling, Andrew A. 2009. *Earth's Catastrophic Past: Geology, Creation and the Flood*. Dallas, Texas: Institute for Creation Research.

Snelling, Andrew A. 2014a. "Radioisotope Dating of Meteorites: I. The Allende CV3 Carbonaceous Chondrite." *Answers Research Journal* 7 (April 16): 103–145. Radioisotope Dating Meteorites: Carbonaceous Chondrite | Answers Research Journal.

Snelling, Andrew A. 2014b. "Radioisotope Dating of Meteorites: II. The Ordinary and Enstatite Chondrites." *Answers Research Journal* 7 (August 20): 239–296. https://answersresearchjournal.org/radioisotope-dating-chondrites-2/.

Snelling, Andrew A. 2014c. "Determination of the Radioisotope Decay Constants and Half-Lives: Rubidium-87 (^{87}Rb). *Answers Research Journal* 7 (September 3): 311–322. https://answersingenesis.org/geology/radiometric-dating/determination-radioisotope-decay-constants-and-half-lives-rubidium-87-87rb/.

Snelling, Andrew A. 2014d. "Determination of the Radioisotope Decay Constants and Half-Lives: Lutetium-176 (^{176}Lu). *Answers Research Journal* 7 (December 3): 483–497. https://answersingenesis.org/geology/radiometric-dating/determination-radioisotope-decay-constants-and-half-lives-lutetium-176/.

Snelling, Andrew A. 2014e. "Radioisotope Dating of Meteorites: III. The Eucrites (Basaltic Achondrites). *Answers Research Journal* 7 (December 31): 533–585. Radioisotope Dating Meteorites: Eucrites | Answers Research Journal.

Snelling, Andrew A. 2015a. Determination of the radioisotope decay constants and half-lives: Rhenium-187 (^{187}Re). *Answers Research Journal* 8 (February 28): 93–111. https://answersingenesis.org/geology/radiometric-dating/determination-radioisotope-decay-constants-and-half-lives-rhenium-187/.

Snelling, Andrew A. 2015b. "Radioisotope Dating of Meteorites: IV. The Primitive and Other Achondrites." *Answers Research Journal* 8 (May 6): 209–252. Radioisotope Dating of Meteorites: IV | Answers Research Journal.

Snelling, A.A. 2015c. "Determination of the Radioisotope Decay Constants and Half-Lives: Samarium-147 (^{247}Sm)." *Answers Research Journal* 8 (June 10): 305–321. https://answersingenesis.org/geology/radiometric-dating/determination-radioisotope-decay-constants-and-half-lives-samarium-147/.

Snelling, Andrew A. 2015d. "Radioisotope Dating of Meteorites: V. Isochron Ages of Groups of Meteorites." *Answers Research Journal* 8 (December 16): 449–478. Radioisotope Dating Meteorites: Isochron Ages | Answers Research Journal.

Snelling, Andrew A. 2016. "Determination of the Radioisotope Decay Constants and Half-Lives: Potassium-40 (^{40}K)." *Answers Research Journal* 9 (August 3): 171–196. https://answersresearchjournal.org/radioisotope-decay-potassium-40/.

Snelling, Andrew A. 2017a. "Determination of the Decay Constants and Half-Lives of Uranium-238 (^{238}U) and Uranium-235 (^{235}U), and the Implications for U-Pb and Pb-Pb Radioisotope Dating Methodologies." *Answers Research Journal* 10 (January 8): 1–38. Decay Constants & Half-Lives: Uranium-238 and -235 | Answers Research Journal.

Snelling, Andrew A. 2017b. "Problems with the U-Pb Radioisotope Dating Methods—1. Common Pb." *Answers Research Journal* 10 (July 26): 121–167. Problems U-Pb Radioisotope Dating Methods | Answers Research Journal.

Snelling, Andrew A. 2018. "Problems with the U-Pb Radioisotope Dating Methods—2. U and Pb Mobility." *Answers Research Journal* 11 (June 13): 85–140. Problems with U-Pb Radioisotope Dating Methods—2. U & Pb Mobility | Answers Research Journal.

Snelling, Andrew A. 2019. "Problems with the U-Pb Radioisotope Dating Methods—3. Mass Fractionation." *Answers Research Journal* 12 (November 13): 355–392. Problems with U-Pb Radioisotope Dating Methods—3. Mass Fractionation | Answers Research Journal.

Snelling, Andrew A. 2022. *The Genesis Flood Revisited*. Green Forest, Arkansas: Master Books, and Petersburg, Kentucky: Answers in Genesis.

Snelling, Andrew A. 2023. "Radiohalos Through Earth History—What Clues Can They Provide Us?" In *Proceedings of the Ninth International Conference on Creationism*. Edited by John H. Whitmore, 540–560. Cedarville, Ohio: Cedarville University International Conference on Creationism.

Staddon, Leanne G., James R. Darling, Winfried H. Schwarz, Natasha R. Stephen, Sheila Schuindt, Joseph Dunlop, and Kimberly T. Tait. 2021. "Dating Martian Mafic Crust: Microstructurally Constrained Baddeleyite Geochronology of Enriched Shergottites Northwest Africa (NWA) 7257, NWA 8679 and Zagami." *Geochimica et Cosmochimica Acta* 315 (15 December): 73–88.

Stauffer, Heinz. 1962. "On the Production Rates of Rare Gas Isotopes in Stone Meteorites." *Journal of Geophysical Research* 67, no. 5 (May): 2023–2028.

Steele, Andrew, M.D. Fries, H.E.F. Amundsen, B.O. Mysen, Marilyn L. Fogel, M. Schweizer, and N.Z. Boctor. 2007. "Comprehensive Imaging and Raman Spectroscopy of Carbonate Globules from Martian Meteorite ALH 84001 and a Terrestrial Analogue from Svalbard." *Meteoritics and Planetary Science* 42, no. 9 (September): 1549–1566.

Stern, Richard A., and Wouter Bleeker. 1998. "Age of the World's Oldest Rocks Refined using Canada's SHRIMP: The Acasta Gneiss Complex, Northwest Territories, Canada." *Geoscience Canada* 25 (3 March): 27–31.

Stolper, Edward M., and Harry Y. McSween Jr. 1979. "Petrology and Origin of the Shergottite Meteorites." *Geochimica et Cosmochimica Acta* 43, no. 9 (September): 1475–1498.

Swindle, Timothy D., Allan H. Treiman, D.J. Lindstrom, M.K. Burkland, Benjamin A. Cohen, J.A. Grier, B. Li, and E.K. Olson. 2000. "Noble gases in Iddingsite from the Lafayette Meteorite: Evidence for Liquid Water on Mars in the Last Few Hundred Million Years." *Meteoritics and Planetary Science* 35, no. 1 (January): 107–115.

Swindle, Timothy D., and Eric K. Olson. 2004. "^{40}Ar-^{39}Ar Studies of Whole Rock Nakhlites: Evidence for the Timing of Formation and Aqueous Alteration on Mars." *Meteoritics and Planetary Science* 39, no. 5 (May): 755–766.

Symes, Steven J.K., Lars E. Borg, Charles K. Shearer Jr., Yemane Asmerom, and Anthony J. Irving. 2005. "Geochronology of NWA 1195 Based on Rb-Sr and Sm-Nd Isotopic Systematics." *Lunar and Planetary Science Conference* 36: #1435.

Symes, Steven J.K., Lars E. Borg, Charles K. Shearer, and Anthony J. Irving. 2008. "The Age of the Martian Meteorite Northwest Africa 1195 and the Differentiation History of the Shergottites." *Geochimica et Cosmochimica Acta* 72, no. 6 (15 March): 1696–1710.

Tait, Kimberly T., and James M.D. Day. 2018. "Chondritic Late Accretion to Mars and the Nature of Shergottite Reservoirs." *Earth and Planetary Science Letters* 494 (15 July): 99–108.

Tanaka, K.L., S.J. Robbins, C.M. Fortezzo, J.A. Skinner, Jr., and T.M. Hare. 2014. "The Digital Global Geologic Map of Mars: Chronostratigraphic Ages, Topographic and Crater Morphologic Characteristics, and Updated Resurfacing History." *Planetary and Space Science* 95 (May): 11–24.

Tartèse, Romain, Mahesh Anand, Francis M. McCubbin, Alison R. Santos, and T. Delhaye. 2014. "Zircons in Northwest Africa 7034: Recorders of Crustal Evolution on Mars." *Lunar and Planetary Science Conference* 45: #2020.

Tatsumoto, Mitsunobu, Daniel M. Unruh, and George A. Desborough. 1976. "U-Th-Pb and Rb-Sr Systematics of Allende and U-Th-Pb Systematics of Orgueil." *Geochimica et Cosmochimica Acta* 40, no. 6 (June): 617–634.

Terada, Kentaro, Tsuyoshi Monde, and Yuji Sano. 2003. "Ion microprobe U-Th-Pb Dating of Phosphates in Martian Meteorite ALH 84001." *Meteoritics and Planetary Science* 38, no. 11: 1697–1703.

Terada, Kentaro, and Yuji Sano. 2004. "Ion Microprobe U-Th-Pb Dating and REE Analyses of Phosphates in the Nakhlites Lafayette and Yamato-000593/000749." *Meteoritics and Planetary Science* 39, no. 12 (December): 2033–2041.

Terribilini, Dario, Otto Eugster, Mario Burger, Alfred Jakob, and Urs Krähenbühl. 1998. "Noble Gases and Chemical Composition of Shergotty Mineral Fractions, Chassigny, and Yamato 793605: The Trapped Argon-40/Argon-36 Ratio and Ejection Times of Martian Meteorites." *Meteoritics and Planetary Science* 33, no. 4 (July): 677–684.

Thomas-Keprta, Kathie L., Dennis A. Bazylinski, Joseph L. Kirschvink, Simon J. Clemett, David S. McKay, Susan J. Wentworth, Hojatollah Vali, Everett K. Gibson, Jr., and Christopher S. Romanek. 2000. "Elongated Prismatic Magnetite Crystals in ALH84001 Carbonate Globules: Potential Martian Magnetofossils." *Geochimica et Cosmochimica Acta* 64, no. 23 (1 December): 4049–4081.

Thomas-Keprta, Kathie L., Simon J. Clemett, David S. McKay, Everett K. Gibson, Jr., and Susan J. Wentworth. 2009. "Origins of Magnetite Nanocrystals in Martian Meteorite ALH84001." *Geochimica et Cosmochimica Acta* 73, no. 21 (1 November): 6631–6677.

Tomkinson, Tim, Martin R. Lee, Darren K. Mark, Katherine J. Dobson, and Ian A. Franchi. 2015. "The Northwest Africa (NWA) 5790 Meteorite: A Mesostasis-Rich Nakhlite with Little or No Martian Aqueous Alteration." *Meteoritics and Planetary Sciences* 50, no. 2 (February): 287–304.

Tornabene, Livio L., Jeffrey E. Moersch, Harry Y. McSween Jr., Alfred S. McEwen, Jennifer L. Piatek,, Keith A. Milam, and Phillip R. Christensen. 2006. "Identification of Large (2–10 km) Rayed Craters on Mars in THEMIS Thermal Infrared Images: Implications for Possible Martian Meteorite Source Regions." *Journal of Geophysical Research: Planets* 111, no. E10 (October): 1–25.

Treiman, Allan H. 1986. "The Parental Magma of the Nakhla Achondrite: Ultrabasic Volcanism on the Shergottite Parent Body." *Geochimica et Cosmochimica Acta* 50: 1061-1070.

Treiman, Allan H. 1990. "Complex Petrogenesis of the Nakhla (SNC) Meteorite: Evidence from Petrography and Mineral Chemistry." *Lunar and Planetary Science Conference* 20: 273–280.

Treiman, Allan H. 1993. "The Parent Magma of the Nakhla (SNC) Meteorite, Inferred from Magmatic Inclusions." *Geochimica et Cosmochimica Acta* 57, no. 19 (October): 4753–4767.

Treiman, Allan H., G.A. Mckay, Donald D. Bogard, David W. Mittlefehldt, M.-S. Wang, L. Keller, M.E. Lipschutz, M.M. Lindstrom, and Daniel H. Garrison. 1994. "Comparison of the LEW88516 and ALHA77005 Meteorites: Similar but Distinct." *Meteoritics* 29, no. 5 (September 1): 581–592.

Treiman, Allan H. 1995. "S ≠ NC: Multiple Source Areas for Martian Meteorites." *Journal of Geophysical Research: Planets* 100, no. E3 (25 March): 5329–5340.

Treiman, Allan H., James D. Gleason, and Donald D. Bogard. 2000. "The SNC Meteorites are from Mars." *Planetary and Space Science* 48: 1213–1230.

Treiman, Allan H. 2003. "Submicron Magnetite Grains and Carbon Compounds in Martian Meteorite ALH84001: Inorganic, Abiotic Formation by Shock and Thermal Metamorphism." *Astrobiology* 3, no. 2 (Summer): 369–392.

Treiman, Allan H. 2005. "The Nakhlite Meteorites: Augite-Rich Igneous Rocks from Mars." *Chem der Erde–Geochemistry* 65, no. 3 (20 July): 203–270.

Treiman, Allan H., M. Darby Dyar, Molly McCanta, Sarah K. Noble, and Carle M. Pieters. 2007. "Martian Dunite NWA 2737: Petrographic Constraints on Geological History, Shock Events, and Olivine Color." *Journal of Geophysical Research: Planets* 112, no. E4 (April): E04002. https://doi.org/10.1029/2006JE002777.

Treiman, Allan H., and Anthony J. Irving. 2008. "Petrology of Martian Meteorite Northwest Africa 998." *Meteoritics and Planetary Science* 43, no. 5 (May): 829–854.

Treiman, Allan H., and Justin Filiberto. 2015. "Geochemical Diversity of Shergottite Basalts: Mixing and Fractionation, and their Relation to Mars Surface Basalts." *Meteoritics and Planetary Science* 50, no. 4 (April): 632–648.

Treiman, Allan H. 2019. "Meteorite Allan Hills (ALH) 84001: Implications for Mars' Inhabitation and Habitability." *The First Billion Years: Habitability*, Abstract #1032.

Turner, Grenville, S.F. Knott, Richard D. Ash, and J.D. Gilmour. 1997. "Ar-Ar Chronology of the Martian Meteorite ALH84001: Evidence for the Timing of the Early Bombardment of Mars." *Geochimica et Cosmochimica Acta* 61, no. 18 (September): 3835–3850.

Turrin, B.D., Jisun Park, G.F. Herzog, F.N. Lindsay, J.S. Delaney, Laurence E. Nyquist, and Carl C. Swisher III. 2013. "^{40}Ar/^{39}Ar Ages of Maskelynite Grains from ALH 77055." *Lunar and Planetary Science Conference* 44: #2979.

Turrin, B.D., J.B. Setera, Jisun Park, J.S. Delaney, Carl C. Swisher III, G.F. Herzog, and Anthony J. Irving. 2018. "^{40}Ar/^{39}Ar Ages of Plagioclase-Bearing Shergottite Northwest Africa 4480." *Lunar and Planetary Science Conference* 49: #2814.

Tyler, David J. 1990. "The Tectonically-Controlled Rock Cycle." In *Proceedings of the Second International Conference on Creationism*. Edited by Robert E. Walsh, and Christopher L. Brooks, vol. 2, 293–301. Pittsburgh, Pennsylvania: Creation Science Fellowship.

Udry, Arya, J. Brian Balta, and Harry Y. McSween, Jr. 2014. "Exploring Fractionation Models for Martian Magmas." *Journal of Geophysical Research: Planets* 119, no. 1 (January): 1–18.

Udry, Arya., Geoffrey H. Howarth, Thomas J. Lapen, and Minako Righter. 2017. "Petrogenesis of the NWA 7320 Enriched Martian Gabbroic Shergottite: Insight into the Martian Crust." *Geochimica et Cosmochimica Acta* 204 (1 May): 1–18.

Udry, Arya, and James M.D. Day. 2018. "1.34 Billion-Year-Old Magmatism on Mars Evaluated from the Co-genetic Nakhlite and Chassignite Meteorites." *Geochimica et Cosmochimica Acta* 238 (1 October): 292–315.

Udry, Arya, Geoffrey H. Howarth, Christopher D.K. Herd, James M.D. Day, Thomas J. Lapen, and Justin Filiberto. 2020. "What Martian Meteorites Reveal About the Interior and Surface of Mars." *Journal of Geophysical Research: Planets* 125, no. 2 (December): e2020JE006523. https://doi.org/10.1029/2020JE006523.

Udry, Arya, Amanda M. Ostwald, and Tomohiro Usui. 2025. "Seeing Red: Retrieving Rocks from Mars and Phobos." *Elements* 21, no. 5 (October): 333–339.

Usui, Tomohiro, Harry Y. McSween, Jr., and Christine Floss. 2008. "Petrogenesis of Olivine-Phyric Shergottite Yamato 980459, Revisited." *Geochimica et Cosmochimica Acta* 72, no. 6 (15 March): 1711–1730.

Usui, Tomohiro, Matthew E. Sanborn, Meenakshi Wadhwa, Harry Y. McSween, Jr. 2010. "Petrology and Trace Element Geochemistry of Robert Massif 04261 and 04262 Meteorites, the First Examples of Geochemically Enriched Lherzolitic Shergottites." *Geochimica et Cosmochimica Acta* 74: 7283–7306.

Váci, Zoltán, Carl B. Agee, Christopher D.K. Herd, Erin L. Walton, Oliver Tschauner, Karen Ziegler, Vitali B. Prakapenka, Eran Greenburg, and Sylvia Monique-Thomas. 2020. "Hydrous Olivine Alteration on Mars and Earth." *Meteoritics and Planetary Sciences* 55, no. 5 (May): 1011–1030.

Valley, John W., John M. Eiler, Colin M. Graham, Everett K. Gibson, Christopher S. Romanek, and Edward M. Stolper. 1997. "Low-Temperature Carbonate Concretions in the Martian Meteorite ALH84001: Evidence from Stable Isotopes and Mineralogy." *Science* 27, no. 5306 (14 March): 1633–1638.

Valley, John W., Aaron J. Cavosie, Takayuki Ushikubo, David A. Reinhard, Daniel F. Lawrence, David J. Larson, Peter H. Clifton, Thomas F. Kelly, Simon A. Wilde, Desmond E. Moser, and Michael J. Spicuzza. 2014. "Hadean Age for a Post-Magma-Ocean Zircon Confirmed by Atom-Probe Tomography." *Nature Geoscience* 7, no. 3 (23 February): 219–223.

Vardiman, Larry, Andrew A. Snelling, and Eugene F. Chaffin, eds. 2005. *Radioisotopes and the Age of the Earth: Results of a Young-Earth Creationist Research Initiative*. El Cajon, California: Institute for Creation Research, and Chino Valley, Arizona: Creation Research Society.

Wadhwa, Meenakshi, and G.W. Lugmair. 1996. "The Formation Age of Carbonates in ALH84001." *Meteoritics and Planetary Science* 31 (January): A145.

Wadhwa, Meenakshi, and Ghislaine Crozaz. 1995. "Trace and Minor Elements in Minerals of Nakhlites and Chassigny: Clues to their Petrogenesis." *Geochimica et Cosmochimica Acta* 59, no. 17 (September): 3629–3645.

Wadhwa, Meenakshi. 2001. "Redox State of Mars' Upper Mantle and Crust from Eu Anomalies in Shergottite Pyroxenes." *Science* 291, no. 5508 (23 February): 1527–1530.

Walton, Erin L., Simon P. Kelley, and Christopher D.K. Herd. 2007. "A Laser Probe ^{40}Ar-^{39}Ar Investigation of Two Martian Lherzolitic Shergottites." *Meteoritics and Planetary Science* 42: A159.

Walton, Erin L., Simon P. Kelley, and Christopher D.K. Herd. 2008. "Isotopic and Petrographic Evidence for Young Martian Basalts." *Geochimica et Cosmochimica Acta* 72, no. 23 (1 December): 5819–5837.

Walton, Erin L., Anthony J. Irving, T.E. Bunch, and Christopher C.D.K. Herd. 2012. "Northwest Africa 4797: A Strongly Shocked Ultramafic Poikilitic Shergottite Related to Compositionally Intermediate Martian Meteorites." *Meteoritics and Planetary Science* 47, no. 9 (September): 1449–1474.

Warren, Paul H. 2011. "Stable-Isotopic Anomalies and the Accretionary Assemblage of the Earth and Mars: A Subordinate Role for Carbonaceous Chondrites." *Earth and Planetary Science Letters* 311, nos. 1_2 (1 November): 93–100.

Weisberg, M.K., Timothy J. McCoy, and Alexander N. Krot. 2006. "Systematics and Evaluation of Meteorite Classification." In *Meteorites and the Early Solar System II*. Edited by D.S. Loretta and Harry Y. McSween Jr., 19–52. Tucson, Arizona: University of Arizona Press.

Werner, Stephanie C., Anouck Z. Ody, and François Poulet. 2014. "The Source Crater of Martian Shergottite Meteorites." *Science* 343, no. 6177 (6 March): 1343–1346.

Wieczorek, Mark A., and Maria T. Zuber. 2004. "The Thickness of the Martian Crust: Improved Constraints from Geoid-to-Topography Ratios". *Journal of Geophysical Research: Planets* 109, no. E1 (January): E01009. https://doi.org/10.1029/2003JE002153.

Wilde, Simon A., John W. Valley, William H. Peck, and Colin M. Graham. 2001. "Evidence from Detrital Zircons for the Existence of Continental Crust and Oceans on the Earth 4.4Gyr Ago." *Nature* 409, no. 6817 (11 January): 175–178.

Wittmann, Axel, Randy L. Korotev, Bradley L. Jolliff, Anthony J. Irving, Desmond E. Moser, Ivan Barker, and Douglas Rumble III. 2015. "Petrography and Composition of Martian Regolith Breccia Meteorite Northwest Africa 7475." *Meteoritics and Planetary Science* 50, no. 2 (February): 326–352.

Wood, C.A., and L.D. Ashwal. 1981. "SNC Meteorites: Igneous Rocks from Mars?" *Lunar and Planetary Science Conference* 12: 1359–1376.

Wooden, J.L., Laurence E. Nyquist, Donald D. Bogard, B.M. Bansal, Henry Wiesmann, Chi-Yu Shih, and G.A. McKay. 1979. "Radiometric Ages for the Achondrites Chervony Kut, Governador Valadares, and Allan Hills 77005." *Lunar and Planetary Science Conference* 10 (March): 1379–1381.

Wooden, J.L., Chi-Y. Shih, Laurence E. Nyquist, B.M. Bansal, Henry Wiesmann, and G.A. McKay. 1982. "Rb-Sr and Sm-Nd Isotopic Constraints on the Origin of EETA 79001: A Second Antarctic Shergottite." *Lunar and Planetary Science Conference* 13: 879–880.

Wu, Yunhua, Weibiao Hsu, Qiu-Li Li, Xiaochao Che, and Shiyong Liao. 2021. "Heterogeneous Martian Mantle: Evidence from Petrology, Mineral Chemistry, and In Situ U-Pb Chronology of the Basaltic Shergottite Northwest Africa 8653." *Geochimica et Cosmochimica Acta* 309 (15 September): 352–365.

Yin, Qing-Zhu, Francis M. McCubbin, Qin Zhou, Alison R. Santos, Romain Tartèse, Xian-Hua Li, Qiu-Li Li, et al. 2014. "An Earth-like Beginning for Ancient Mars Indicated by Alkali-Rich Volcanism at 4.4Ga." *Lunar and Planetary Science Conference* 45: #1320.

Zhou, Qin, Christopher D.K. Herd, Qing-Zhu Yin, Xian-Hua Li, Fu-Yuan Wu, Qiu-Li Li, Yu Liu, Guo-Qiang Tang, and Timothy J. McCoy. 2013. "Geochronology of the Martian Meteorite Zagami Revealed by U–Pb Ion Probe Dating of Accessory Minerals." *Earth and Planetary Science Letters* 374 (15 July): 156–163.